State of the Earth's Cryosphere at the Beginning of the 21st Century: Glaciers, Global Snow Cover, Floating Ice, and Permafrost and Periglacial Environments—

FLOATING ICE: SEA ICE

By CLAIRE L. PARKINSON, *and* DONALD J. CAVALIERI

SATELLITE IMAGE ATLAS OF GLACIERS OF THE WORLD

Edited by RICHARD S. WILLIAMS, JR., *and* JANE G. FERRIGNO

U.S. GEOLOGICAL SURVEY PROFESSIONAL PAPER 1386–A–4–I

Sea ice covers vast areas of the polar oceans, ranging in extent from ~5–7×10^6 km^2 in September to ~15×10^6 km^2 in March in the Northern Hemisphere and from ~3×10^6 km^2 in February to ~18×10^6 km^2 in September in the Southern Hemisphere. The extensive cover of sea ice has major impacts on the atmosphere, oceans, and terrestrial and marine ecosystems of the polar regions. Satellite data document considerable interannual variability in the spatial distributions of both polar sea-ice covers, suggesting possible connections between the sea ice and various oscillations within the global climate system. There are statistically significant 25-year trends, including overall trends of a decrease in the extent of sea ice in the Arctic Ocean and adjacent seas and an increase in the extent of sea ice in the Southern Ocean around Antarctica from late 1978 through the end of 2003.

CONTENTS

STATE OF THE EARTH'S CRYOSPHERE AT THE BEGINNING OF THE 21ST CENTURY: GLACIERS, GLOBAL SNOW COVER, FLOATING ICE, AND PERMAFROST AND PERIGLACIAL ENVIRONMENTS

FLOATING ICE: SEA ICE

By CLAIRE L. PARKINSON[1] *and* DONALD J. CAVALIERI[1]

Abstract

Sea ice covers vast areas of the polar oceans, ranging in extent from ~5–7×10^6 km^2 in September to ~15×10^6 km^2 in March in the Northern Hemisphere and from ~3×10^6 km^2 in February to ~18×10^6 km^2 in September in the Southern Hemisphere. The extensive cover of sea ice has major impacts on the atmosphere, oceans, and terrestrial and marine ecosystems of the polar regions. As changes occur in the sea-ice cover, there are potential widespread climatological and ecological consequences from both regional and global perspectives. Satellite data document considerable interannual variability in the spatial distributions of the two polar sea-ice covers, and many studies suggest possible connections between the sea ice and various oscillations within the global climate system, such as the Arctic Oscillation, North Atlantic Oscillation, and Antarctic Oscillation (or Southern Annular Mode). Nonetheless, there are statistically significant 25-year trends, including overall trends of a decrease in the extent of sea ice in the Arctic Ocean and adjacent seas and an increase in the extent of sea ice in the Southern Ocean around Antarctica from late 1978 through the end of 2003. For a detailed picture of the seasonally varying ice cover at the start of the 21st century, this chapter includes maps of sea-ice concentration for each month of 2001 for both the Arctic and Antarctic regions, as well as an overview of what the satellite record has shown about changes in the two polar sea-ice covers from the late 1970s through 2003.

Introduction

Areal Coverage

Sea ice covers vast regions of the Earth's surface at any given moment, with major impacts on local and regional climates and terrestrial and marine ecosystems. Globally, the areal extent of sea ice ranges from ~18×10^6 km^2 to ~27×10^6 km^2, with the distribution of the sea ice between the Northern and Southern Hemispheres varying systematically with season.

In the Northern Hemisphere, sea ice covers ~15×10^6 km^2 at its winter maximum in February and March, spreading throughout the Arctic Ocean, Canadian Archipelago, Hudson Bay, Baffin Bay, and the Kara Sea, and also extending well into the Sea of Okhotsk, the Bering Sea, the Labrador Sea, the Barents Sea, and the Greenland Sea. This vast area of sea-ice cover is reduced in summer by at least half, to ~6×10^6 km^2 or less by mid-September, at its summer minimum, when it is confined mostly to the Arctic Ocean (fig. 1). The winter maximum sea-ice extent is 1.5 times the area of Canada; even at

[1] National Aeronautics and Space Administration, Goddard Space Flight Center, Cryospheric Sciences Laboratory, Cryospheric Sciences Branch (Code 614.1), Greenbelt, MD 20771 U.S.A.

the summer minimum, the sea-ice extent has generally exceeded the combined areas of India, Pakistan, Afghanistan, Iran, and Iraq. Ice thicknesses tend to be less than 6 m, and the average ice thicknesses in the central Arctic are probably in the range of 2 to 4 m (see Swithinbank, 1972; Rothrock and others, 1999; and Winsor, 2001, for sea-ice-thickness measurements based on observations from upward-looking submarine sensors; see Laxon and others, 2003, for ice-thickness estimates based on satellite radar altimetry). Ice thicknesses in the surrounding seas and bays are probably less than 2.5 m; the thickness of sea ice is considerably harder to measure on a hemispheric basis than the areal extent of sea ice and, consequently, is much less well known.

In the Southern Hemisphere, winter sea-ice extent is even higher than in the Northern Hemisphere, peaking at ~18×10^6 km^2, usually in September. By the summer minimum, generally in late February, the sea-ice cover decreases to ~3×10^6 km^2 (fig. 2). The much larger range in extent of sea ice during the annual cycle in the Antarctic compared with the Arctic is the result of the different geographical distribution of land and ocean in the two hemispheres. In the Northern Hemisphere, the central polar region is occupied by the Arctic Ocean, which is largely surrounded by land (fig. 1). The surrounding land areas restrict the expansion of sea ice in winter but also help maintain a large perennial ice cover by restricting the input of warm water in summer. In the Southern Hemisphere, by contrast, the central polar region is occupied by the Antarctic continent, which is surrounded by vast ocean areas largely unrestricted by land masses (fig. 2). Any summer sea ice in the Southern Hemisphere is ice that has survived the summer heating despite being at latitudes equatorward of 78° S., whereas winter ice in the Southern Hemisphere is unconstrained by land in its northward expansion. Because of the limited amount of ice that survives the summer, sea ice in the Southern Hemisphere tends, overall, to be thinner than the ice in the Northern Hemisphere. Southern Hemisphere ice thicknesses generally are less than 1 m (see, for example, Worby and others, 1996, 1998; Jeffries and others, 1998).

Impacts of Sea-Ice Cover on the Ocean and Atmosphere

The vast area of sea-ice cover in the two polar regions has many impacts on the climate and on terrestrial and marine ecosystems. Climatologically, sea ice provides insulation between the ocean and atmosphere, reflects much of the solar radiation incident on it, expels salt as the ice forms, releases relatively fresh water to the upper layer of the ocean as the ice melts, and transports cold, relatively fresh water equatorward.

The insulation effect is one of the most important, restricting ocean-atmosphere exchanges of heat, mass, and momentum. The heat insulation is particularly important in winter, when the sea-ice cover greatly restricts loss of heat from the ocean to the very cold polar atmosphere. Maykut (1978) calculated that the January sensible heat flux from the ocean to the atmosphere in the central Arctic is ~550 watts per square meter (Wm^{-2}) in areas where the ocean and atmosphere are in direct contact with each other but is less than 50 Wm^{-2} where the two are separated by sea ice of 80 cm thickness and is 0 Wm^{-2} where the two are separated by an ice layer as thick as 3 m. His calculations for latent heat flux in January indicate a flux of ~145 Wm^{-2} for an ice-free ocean area, reduced to <10 Wm^{-2} for a sea-ice cover of 40 cm.

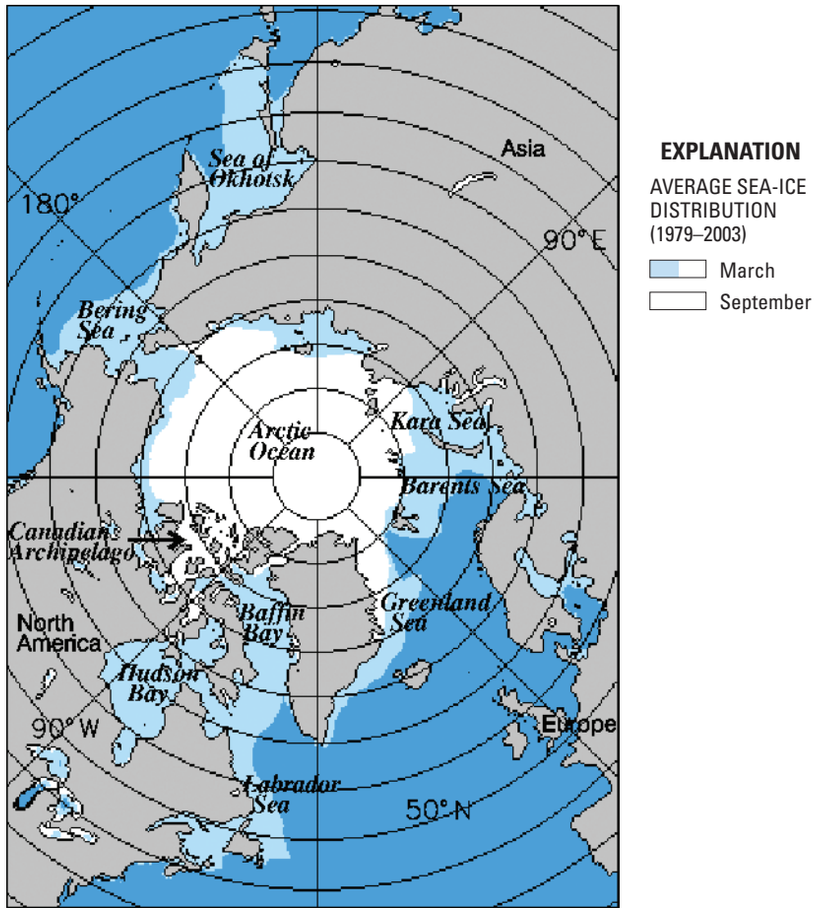

Figure 1.—*North polar location map and monthly sea-ice distribution in March (white and light blue) and September (white), averaged for the 25-year period from 1979 to 2003. The sea-ice distributions are derived from satellite data discussed in the "Annual Cycle of Sea Ice" section.*

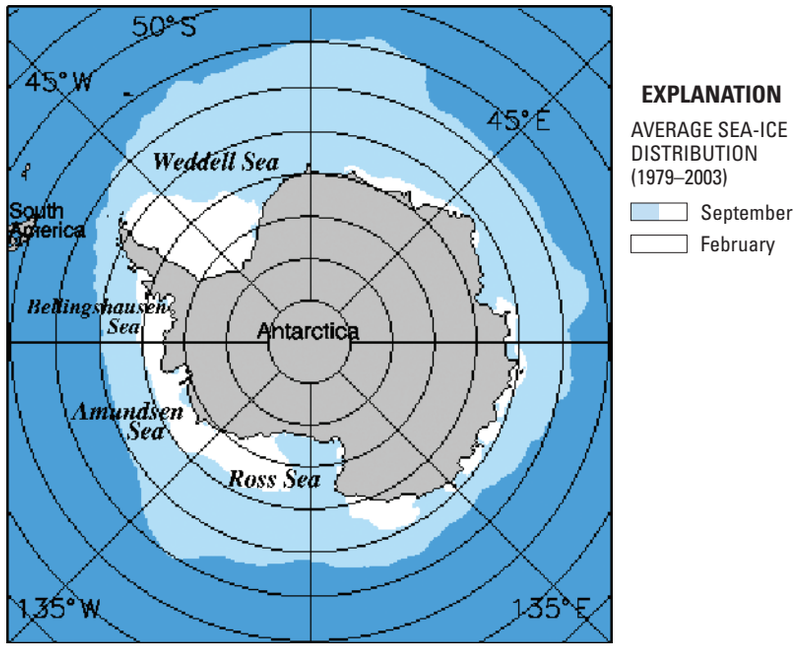

Figure 2.—*South polar location map and monthly sea-ice distribution in February (white) and September (white and light blue), averaged for the 25-year period from 1979 to 2003. The sea-ice distributions are derived from satellite data discussed in the "Annual Cycle of Sea Ice" section.*

Another of the most important effects of the sea ice is the reflection of solar radiation. An ice-free ocean tends to have a low albedo (or reflectivity), typically in the range of 3 to 15 percent. Ice, on the other hand, tends to have a much higher albedo, especially if covered by a layer of fresh snow, when the albedo can be as high as 98 percent. More typically, the ice albedo is in the range of 40 to 80 percent, but even that percentage is significantly higher than the ocean albedo. The contrast between ice and liquid water albedos leads to an important positive feedback in the climate system: under conditions of regional warming, the sea-ice cover is expected to retreat, creating a reduced overall surface albedo. This leads to an increased absorption of solar radiation and, consequently, further warming. Similarly, cooling leads to ice expansion, increased albedo, decreased absorption of solar radiation, and further cooling. A similar positive feedback applies to other types of ice as well (for example, glaciers, snow cover, lake and river ice, and permafrost), which, working in concert, creates a process that enhances climate change in the polar regions, where marine and terrestrial ice are widespread.

As sea ice forms, some of the original water's salt content is expelled to the water below, while some of the salt collects into pockets within the ice. Additional salt is released from the ice as the ice gets older, due either to gravitational downward migration or to a flushing out of the salt by meltwater. This expelling of salt to the upper layer of the ocean during ice formation and aging can affect ocean circulation if the density profile directly under the ice is weak enough that the addition of the expelled salt leads to overturning. Consequences can include mixed-layer deepening, downwelling, and, in some instances, even bottom-water formation, the latter arising when the surface water downwells to the ocean depths. In contrast, as ice undergoes surface melting during the summer, the relatively fresh, low-density meltwater tends to stabilize the upper ocean layer.

Another climatological effect of sea ice is the influence of the freeze/melt cycle on seasonal temperature contrasts. Because energy is released during freezing (exothermic reaction), which occurs predominantly during fall and winter, and is absorbed during melting (endothermic reaction), which occurs predominantly during spring and summer, the freeze/melt cycle contributes to the reduction (that is, dampening down) of seasonal temperature extremes.

Impacts of Sea-Ice Cover on Terrestrial and Marine Ecosystems

The presence of sea ice affects polar life forms in a wide variety of ways. Sea ice provides a habitat for many very small organisms, provides a platform for larger animals, and restricts light transmission to organisms in the ocean underneath the ice, while also insulating such organisms from the cold polar atmosphere.

Even a small polar ice floe can be the habitat for an abundance of organisms, including millions of algae, with a biomass sometimes as high as 100 mg of chlorophyll *a* m^{-2} (Gradinger, 1995). Algae are consumed by protozoans, crustaceans, and nematodes, all also living within the ice; under favorable conditions, densities of protozoans, crustaceans, and nematodes can exceed 100,000 organisms m^{-3} (Melnikov, 1997). Within the Arctic sea ice, rotifers and nematodes are abundant, whereas within the Antarctic ice, the dominant metazoan fauna are copepods and acoelomous turbellarians (Schnack-Schiel,

2003). When sea ice melts in the spring and summer, algae are released into surrounding waters, at times leading to major algal blooms near the ice edge (Arrigo and others, 2002).

Sea ice also affects larger organisms, many of which take advantage of the platform that the ice provides. In both polar regions, seals (*Pinnipedia*) give birth and nurse their young on sea-ice floes; ice floes further provide the seals with places of rest and safety from killer whales (*Orcinus orca*) and leopard seals (*Hydrurga leptonyx*) in the Antarctic. In the Arctic, polar bears (*Ursus maritimus*) and Arctic foxes (*Alopex lagopus*) traverse the sea ice, with polar bears sometimes staying on the ice for months at a time (Stirling and Derocher, 1993). In the Antarctic, the most noted wanderers on the sea ice are penguins (*Spheniscidae*), although in both polar regions, many mammal and avian species frequent the ice and are significantly affected by it (Ainley and others, 2003). As the sea-ice cover changes, whether caused by regional climate warming or other reasons, the associated terrestrial and marine ecosystems must adjust as well (Croxall and others, 2002; Derocher and others, 2004).

The presence of sea ice also affects human activities in many ways, such as hindering movement of ships (often requiring icebreakers to provide passage for cargo ships and research vessels) and complicating the interpretation of submarine acoustics. On the positive side, sea-ice floes (and also tabular icebergs calving from glaciers and ice shelves) can serve as floating platforms for ice fishing and for scientific measurements on and under the ice.

Sea-Ice Records

Many data products detailing various aspects of the polar sea-ice cover are now available; some of the more important of these records are discussed in this section.

Pre-Satellite Records

The very nature of polar seas covered with millions of square kilometers of uneven, broken, and moving sea ice makes these regions particularly inhospitable and not easily navigable by surface ships. Prior to 1960, sea-ice observations were made by observers from the shore, ships, and aircraft. Many of the earliest sea-ice data records were made by explorers and those hunting various species of seals (pinnipeds) and whales (cetaceans), although the longest sea-ice record probably is the record of the number of weeks per year of ice along the northern coast of Iceland, made by Icelanders, that dates back to about 870. The latter record is less complete prior to 1600 than afterwards (Thoroddsen, 1916–17; Koch, 1945; Bergþórsson, 1969, 1970; Vilmundarson, 1969).

Efforts are underway to piece together many of the historical records, although sparse in both spatial and temporal coverage, for the purpose of creating a longer term perspective than would be possible with only the satellite observations (the earliest coming in the 1960s). The key compilations completed so far include the following: Walsh and Johnson (1979) compiled Arctic sea-ice data for the period from 1953 to 1977, digitizing the data into monthly grids covering most of the Northern Hemisphere sea-ice

region; Jevrejeva (2001) compiled a long-term time series of the date of sea-ice breakup in the northern Baltic Sea spanning the period from 1529 to 1990; the Arctic and Antarctic Research Institute (AARI), in St. Petersburg, Russia, compiled historical Russian sea-ice extent and thickness observations from the beginning of the 20th century for parts of the Arctic marginal seas (Polyakov and others, 2003); Fetterer and Troisi (1997) further processed digitized 10-day Arctic charts of sea-ice concentration (percent areal ice coverage) and sea-ice type for 1953–1990 from the AARI data set, to provide a product on the Equal-Area Scalable Earth (EASE) grid; the U.S. National Snow and Ice Data Center (NSIDC, 2004) compiled measurements of 23 central Arctic snow-and-ice parameters from the former Soviet Union's Sever airborne and North Pole drifting-station programs for the period from 1928 to 1989; and Colony and Thorndike (1984) generated ice-drift velocities for the period from 1872 to 1973, from data from drifting ships, manned research stations on ice floes and tabular icebergs, and data buoys in the Arctic Ocean. Additionally, a comprehensive Joint U.S.-Russian Arctic Sea Ice Atlas compiled in 1996 provides a historical record of sea-ice charts and monthly sea-ice motion fields from Russian and U.S. sources (including ice-station, ice-buoy, and ice-breaker data) from 1950 to 1994 (Arctic Climatology Project, 2000), and a 200-year record of the areal extent of sea ice on the Scotian Shelf in the Gulf of St. Lawrence, Canada, has been generated from ice-patrol and shipping reports, local newspaper stories, and lighthouse records (Hill and others, 2002). Going back even further in time, historical ice charts of the Nordic Arctic seas spanning a period of more than 400 years (1553–2002) have been archived at *http://acsys.npolar.no/ahica/summary.htm*, under the auspices of the World Climate Research Program (WCRP) Arctic Climate System Study (ACSYS). The earliest of these charts were derived from ship logs and diaries, and the more recent observations were from ships, aircraft, and satellites.

In some cases, sea-ice records have been generated from proxy records instead of direct sea-ice observations. For instance, Grumet and others (2001) generated a 1,000-year record of spring sea-ice conditions in the Arctic region of Baffin Bay using sea-salt records from an ice core obtained from the Penny Ice Cap on Baffin Island. Additionally, Bergþórsson (1970) used temperature measurements at two meteorological stations in Iceland (Stykkishólmur and Teigarhorn) to correlate mean annual temperature and presence of drift ice around Iceland from 1846 to 1969. He then used that correlation to relate annual temperature and sea-ice duration by month for the period from 1591 to 1846 and estimated temperature and sea-ice duration for the period from 930 to 1591.

With the advent of satellite observations in the 1960s, more consistent data records became possible, and hybrid sea-ice data sets combining both pre-satellite and satellite data have been compiled. In particular, Walsh and Chapman (2001) expanded upon the Walsh and Johnson (1979) 1953–1977 record of the Northern Hemisphere sea ice by adding satellite data for the post-1972 period and additional pre-satellite data, generating a record for the entire 20th century. Also, the U.K. Met Office Hadley Centre has produced global sea-ice and sea-surface temperature data sets for the period 1871 onward (Rayner and others, 2003). Additionally, based on aerial reconnaissance and ship and satellite observations during the period from 1953 to 1986, a collection of about 6,000 historical sea-ice charts showing areal extent and

compactness of sea ice in parts of the Bering Sea, Chukchi Sea, and Beaufort Sea adjacent to Alaska and the western Canadian Arctic is archived at the NSIDC in Boulder, Colorado (Dehn, 2002).

Visible and Infrared Satellite Records

The first U.S. environmental satellite, the Television and Infrared Observation Satellite (TIROS), was launched by the U.S. National Aeronautics and Space Administration (NASA) on 1 April 1960; it provided the first visible (daytime) and thermal-infrared (nighttime) satellite images of the Earth's surface and its cloud cover. The early TIROS satellites orbited at a relatively low inclination (angle with the Equator) and, hence, sea-ice observations were limited to latitudes between 60° N. and S.

In spite of the serious problem of cloud cover, visible and thermal-infrared satellite imagery provided the first glimpses of sea-ice cover from space in both polar regions. In 1963, images of sea ice in the Labrador Sea from TIROS 5 and 6 became the first satellite images to be used in official advisories (Notice to Mariners or NTMs) for ships (Massom, 1991). In 1964, NASA's Nimbus 1 satellite was the first to be placed in a polar orbit (98.6° inclination), and this allowed it to provide data coverage poleward to latitudes 82.5° N. and S. Complete coverage of sea ice was thereby achieved in the Southern Ocean around Antarctica, and the coverage in the Arctic Ocean was to within 7.5° of the North Pole. Beginning with TIROS 9 in 1965, many more polar-orbiting environmental satellites have been successfully launched and become operational.

The TIROS series of satellites was followed by the Environmental Science Services Administration (ESSA) series, named for the government agency (1965–1970) within the Department of Commerce (DOC) that operated the satellites, and by the Nimbus and National Oceanic and Atmospheric Administration (NOAA) series, the latter named for the DOC agency (1970–present) that was the successor to ESSA. The first satellite in the operational NOAA series, NOAA 1, was launched in December 1970; NOAA 17 was launched in June 2002.

A major advance in sea-ice remote sensing was achieved with the launch of the Advanced Very High Resolution Radiometer (AVHRR) on the TIROS-N satellite in 1978. AVHRR provided improved spectral and spatial resolution compared with previous radiometers. More recent satellites in the NOAA series also have included AVHRR sensors; the AVHRR sensor provides sea-ice imagery at a picture element (pixel) resolution at nadir of 1.1 km. Under cloud-free conditions, this sensor, with its wide swath, has proved quite useful for producing sea-ice charts (fig. 3). NSIDC archives a variety of gridded sea-ice products derived from AVHRR data, including a 1-km pixel resolution, Level 1b polar data set useful for monitoring melt ponds on sea ice. Another gridded data set is the daily sea-ice motion vectors for both polar regions spanning the period from November 1978 to March 2003 (Fowler, 2003). Sea-ice surface temperature also is derived from AVHRR data and is archived as part of NSIDC's Polar Pathfinder EASE-grid composites (Key and Haefliger, 1992; Fowler and others, 2000).

The first satellite series designed specifically to monitor the Earth's surface was the Earth Resources Technology Satellite-1 (ERTS-1), launched by NASA on 23 July 1972 and later renamed Landsat 1. Since 1972, six more Landsat

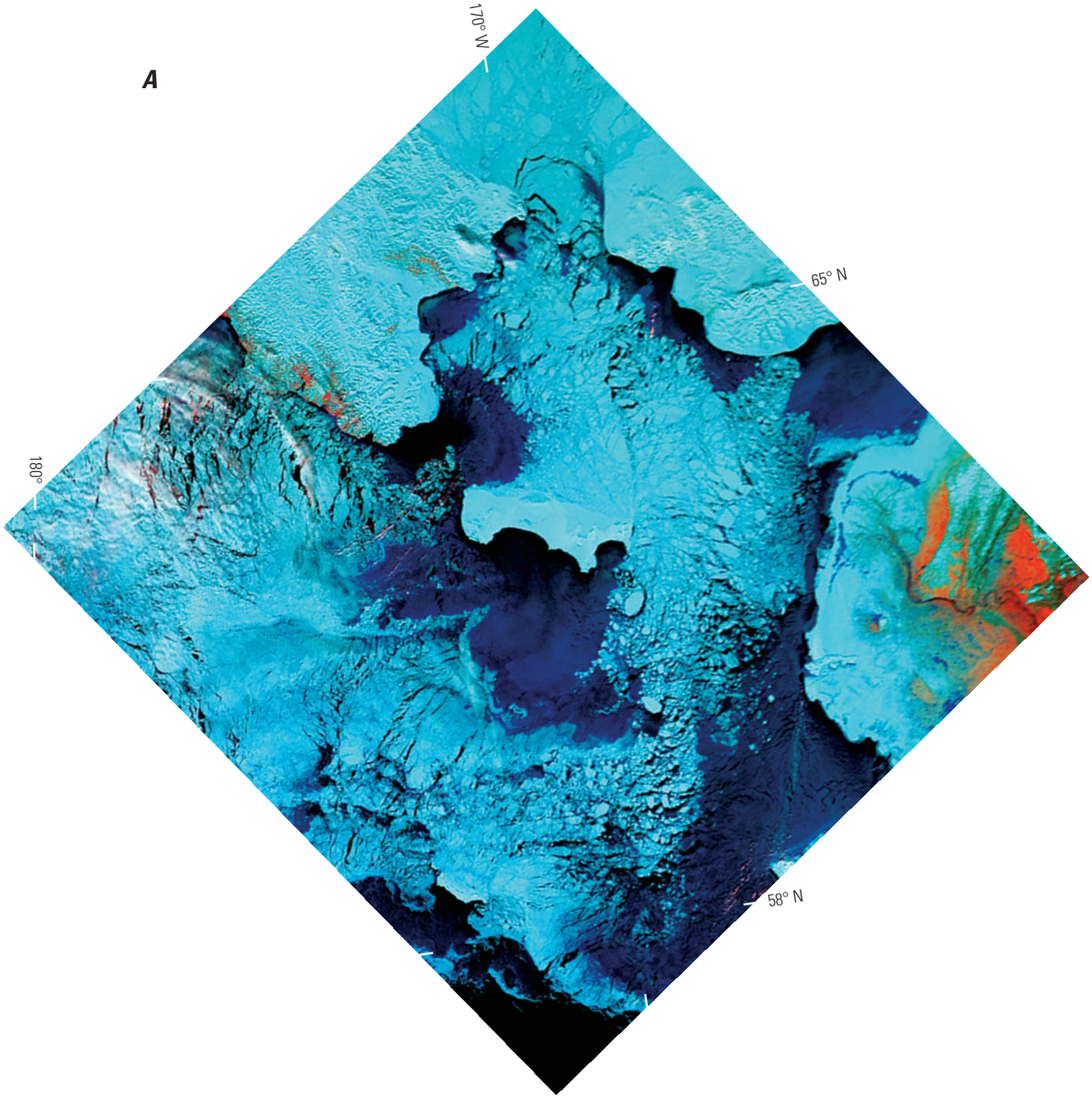

Figure 3.—**A**, *NOAA 17 Advanced Very High Resolution Radiometer (AVHRR) image of the Bering Sea for 16 March 2003.* **B**, *National Ice Center (NIC) sea-ice-analysis chart for the week of 17–21 March 2003.*

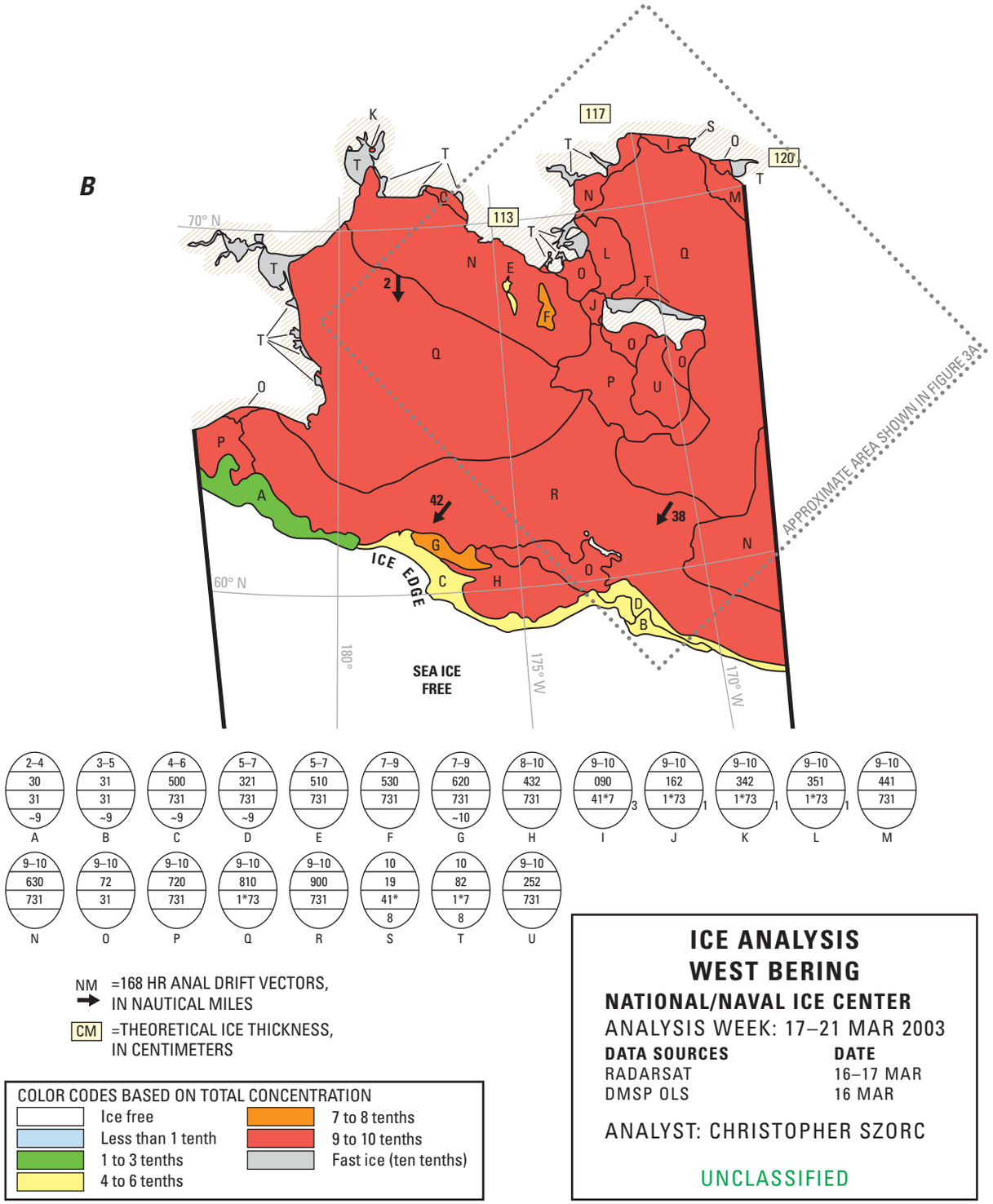

The numbers in the 21 ellipses ("eggs") contain ice information for the corresponding regions (labeled A through U) on the map. Numbers on the top line present the ice concentrations in tenths. Numbers on the second line refer to ice concentrations (in tenths) of the thickest, medium, and thinnest ice in the region (or, in cases with just two digits, of the thick and thin ice, respectively). Numbers on the third line refer to stages of development of the ice, in order of decreasing ice thickness. Numbers at the bottom of the ellipse, when present, relate to floe size. Further details can be found at the National Ice Center web page at <*http://natice.noaa.gov*>.

***Figure 3.*—A**, *NOAA 17 Advanced Very High Resolution Radiometer (AVHRR) image of the Bering Sea for 16 March 2003.* **B**, *National Ice Center (NIC) sea-ice-analysis chart for the week of 17–21 March 2003.—Continued*

satellites have been launched; only Landsat 6 failed to achieve orbit. The most recent, Landsat 7, was launched in 1999 and carries the Enhanced Thematic Mapper Plus (ETM+) sensor, which is an improved version of the Thematic Mapper flown on Landsat 4 and 5 and the Enhanced Thematic Mapper flown on the failed Landsat 6. The ETM+ sensor measures radiances from visible to near- and thermal-infrared wavelengths in six spectral bands at a pixel resolution of 30 m. A seventh, panchromatic band provides a pixel resolution of 15 m. The Landsat series of visible and infrared observations has been used widely over the years for studying the movement and deformation of sea ice, sea-ice type, and sea-ice concentration (fig. 4) and for generating regional sea-ice atlases (Ito, 1982).

Another visible and infrared sensor is the Moderate Resolution Imaging Spectroradiometer (MODIS) designed to measure biological and physical processes on the Earth and in its atmosphere. The first MODIS was launched on NASA's Earth Observing System (EOS) satellite Terra on 18 December 1999; the second MODIS was launched on the EOS Aqua satellite on 4 May 2002. MODIS provides visible, near-infrared, and thermal-infrared imagery in 36 bands within the wavelength range of 0.4 to 14.5 μm. MODIS sea-ice products from Terra and Aqua include the areal extent and surface temperature of sea ice; the two products are available as Level 2 swath data and as Level 3 gridded data. The MODIS sea-ice extent algorithm distinguishes sea ice from open ocean based on reflective characteristics. Thermal-infrared data are used to derive ice-surface temperature (Hall and others, 2004). Global sea-ice extent and ice-surface temperature are mapped daily at 1-km pixel and 0.05-degree spatial resolutions, respectively. Eight-day composite data are available at 1-km pixel resolution and are planned for the 0.05-degree spatial-resolution product. These products are archived at NSIDC. More detailed information on MODIS sea-ice products can be obtained from the MODIS sea-ice user's guide (Riggs and others, 2003).

Active-Microwave and Laser Satellite Records

A serious limitation with visible and infrared satellite imaging is that cloud cover hinders visible and infrared radiation that is reflected by or emitted from the Earth's surface from reaching the satellite sensors. This problem has been circumvented through the development of microwave sensors—both active and passive. Furthermore, microwave sensors have the additional advantage over visible imagery of not needing daylight (solar-illumination) conditions, because microwave radiation is emitted either from the satellite instrument (in the case of active-microwave instruments) or from the Earth/atmosphere system (in the case of passive-microwave instruments).

Radar Altimeters and Scatterometers

Active-microwave sensors transmit and receive a microwave signal; users depend on surface backscatter to determine geophysical properties of the surface. These sensors include radar altimeters, scatterometers, side-looking real aperture radars (SLR or SLAR), and synthetic aperture radars (SAR). The primary difference between radar altimeters and scatterometers is that the altimeter is a nadir-pointing sensor that collects data along a narrow beam, whereas the scatterometer collects data within a swath centered on the satellite track. The primary application of these sensors has been in oceanographic

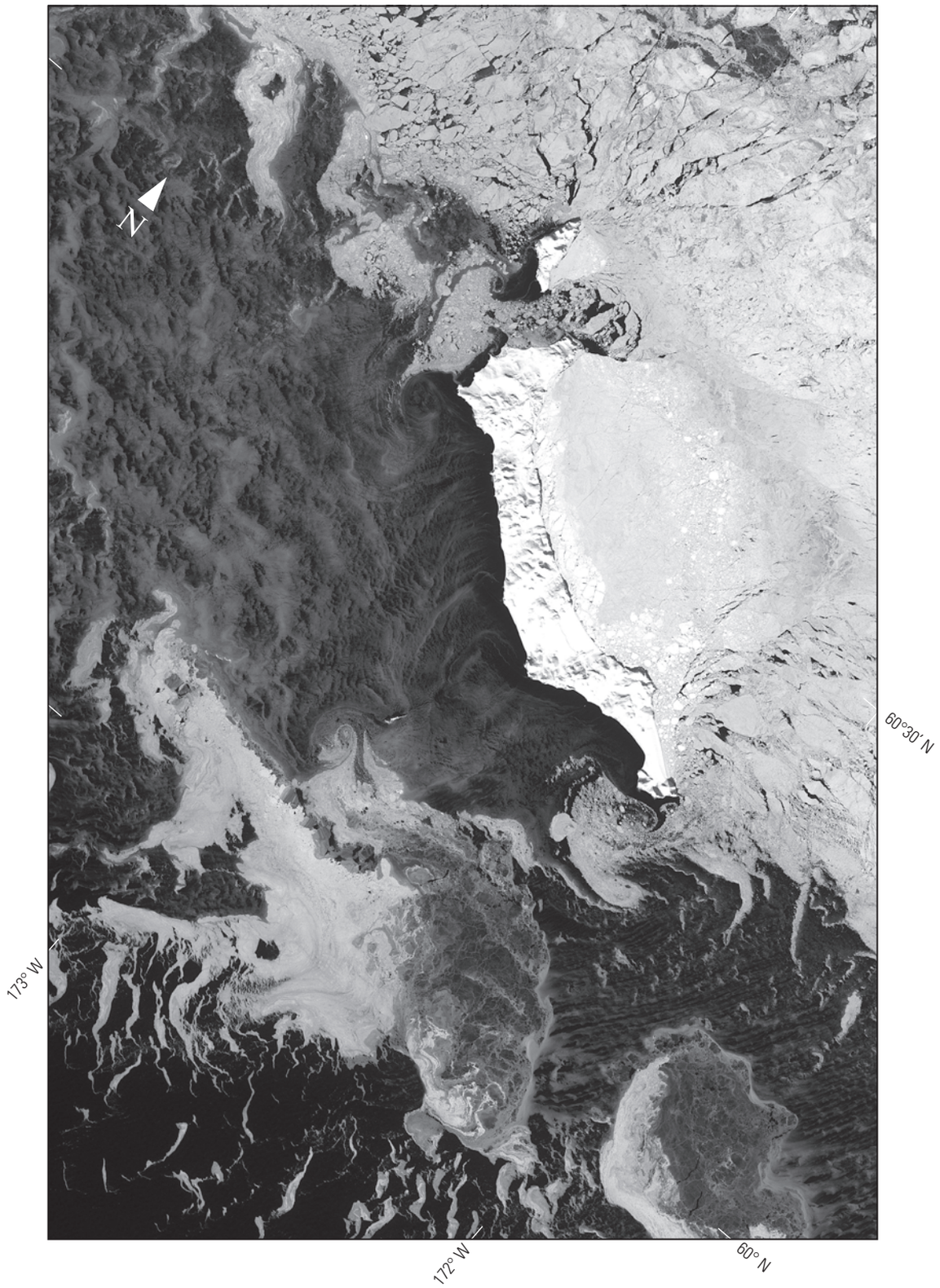

Figure 4.—*Landsat 7 Enhanced Thematic Mapper Plus (ETM+) image of St. Matthew Island, Alaska, in the Bering Sea on 13 March 2003. The image shows the detailed structure of the sea-ice edge near the island.*

studies, providing, for example, information on ocean topography and on the speed and direction of the wind directly above the ocean surface. The first spaceborne radar altimeter and scatterometer flew onboard Skylab in 1973 and 1974, but it was only after the launch of the Geodetic Earth Orbiting Satellite 3 (GEOS-3) in 1975 that sea ice was recorded by an altimeter from space. Launched in 1983, the Russian satellite COSMOS-1500 carried a real-aperture radar that was used for navigation through ice-choked waters. More recently, radar altimeters on board the European Remote Sensing (ERS) satellites ERS-1 and ERS-2 have been used to estimate sea-ice thicknesses in the Arctic region (Laxon and others, 2003).

The Seasat-A Satellite Scatterometer (SASS) operated for only 4 months after its launch in June 1978, but it provided a major impetus for using active sensors to study sea ice. Most existing sea-ice records from scatterometer data are derived from microwave scatterometers onboard the European satellites ERS-1 and ERS-2, launched in 1991 and 1995, respectively, and the Japanese Advanced Earth Observing Satellite-1 and 2 (ADEOS-1, -2), launched in 1998 and 2002, respectively. NASA's Quick Scatterometer (QuikSCAT) was launched in 1999 to provide scatterometry coverage shortly after ADEOS-1 failed. Sources of scatterometer sea-ice datasets include:

- Centre ERS d'Archivage et de Traitement [CERSAT - French ERS Processing and Archiving Facility]. CERSAT is part of the French Research Institute for Exploitation of the Sea [Institut français de recherche pour l'exploitation de la mer or IFREMER] and is the node of the European Space Agency (ESA) for archiving, processing, and validating data from spaceborne sensors. Among the products archived are Level 3 products of backscatter coefficients over sea ice for north and south polar regions, presented on polar stereographic 25-km resolution grids. From these gridded products, it is possible to calculate the areal extent of sea ice and to categorize three ice types: multiyear ice, consolidated first-year ice,[2] and marginal ice. Weekly data products are available from the Active Microwave Instrument (AMI) in its Wind Scatterometer (AMI-Wind) mode on the ERS-1 (5 August 1991–26 May 1996) and ERS-2 (25 March 1996–15 January 2001) missions; 3-day products are available from the NASA Scatterometer (NSCAT) sensor on the ADEOS-1 (19 September 1996–29 June 1997) satellite; and daily products at both 12.5-km and 25-km spatial resolutions are available from the SeaWinds sensor on the NASA QuikSCAT satellite (20 July 1999–30 June 2001) platform. In addition, 3-day and 6-day sea-ice-drift products are available for the central Arctic at a spatial resolution of 62.5 km for the winter (October–April) periods 1999–2000 through 2002–2003. Further details about these products can be found at *http://www.ifremer.fr/cersat/en/data/gridded.htm*.

- Brigham Young University (BYU) Center for Remote Sensing. The BYU Center for Remote Sensing archives Arctic and Antarctic sea-ice extents derived from QuikSCAT and NSCAT. The QuikSCAT data cover the period from 19 July 1999 to 7 June 2004 and are available in two formats: a masked image where ocean areas outside the sea-ice limit are set to the no-data value and an ASCII file containing latitude and longitude pairs corresponding to contour points on the ice edge.

[2] For an illustrated glossary of the numerous technical terms used by glaciologists to describe floating ice, including the more than two dozen terms for pack ice, the reader is referred to Armstrong and others (1973). Several of the sea-ice terms described in the glossary are used in this report.

The NSCAT data cover the period from 14 September 1996 to 28 June 1997 and consist of ice-masked Scatterometer Image Reconstruction with Filtering (SIRF) images (Long and others, 1993) along with similar ASCII files to those for the QuikSCAT data. A sea-ice motion data set derived from a merged scatterometer (QuikSCAT)/passive-microwave (Special Sensor Microwave Imager [SSMI]) product (Liu and others, 1999) also is available at BYU. The ice-motion products are available as postscript images of the ice motion and as ASCII files describing the ice-motion vectors. Further details of the BYU scatterometer sea-ice data sets can be found at *http://www.scp.byu.edu/derived.html*.

- The Physical Oceanography Distributed Active Archive Center (PO.DAAC) at the Jet Propulsion Laboratory, California Institute of Technology. PO.DAAC is the long-term archive of sigma-0 (normalized radar cross section) data from most of the spaceborne scatterometers. It also archives the following data sets from the BYU Center for Remote Sensing: daily browse images of QuikSCAT sigma-0 measurements, daily browse images of SeaWinds sigma-0 measurements, and high-resolution images of Seasat sigma-0 measurements. The Web site for PO.DAAC is *http://podaac.jpl.nasa.gov/*.

Laser Altimeters

The laser altimeter offers an improvement over radar altimeters for estimating sea-ice thickness, because it has the capability for higher spatial resolution and better precision. The first laser altimeter in Earth orbit was launched by NASA, as part of the EOS Program, on the Ice, Cloud, and land Elevation Satellite (ICESat) in January 2003. The Geoscience Laser Altimeter System (GLAS) on ICESat was launched primarily to measure ice-sheet elevations, but it also provides the potential for monitoring the third dimension of the polar sea-ice cover—ice thickness—derived from measured surface elevation (Kwok and others, 2004). Level 2 sea-ice elevation data are archived at NSIDC (Zwally and others, 2003). The ICESat mission ended in late 2009; the ICESat 2 mission is scheduled for launch in early 2016.

A European satellite named CryoSat (Wingham and others, 2006) was designed to measure the thickness variability of both land and sea ice for 3 years, using a newly designed radar altimeter. CryoSat "was intended to be the first project in ESA's Earth Explorer Programme, a series of satellites designed to collect data on global environmental issues" (Nature, v. 437, no. 7062, 20 October 2005, p. 1,078). This mission would have complemented ICESat's sea-ice elevation measurements, with a coarser spatial resolution but the advantage of being able to map ice thicknesses through cloud cover. However, CryoSat was destroyed during an unsuccessful launch attempt on a modified Russian rocket (Rockot/Breeze) on 8 October 2005. ESA approved a CryoSat 2 mission in February 2005; the satellite was launched 8 April 2010.

Synthetic Aperture Radar

Synthetic aperture radars (SARs) provide narrow-swath, very high spatial-resolution imagery. Because of their high spatial resolution and availability under dark or light and cloudy or clear conditions, SAR sensors are particularly useful for studies of sea-ice processes. Spaceborne SARs were launched by the

United States on Seasat in June 1978 and by Russia on COSMOS-1870 in July 1987. Subsequently, other SAR sensors were launched by the Europeans on ERS-1 and ERS-2, by the Japanese on the Japanese Earth Resources Satellite-1 (JERS-1), and by the Canadians on RADARSAT. The Alaska SAR Facility (ASF) at the University of Alaska, Fairbanks, is under contract to NASA to acquire, process, archive, and distribute SAR data from the European Space Agency ERS-1 and ERS-2 satellites, the Japan Aerospace Exploration Agency (JAXA) JERS-1 satellite, and the Canadian Space Agency RADARSAT-1 satellite. ASF is the primary repository of spaceborne SAR data, including derived sea-ice products.

The Geophysical Processor System at ASF produces two products based on sea-ice-type classification from the ERS-1 SAR. Sea-ice types are classified as multiyear ice, deformed first-year ice, undeformed first-year ice, and new ice/smooth open water. The two products are (1) sea-ice classification images color-coded according to sea-ice type and (2) files listing the percentage of each sea-ice type found in 5-km × 5-km image blocks.

In addition to sea-ice-type classification products, the ASF Geophysical Processor System produces and archives sea-ice motion vectors from ERS-1 SAR data. During the "ice phases" of ERS-1 operations, the satellite retraced its ground track about every 3 days, in part to facilitate the determination of sea-ice motion vectors. Each sea-ice motion product gives the initial and final latitude and longitude of an ice feature as well as its displacement in kilometers and its rotation in degrees. About 60 of these products were generated for each winter week from September 1991 until December 1994. Most of the sea-ice motion vectors are for the Beaufort Sea and the high Arctic region up to lat 85° N., although some are for the Chukchi and East Siberian Seas and a few are for areas south of lat 65° N.

Passive-Microwave Satellite Records

The most spatially and temporally complete global sea-ice data records are provided by satellite passive-microwave observations dating from 1973 to the present, especially those from November 1978 to the present. These records are used in the following "Annual Cycle of Sea Ice," "Trends in the Sea-Ice Cover," and "Interannual Variability of Sea Ice" sections of this report to describe the state of the sea-ice cover. Satellite passive-microwave records are derived from measurements of radiation emitted from within the Earth/atmosphere system and have the advantages of being equally available under nighttime and daylight conditions, typically being unaffected by most cloud cover, and being obtainable near globally at a frequency of every few days or better.

The first passive-microwave observations of the Earth's surface from space were made from the Russian COSMOS-243 satellite in 1968, with a nadir-viewing radiometer operating at frequencies of 3.5, 8.8, 22.2, and 37 GHz (Massom, 1991). The first spaceborne radiometer to produce images of the polar sea-ice cover was the Electrically Scanning Microwave Radiometer (ESMR) on NASA's Nimbus 5 satellite. The ESMR, a single-channel sensor operating at 19 GHz that was launched on 11 December 1972, provided images of the ice cover and data to determine the position of the ice edge, calculate ice extents, and calculate approximate sea-ice concentrations. The ESMR provided useful sea-ice data for most of the period from 11 December

1972 through 31 December 1976. The first sea-ice atlases based on satellite microwave imagery were created from ESMR data, for both the Antarctic (Zwally and others, 1983) and the Arctic (Parkinson and others, 1987). As the first global-scale, frequent coverage sea-ice data set, ESMR data revealed many previously unknown details, such as how uneven the annual advance and retreat of the ice are when viewed geographically and how large the differences in the spatial patterns are from one year to another (Zwally and others, 1983; Parkinson and others, 1987).

The next major advance in imaging microwave radiometers was provided by the Scanning Multichannel Microwave Radiometer (SMMR) launched on the Nimbus 7 spacecraft on 24 October 1978 (Gloersen and Barath, 1977). The SMMR overcame several limitations of the single-channel ESMR and provided more accurate retrievals of sea-ice concentration by covering a range of frequencies from 6.6 GHz to 37 GHz with dual polarization. With polarization and spectral information available, SMMR data were used to provide maps of Arctic and Antarctic sea-ice concentrations as well as the first satellite-derived maps of sea-ice type and temperature (Cavalieri and others, 1984). Based on more than 8 years of observations, from November 1978 to August 1987, a SMMR sea-ice atlas was produced that documented changes in Arctic and Antarctic sea-ice concentration, shifts of Arctic multiyear-ice distribution, and sea-ice temperature in both polar regions (Gloersen and others, 1992). However, the main ESMR and SMMR records did not overlap.

In August 1987, the Nimbus 7 SMMR stopped scanning, terminating the SMMR sea-ice record. However, this did not end the passive-microwave sea-ice record because in July 1987, a scanning microwave radiometer was launched on the operational Defense Meteorological Satellite Program (DMSP) satellite series. [DMSP was originally called the Defense System Applications Program (DSAP) and the Defense Acquisition and Processing Program (DAPP). DMSP data were declassified in December 1972, thus making past and future data available to the scientific community.] This sensor, the Special Sensor Microwave Imager (SSMI), operates at a range of frequencies from 19 GHz to 85 GHz and has been flown on several DMSP satellites since 1987. In October 2003, the first enhanced SSMI, the SSMI/Sounder (SSMIS) was launched; and as of 2012 a successor SSMIS continues to provide polar data coverage.

One of the first sea-ice applications of the DMSP SSMI data was the compilation by the Canadian Atmospheric Environment Service and the Canadian Space Agency of a Northern Hemisphere sea-ice atlas covering the period July 1987 through June 1990 (LeDrew and others, 1992). The atlas documents seasonal and interannual changes in the total sea-ice cover and first-year and multiyear ice types.

Analyses of the SMMR and SSMI satellite microwave-data records have shown substantial year-to-year variability in the polar sea-ice cover, as well as statistically significant longer term trends (see the following sections "Trends in the Sea-Ice Cover" and "Interannual Variability of Sea Ice"). In order to determine the trends, a multiyear effort was undertaken at NASA's Goddard Space Flight Center in the 1990s to blend the records of sea-ice extent from the SMMR and three SSMIs, generating a continuous, seamless sea-ice record from 1978 through 1996 (Cavalieri and others, 1997, 1999). Results from analyses of the combined SMMR/SSMI record have been published for both hemispheres (Parkinson and others, 1999; Gloersen and others, 1999; Zwally

and others, 2002). The SMMR/SSMI time series was extended further back to 1972/1973, with lesser quality data, through the combined use of the 4-year ESMR data set and a data set from the United States National Ice Center (NIC)[3] based on surface, airborne, and satellite visible, infrared, and microwave observations (Cavalieri and others, 2003). All of these time series, including hemispheric and regional sea-ice extents for both the Arctic and Antarctic, are archived at NSIDC. Other scientists also have analyzed the SMMR/SSMI record, including Johannessen and others (1995), Bjørgo and others (1997), Stammerjohn and Smith (1997), and Watkins and Simmonds (2000).

In May 1999, India launched the Indian Remote Sensing (IRS) satellite IRS P4 (also called Oceansat 1), carrying a Multi-frequency Scanning Microwave Radiometer (MSMR). MSMR provides dual-polarized images of sea ice at four frequencies: 6, 10, 18, and 21 GHz. A research group at the Indian National Centre for Antarctic and Ocean Research in Goa, India, published an atlas of Antarctic sea-ice cover based on the sharp contrast between the observed microwave brightnesses of an ice-free ocean and an ice-covered ocean for the period June 1999 through September 2001 (Vyas and others, 2004).

The next generation passive-microwave imager, the Advanced Microwave Scanning Radiometer for EOS (AMSR-E) (Kawanishi and others, 2003), was designed and built by the Japanese National Space Development Agency (NASDA, which subsequently was merged into JAXA) and was launched on NASA's Aqua satellite on 4 May 2002. AMSR-E operates at a wider range of frequencies (6–89 GHz) than either SMMR or SSMI and provides a higher spatial resolution, about twice that of the SSMI. These AMSR-E attributes have led to the development of more sophisticated passive-microwave sea-ice algorithms (Comiso and others, 2003). AMSR-E data, when combined with data from other sensors, promise to yield new information on how the polar sea-ice cover interacts with the global climate system and on the role of sea ice in climate feedback mechanisms. Coincident Arctic sea-ice images from the Aqua AMSR-E and Aqua MODIS data are shown in figure 5.

Two other passive-microwave radiometers, both launched in 2003, provide additional observations for developing improved sea-ice data records. The first is WindSat, a U.S. Navy instrument launched on the U.S. Air Force Coriolis satellite in January 2003; the second is the first (of five) Special Sensor Microwave Imager Sounder (SSMIS), launched on 18 October 2003 on a DMSP platform. WindSat is a multifrequency, polarimetric microwave radiometer designed primarily for measuring ocean surface wind vectors from space but also producing fully polarimetric data for studying other geophysical parameters, including sea ice. WindSat data are archived at PO.DAAC [*http://podaac.jpl.nasa.gov/windsat*]. The SSMIS, a joint U.S. Air Force/U.S. Navy multichannel passive-microwave sensor, replaces, enhances, and extends the imaging and sounding capabilities of the DMSP Special Sensor Microwave Temperature sounder (SSMT), SSMT-2, and SSMI microwave sensors (Poe and others, 2001). SSMIS, a conically scanning instrument, has atmo-

[3] The National Ice Center (NIC) is a multiagency operational center representing the Department of Defense (Navy), the Department of Commerce's National Oceanic and Atmospheric Administration (NOAA), and the United States Coast Guard under the Department of Homeland Security. The Web site for NIC is *http://www.natice.noaa.gov*.

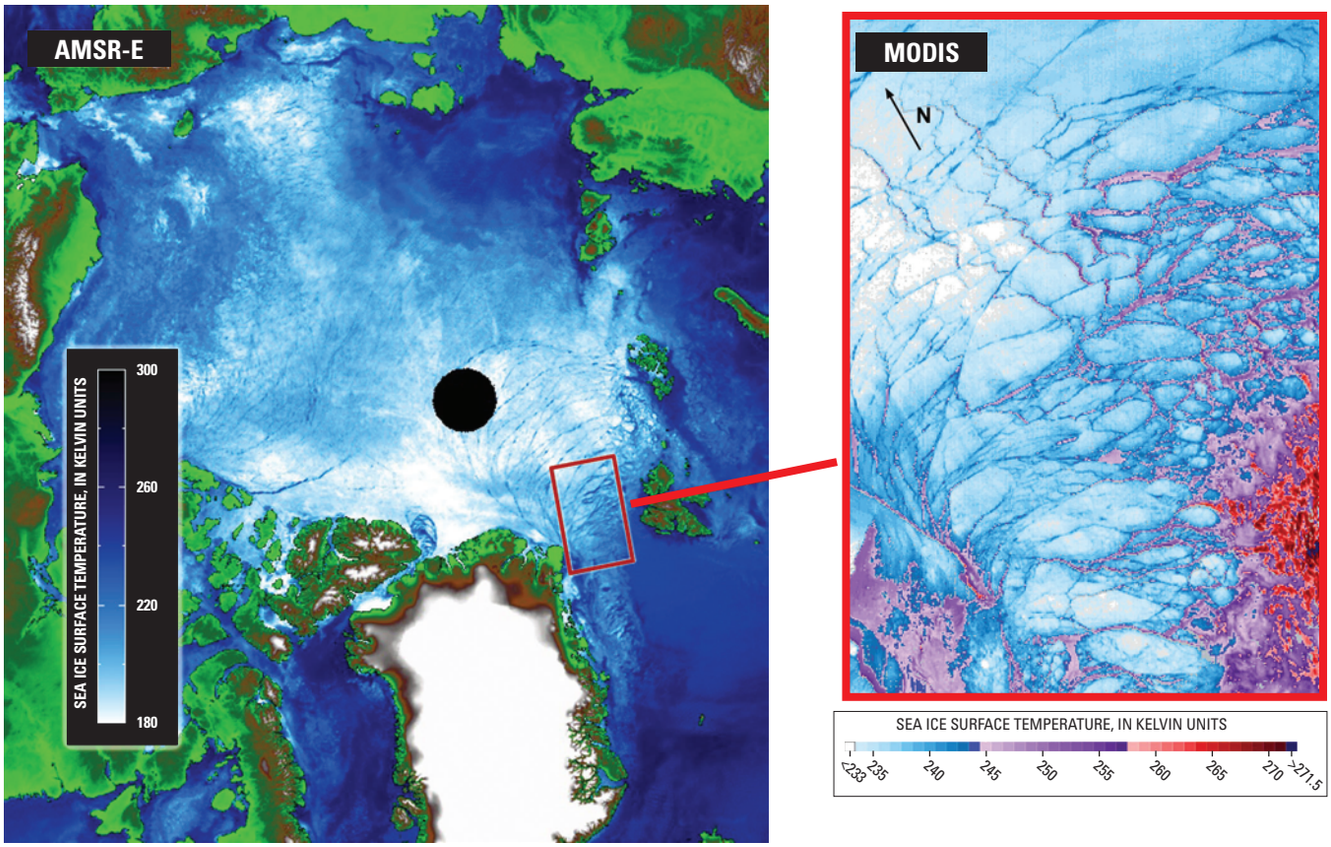

Figure 5.—*Same-day sea-ice images from microwave and visible/infrared sensors. Left: The Arctic region on 12 March 2003, as imaged from the 89-GHz vertically polarized channel of the Earth Observing System (EOS) Aqua Advanced Microwave Scanning Radiometer for EOS (AMSR-E), at a pixel resolution of 5 km. Right: Ice-surface temperature in the Fram Strait on 12 March 2003, as determined from data from the EOS Terra Moderate Resolution Imaging Spectroradiometer (MODIS). (Images from Hall and others, 2004.)*

spheric-sounding channels [Lower Atmospheric Sounding (LAS) and Upper Atmospheric Sounding (UAS)] that potentially can be used to improve atmospheric corrections to sea-ice retrievals.

In May 1994, the U.S. Congress developed a convergence plan designed to reduce the overall cost of developing and operating polar-orbiting environmental satellite systems, by merging efforts by NASA and the Departments of Defense and Commerce. This plan led to the development of the National Polar-orbiting Operational Environmental Satellite System (NPOESS) and launch of the NPOESS Preparatory Project (NPP), an interim satellite launched on 28 October 2011. NPP was renamed the Suomi National Polar-orbiting Partnership (Suomi NPP) after launch. The NPOESS partnership was dissolved in 2010 and replaced in part by a NASA/NOAA Joint Polar Satellite System (JPSS). Among the five Earth-observing imaging systems on NPP is a Visible Infrared Imaging Radiometer Suite (VIIRS), which is a MODIS follow-on instrument. In addition, in May 2012, JAXA launched AMSR-2, a follow-on to AMSR-E.

Annual Cycle of Sea Ice

To depict the state of the sea-ice cover at the start of the 21st century, while taking into account the large seasonal variations, this section provides images of sea-ice concentrations for each month of 2001 for both polar regions. These images for 2001 are accompanied by corresponding images for the 25-year monthly average data for the period from 1979 to 2003 and by graphs of the annual cycle of sea-ice extent, which is defined as the ocean area with ice concentrations of at least 15 percent (when gridded to pixels of approximately 25×25 km). This definition of sea-ice extent follows the usage in the Antarctic and Arctic sea-ice volumes by Zwally and others (1983) and Parkinson and others (1987) and many subsequent sea-ice analyses. All the images in this section are derived from the passive-microwave satellite data of the Nimbus 7 SMMR and the DMSP SSMI, using the NASA Team algorithm detailed in Cavalieri and others (1984) and Gloersen and others (1992) and the SMMR/SSMI data-set matching procedures described in Cavalieri and others (1999).

Arctic Region

Images of monthly average Arctic sea-ice concentration for each month of 2001 are presented in figure 6, and the corresponding images for the monthly averages of the 25-year period from 1979 to 2003 are presented in figure 7. The black circular region centered at the North Pole indicates missing data; because of the inclination of the Nimbus 7 and DMSP satellite orbits, respectively, the SMMR data do not extend north of lat 84.6° N. and the SSMI data do not extend north of lat 87.6° N.

As shown in figure 7, the Arctic sea-ice cover typically is close to its maximum extent in January, although it expands outward a bit further in February and March. During this January–March period, the sea-ice cover tends to be highly compact (more than 92 percent sea-ice concentration) throughout almost all of the Arctic Ocean, the Canadian Archipelago, Hudson Bay, Baffin Bay, and the Kara Sea, with ice of lesser concentrations extending well into the Sea of Okhotsk, Bering Sea, Labrador Sea, Greenland Sea, and Barents Sea. The decay of sea ice in spring and summer is apparent both in a lessening of sea-ice concentrations, starting in the marginal seas and progressing to the central Arctic, and in a marked retreat of the sea-ice edge. By the end of summer, at the minimum sea-ice extent in September, the remaining sea ice is predominantly in the Arctic Ocean, with some sea ice also remaining in the Canadian Archipelago and the Greenland Sea. In autumn and early winter, the sea-ice cover then expands outward fairly systematically to its wintertime distribution (fig. 7). Monthly sea-ice extent averaged for the 25 years ranges from a minimum of 6.8×10^6 km^2 in September to a maximum of 15.3×10^6 km^2 in March (fig. 8).

The year 2001 had basically the same annual cycle in sea-ice extent as the 25-year average (1979–2003), although some differences were apparent in every month. Among the prominent differences visible between figure 6 and figure 7: February and March 2001 had more sea ice in the Sea of Okhotsk than the 25-year average February and March; April and May 2001 had less sea ice in the Bering Sea than the average April and May; June and July 2001 had less sea ice in Hudson Bay than the average June and July; August and September 2001 had less sea ice in the Greenland Sea and lower concentration sea ice in much of the central Arctic than the average August and September;

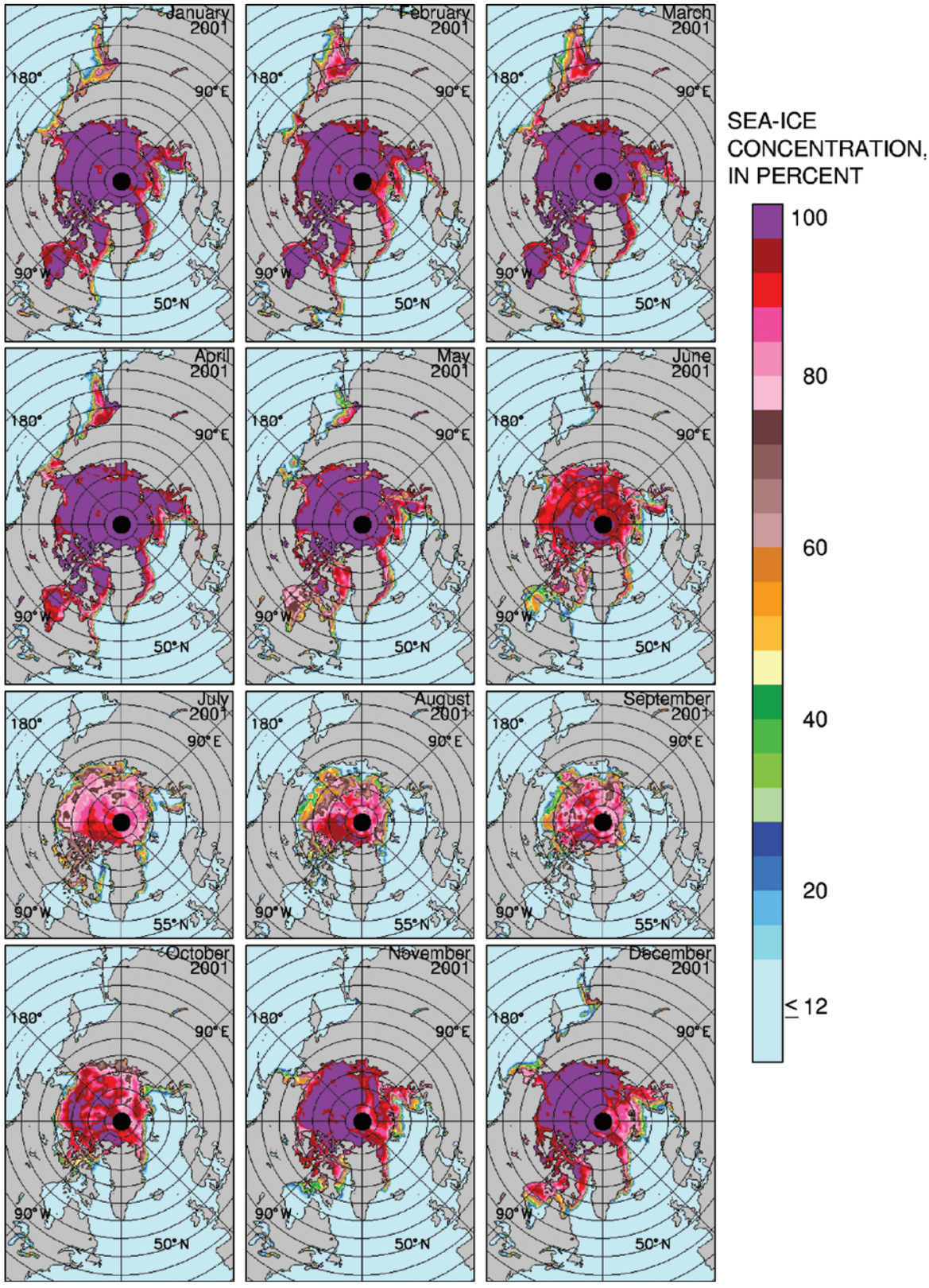

***Figure 6.**—Monthly average sea-ice concentrations in the Northern Hemisphere for January–December 2001, as derived from data from the Defense Meteorological Satellite Program (DMSP) Special Sensor Microwave Imager (SSMI).*

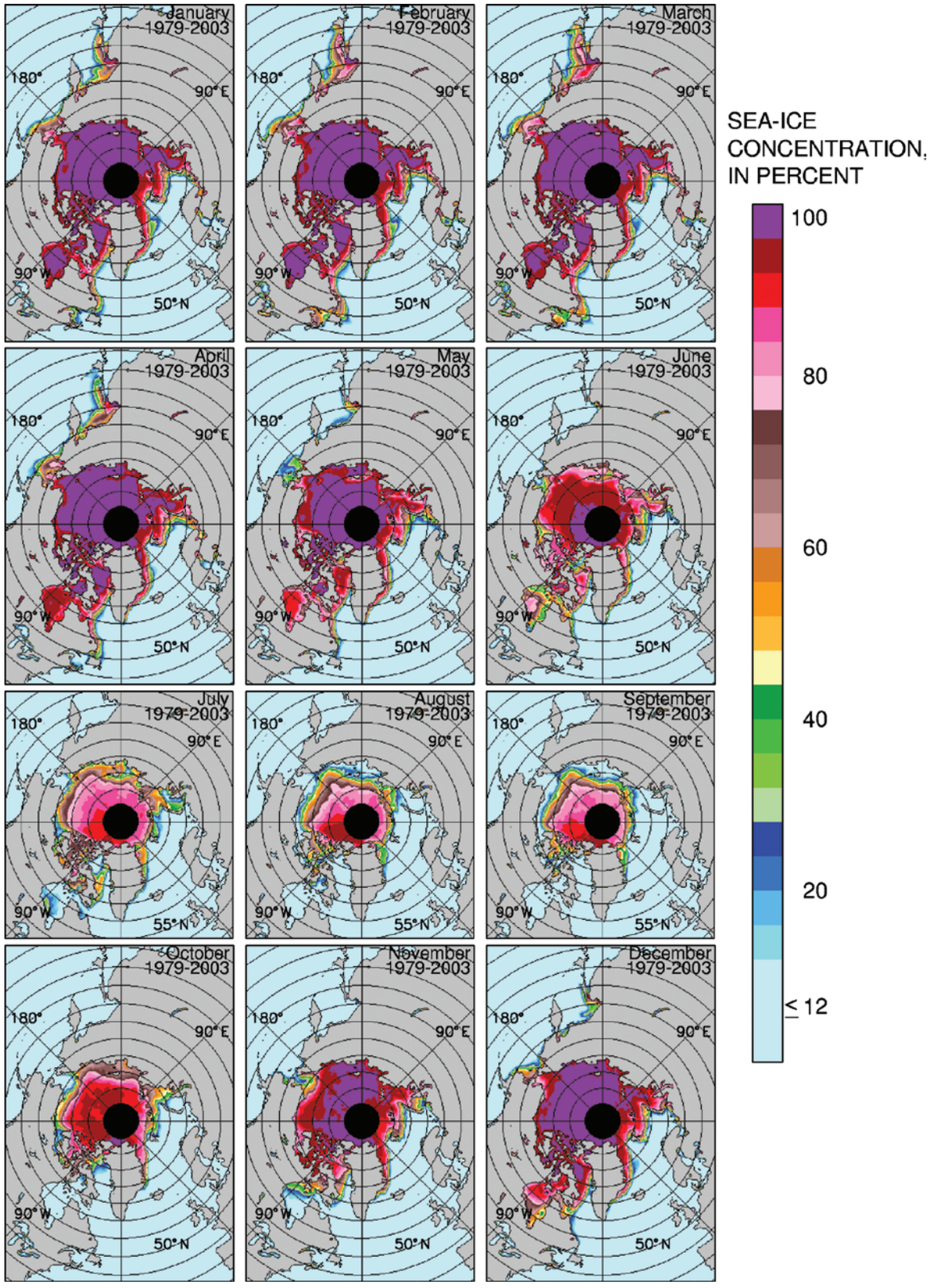

Figure 7.—*Monthly average sea-ice concentrations in the Northern Hemisphere for January–December, averaged for the 25-year period from 1979 to 2003. The sea-ice concentrations are derived from data from NASA's Nimbus 7 Scanning Multichannel Microwave Radiometer (SMMR) and the Defense Meteorological Satellite Program (DMSP) Special Sensor Microwave Imager (SSMI).*

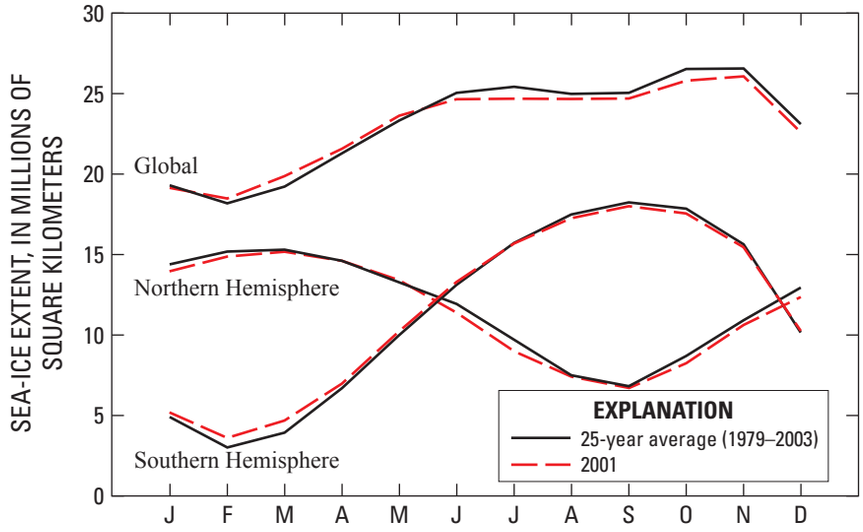

***Figure 8.**—The 2001 (dashed lines) and the 25-year average (solid lines) (1979–2003) annual cycles of monthly average sea-ice extent for the Northern Hemisphere, the Southern Hemisphere, and the total (Global).*

October 2001 had somewhat higher concentration sea ice just north of Alaska and eastern Siberia than the average October; November 2001 had somewhat more sea ice in the Bering Sea but less sea ice in the Barents Sea than the average November; and December 2001 had less sea ice in Hudson Bay than the average December.

Monthly sea-ice extent in 2001 ranged from 6.7×10^6 km^2 in September to 15.2×10^6 km^2 in March (fig. 8). Overall, monthly average sea-ice extent tended to be slightly less in 2001 than in the 25-year average. However, even in the month with the largest difference, July, the 2001 sea-ice extent (9.0×10^6 km^2) was 93 percent of the 25-year average July sea-ice extent (9.7×10^6 km^2) (fig. 8). The 2001 July sea-ice extent is outside the 1-standard deviation bounds of the average extent for the 25 Julys (9.7×10^6 km^2 $\pm$ 0.5×10^6 km^2) but not outside the 2-standard deviation bounds.

Antarctic Region

Images of monthly average Antarctic sea-ice concentration for each month of 2001 are presented in figure 9, and the corresponding images for the monthly averages of the 25-year period from 1979 to 2003 are presented in figure 10. On average, the sea-ice cover by January has retreated to the Antarctic coast at a few locations around the continent, most prominently in front of the Ross Ice Shelf; it has retreated to a greater portion of the coast by the time of its minimum, in February. The largest amount of sea ice remaining in February is in the western Weddell Sea, with much smaller but still sizable amounts of sea ice remaining in the Bellingshausen, Amundsen, and eastern Ross Seas (fig. 10).

A few sizable areas of open water (termed "polynyas") in coastal regions and internal to the ice pack are apparent in the 25-year averages for both January and February. These open-water areas generally have closed up by March, as the sea-ice cover begins its late-summer/early-autumn advance. By April, the sea ice has spread northward around much of the continent and toward the northeast in the western Weddell Sea, in conjunction with the cyclonic or Circumpolar Current (West Wind Drift), and the only part of the coast still free of sea ice is along the northwestern coast of the Antarctic Peninsula (fig. 10).

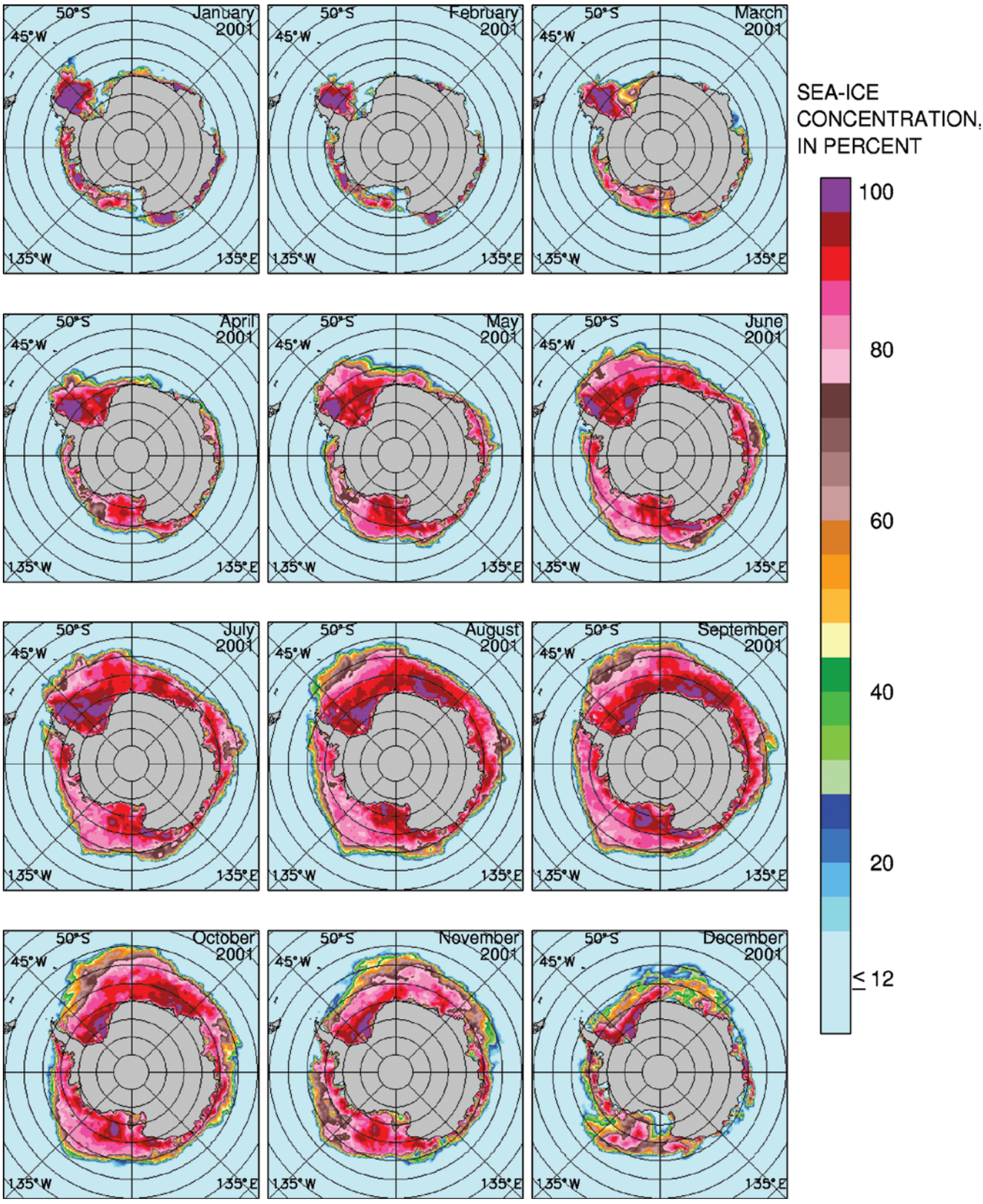

Figure 9.—*Monthly average sea-ice concentrations in the Southern Hemisphere for January–December 2001, as derived from data from the Defense Meteorological Satellite Program (DMSP) Special Sensor Microwave Imager (SSMI).*

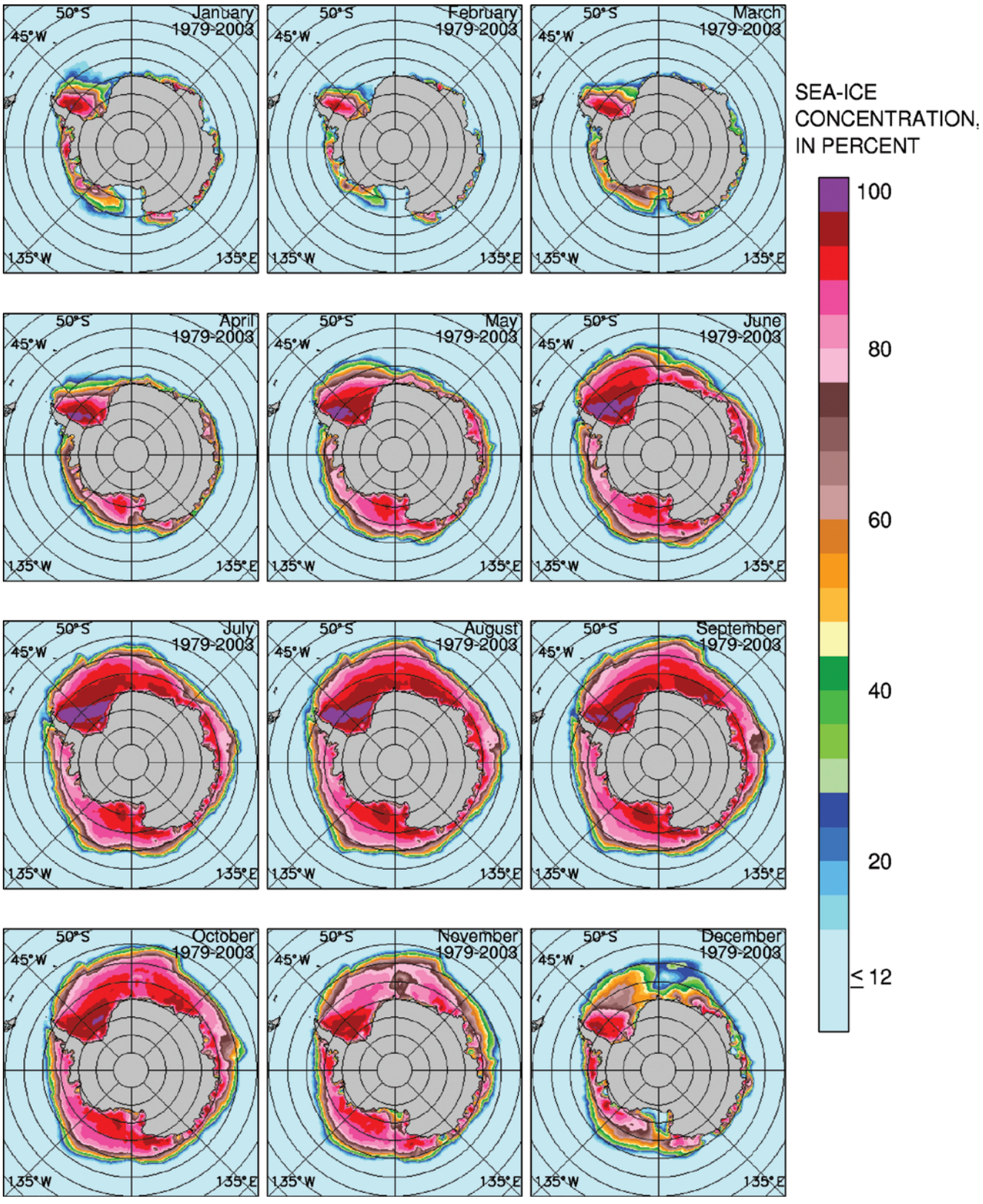

Figure 10.—*Monthly average sea-ice concentrations in the Southern Hemisphere for January–December, averaged for the 25-year interval from 1979 to 2003. The sea-ice concentrations are derived from data from NASA's Nimbus 7 Scanning Multichannel Microwave Radiometer (SMMR) and the Defense Meteorological Satellite Program (DMSP) Special Sensor Microwave Imager (SSMI).*

The sea-ice cover typically continues to expand outward from May to August, by which time it has reached lat 55° S. in the far eastern Weddell Sea and lat 60° S. to 65° S. in the Ross Sea. The sea-ice cover increases slightly from August to September, although all three months—August, September, and October—have comparably large sea-ice extents, preceding the substantial decay that takes place during the following three months (fig. 10). The minimum monthly average sea-ice extent is 3.0×10^6 km^2 in February, and the maximum is 18.2×10^6 km^2 in September (fig. 8), averaged for the 25-year period. Decay, lasting five months, is more rapid than the seven-month ice advance, in contrast to the situation in the Arctic, where the most rapid rates of change are during the growth period, particularly in September to December (fig. 8). In the Antarctic, the rates of decay are greatest from November to December and December to January, with rates of change noticeably greater than those of any other 25-year-average one-month shift in either hemisphere (fig. 8).

As with the Arctic sea-ice cover, although the basic seasonal contrast in the Antarctic sea-ice cover remains valid for each year, details of the annual cycle vary. This variation is illustrated by the contrasts between the 2001 monthly images (fig. 9) and the 1979 to 2003 average images (fig. 10). Among the clearly visible contrasts: January 2001 had a more concentrated but less expansive sea-ice cover in the western Weddell Sea than the 25-year average January; February and March 2001 had more sea ice in the western Ross Sea than the 25-year average February and March; April–June 2001 had less expansive sea ice in the Bellingshausen and Amundsen Seas than the average April–June; July and August 2001 had less expansive sea ice near the Greenwich Meridian but more expansive sea ice at about long 80° E. than the average July and August; November and December 2001 had noticeably less expansive sea ice in the western Weddell Sea but more expansive sea ice near long 45° E. and long 135° W. than the average November and December; and December 2001 also had a noticeably larger open-water area (polynya) off the Ross Ice Shelf than the average December (figs. 9, 10).

Integrating over each of the images in figures 9 and 10, sea-ice extent in 2001 tended to be somewhat larger than the 25-year average in the summer months but slightly smaller than the 25-year average in the winter months; the largest differences were in February and March (fig. 8). The February and March 2001 sea-ice extents were 3.6×10^6 km^2 and 4.7×10^6 km^2, respectively, compared to the 25-year average values of 3.0×10^6 $\pm0.3\times10^6$ km^2 and 3.9×10^6 $\pm0.4\times10^6$ km^2. This translates to the 2001 sea-ice extents being greater than the 25-year averages by approximately 20 percent in each of these 2 months and approximately at the 2-standard deviation range. The September maximum sea-ice extent in 2001 was 18.0×10^6 km^2, which is approximately 1 percent less than the 25-year average value.

The values in the two hemispheres were added together to determine global sea-ice extent. The global annual cycle is roughly in phase with the cycle in the Southern Hemisphere, reflecting the much greater range in seasonal variation of ice cover in the Southern Hemisphere than the Northern Hemisphere. The global cycle has a smaller amplitude, which is modulated by the out-of-phase nature of the two sea-ice covers (fig. 8). Global sea-ice extent averaged for the period from 1979 to 2003 ranges from a minimum of about 18.2×10^6 km^2 in February to a maximum of about 26.5×10^6 km^2 in October and November (fig. 8). Sea-ice extent in 2001 was slightly above average during February to May and slightly below average in June to December (fig. 8).

Trends in the Sea-Ice Cover

The prominent annual cycle of sea-ice cover in both polar regions tends to mask any long-term trends when time series of monthly or daily sea-ice extents are plotted. Non-0 trends do exist, however, and can become apparent through various representations of the data. In this section, results are plotted as monthly deviations and yearly, seasonal, and monthly averages. Monthly deviations are calculated for each year by taking an individual month's data and subtracting the average of that month's data for either a 25- or 26-year interval (for example, February 1983 minus the February average for 1979–2003). Because the SMMR data start at the end of October 1978, the monthly average and monthly deviation plots start with November 1978 and go through December 2003, so November and December have 26 years of data, while the other months have 25 years of data. Yearly and seasonal averages are all 25-year averages, calculated for each year 1979 to 2003 by averaging the daily average sea-ice extents.

Arctic Region

Time series of Northern Hemisphere monthly sea-ice extent for the period November 1978 to December 2003 and monthly deviations for the same time period are shown in figures 11*A* and 11*B*, respectively; yearly and seasonal averages for 1979 to 2003 are shown in figure 11*C*. The annual cycle dominates the time series of monthly averages (fig. 11*A*), but a prominent trend toward decreasing sea-ice cover becomes visible when the data are plotted as monthly deviations and yearly averages (figs. 11*B*, 11*C*). The slopes of the trend lines are -36,700 ±2,200 km^2 a^{-1} for the monthly deviations and -36,600 ±4,400 km^2 a^{-1} (-3.0 ±0.4 percent $decade^{-1}$) for the yearly averages; both trends are statistically significant, as non-0, at the 99-percent confidence level. These trends are somewhat greater in magnitude than the trends of -34,300 ±3,700 km^2 a^{-1} (for monthly deviations) and -34,000 ±8,300 km^2 a^{-1} (-2.8 percent $decade^{-1}$, for yearly averages) calculated by Parkinson and others (1999) for the same SMMR/SSMI data for the period from November 1978 to December 1996 and the -32,000 ±4,000 km^2 a^{-1} trend calculated by Bjørgo and others (1997) for the period from November 1978 to August 1995. The higher values for the period through December 2003 (fig. 11) reflect the acceleration of the downward trend in recent years. A similar acceleration is also apparent from the lower values obtained when extending the SMMR/SSMI data set backward in time through incorporation of the ESMR and NIC data sets (Cavalieri and others, 2003).

The downward trend in Arctic sea-ice extent is present in all four seasons (fig. 11*C*). The steepest seasonal slope is -46,100 ±9,300 km^2 a^{-1} (-5.4 ±1.1 percent $decade^{-1}$) for summer, but even the slope with the smallest magnitude, at -28,300 ±5,100 km^2 a^{-1} (-1.8 ±0.3 percent $decade^{-1}$) for winter, is statistically significant at the 99-percent confidence level, as are the other three seasonal trend values.

The downward trend in Arctic sea-ice extent revealed by the satellite data (fig. 11) seems to be accompanied by a decrease in ice thicknesses (Rothrock and others, 1999; Wadhams and Davis, 2000). However, the ice-thickness information has come largely from in-situ and submarine measurements. Data from both of these sources are spotty in time and space, and some studies have found the data insufficient to conclude either upward or downward trends

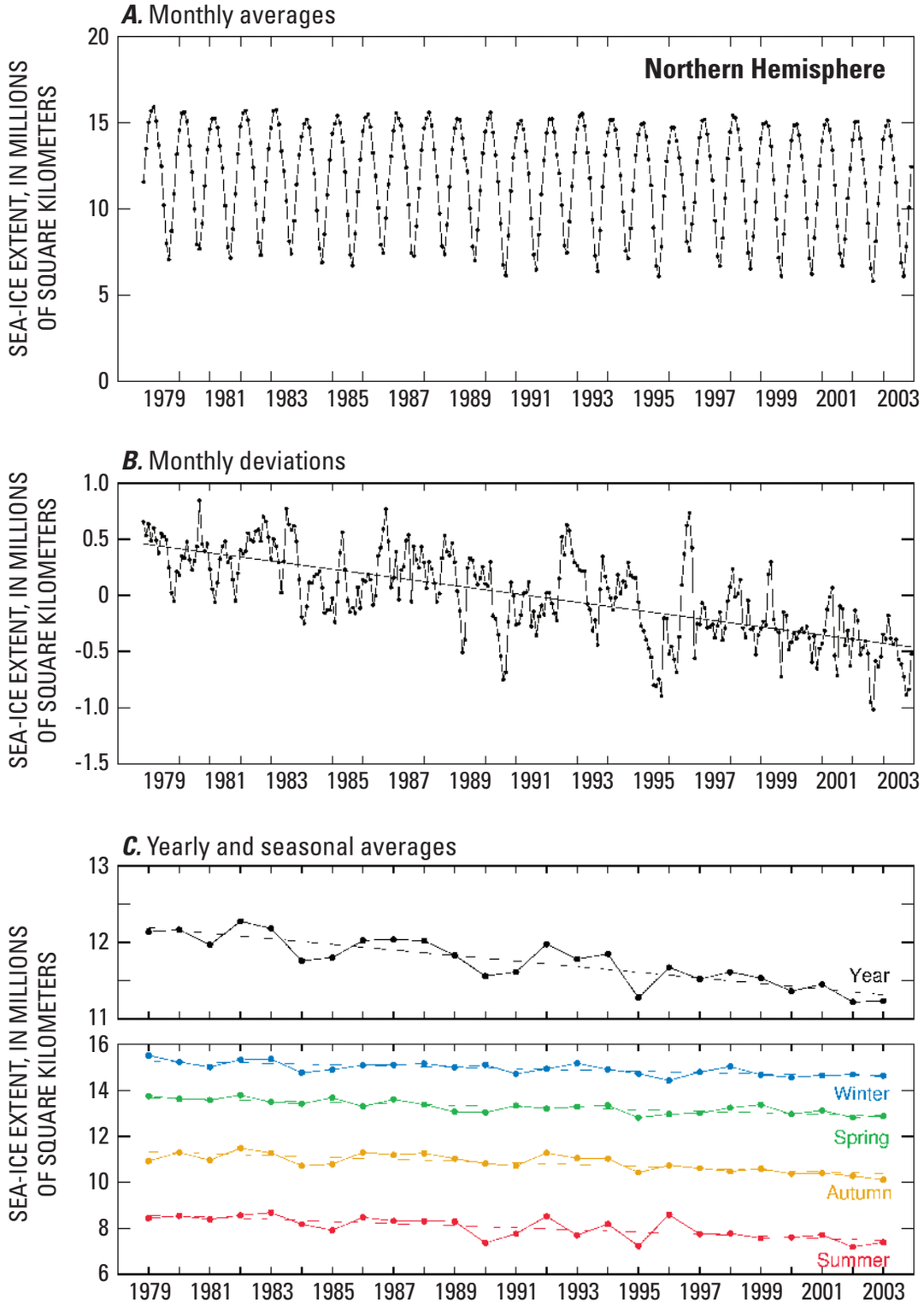

Figure 11.—**A**, *Monthly average sea-ice extent in the Northern Hemisphere, November 1978–December 2003.* **B**, *Deviations in monthly sea-ice extents in the Northern Hemisphere, November 1978–December 2003.* **C**, *Yearly and seasonal average sea-ice extents in the Northern Hemisphere, 1979–2003. Winter is averaged for January–March; spring is averaged for April–June; summer is averaged for July–September; and autumn is averaged for October–December. All values are derived from data from NASA's Nimbus 7 Scanning Multichannel Microwave Radiometer (SMMR) and the Defense Meteorological Satellite Program (DMSP) Special Sensor Microwave Imager (SSMI). (Updated from Parkinson and others, 1999.)*

(McLaren and others, 1992, for the North Pole for 1977–1990; Winsor, 2001, for the Arctic during the 1990s). In an early study on ice thicknesses, based on observations in late winter 1971 from upward-looking echo sounders on the nuclear-powered submarine H.M.S. *Dreadnought*, Swithinbank (1972) determined a mean sea-ice thickness of 2.6 m along survey tracks under the Arctic Ocean; he also noted (Swithinbank, 1972, p. 246), based on data prior to 1972, that "There is no evidence of secular changes in the mean thickness of the Arctic Ocean pack ice." Analysis of additional submarine data and eventual development of a long-term ice-thickness data set from satellite altimetry (Laxon and others, 2003; Zwally and others, 2003; Wingham and others, 2006) should help establish a more definitive record of changes in sea-ice thickness.

Antarctic Region

Time series of monthly sea-ice extent in the Southern Hemisphere for the period November 1978 to December 2003 and monthly deviations for the same period are presented in figures 12*A* and 12*B*; yearly and seasonal averages for 1979–2003 are shown in figure 12*C*. The monthly averages highlight the prominent annual cycle (fig. 12*A*), and the monthly deviations and yearly averages show the trend toward increasing sea-ice cover (figs. 12*B*, 12*C*, respectively). The positive trends, at 11,200 ±3,100 $km^2\ a^{-1}$ for the monthly deviations and 11,700 ±5,400 $km^2\ a^{-1}$ (1.0 ±0.5 percent $decade^{-1}$) for the yearly averages are less than a third of the magnitude of the corresponding negative trends in the Arctic, although the trends are still statistically significant, with confidence levels of 99 percent for the monthly deviations and 95 percent for the yearly averages.

Seasonally, the Southern Hemisphere sea-ice cover shows upward trends in sea-ice extent for the 1979 to 2003 period in each of the four seasons, although none at a statistically significant level. The largest positive trend is for autumn, at 22,600 ±12,500 $km^2\ a^{-1}$ (2.3 ±1.3 percent $decade^{-1}$) (fig. 12*C*).

The overall upward trend in sea-ice coverage in the Antarctic since November 1978 has been reported by Stammerjohn and Smith (1997) for the period 1979 to 1994, by Cavalieri and others (1997) and Watkins and Simmonds (2000) for the period November 1978 to December 1996, and by Zwally and others (2002) for the period November 1978 to December 1998. This upward trend was preceded by sharp declines in the Antarctic sea-ice cover during the 1970s (Kukla and Gavin, 1981). In fact, the declines in the 1970s were so large that when the SMMR/SSMI data record is extended back to 1973 through incorporation of ESMR and NIC data, the overall 1973 to 2002 trend in Antarctic sea-ice extent is downward, not upward like the 1979 to 2003 trend (Folland and others, 2001; Cavalieri and others, 2003). The Antarctic sea-ice cover declined markedly in the 1970s and has slowly been rebounding since the late 1970s, although it has not yet rebounded to its 1973 to 1975 levels.

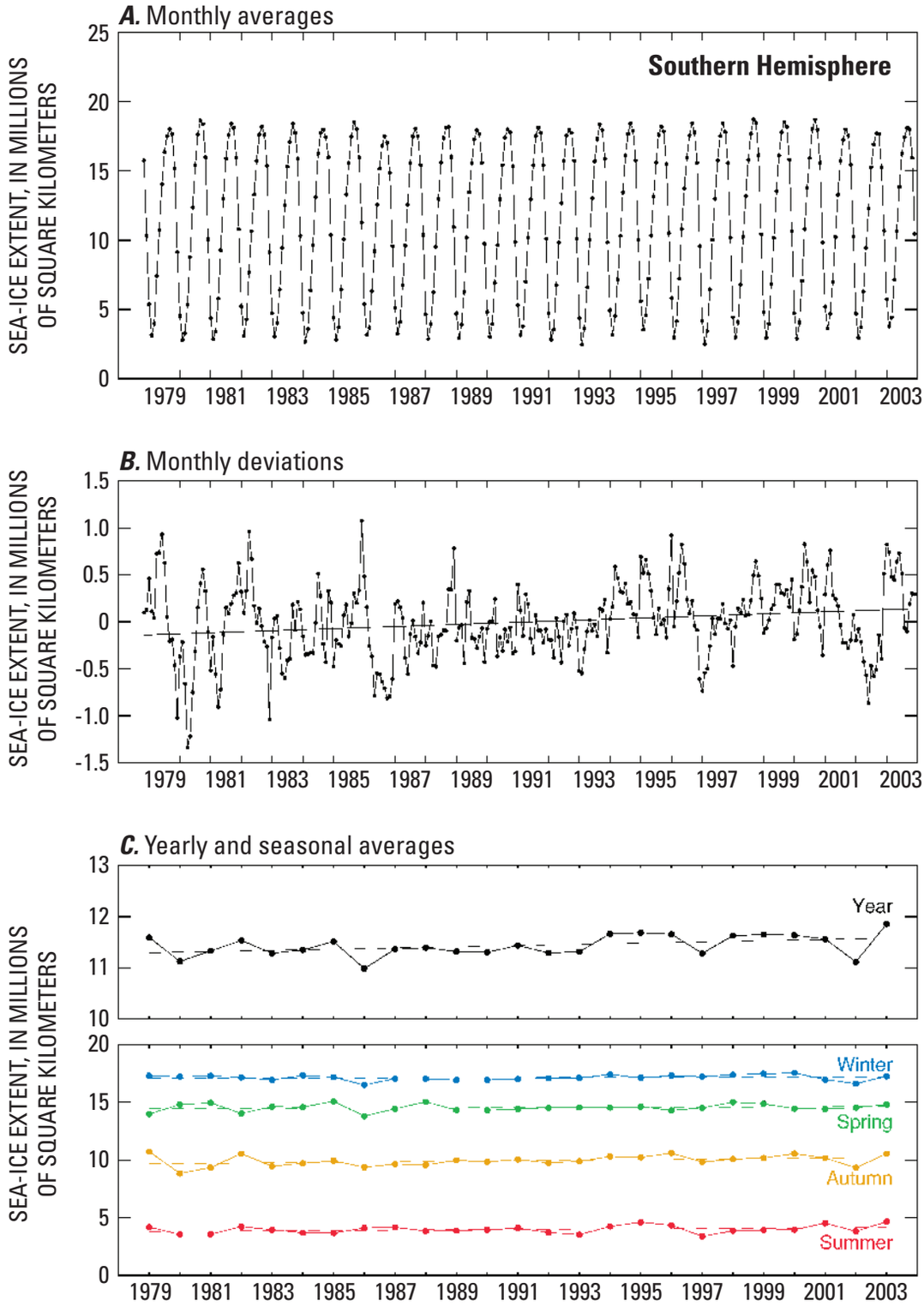

***Figure 12.*—A**, *Monthly average sea-ice extents in the Southern Hemisphere, November 1978–December 2003.* **B**, *Deviations in monthly sea-ice extents in the Southern Hemisphere, November 1978–December 2003.* **C**, *Yearly and seasonal average sea-ice extents in the Southern Hemisphere, 1979–2003. Summer is averaged for January–March; autumn is averaged for April–June; winter is averaged for July–September; and spring is averaged for October–December. All values are derived from data from NASA's Nimbus 7 Scanning Multichannel Microwave Radiometer (SMMR) and the Defense Meteorological Satellite Program (DMSP) Special Sensor Microwave Imager (SSMI). (Updated from Zwally and others, 2002.)*

Interannual Variability of Sea Ice

In addition to the statistically significant overall trends in the Arctic and Antarctic sea-ice extent, considerable non-uniform interannual variability is present in both hemispheres, and this is true for each month of the year. The interannual variability is illustrated in this section with a complete set of sea-ice cover images in early summer for both hemispheres (July in the Northern Hemisphere, January in the Southern Hemisphere) for the 25-year period 1979 to 2003.

Arctic Region

Images of July sea-ice concentrations in the Northern Hemisphere in each year of the period 1979–2003 are presented in figure 13. Examination of the images shows interannual variability throughout the Arctic and no steady direction of change (toward increasing or decreasing sea-ice covers) through the 25 years. In Hudson Bay, which typically has a nearly complete sea-ice cover in winter (figs. 6, 7), sea ice with concentrations of at least 44 percent covered a sizable part of the bay in July 1992, much of the southern coastal area in July 1982, 1985, 1986, 1994, 1995, and 2000, but almost none of the bay in July of most of the other years, with some Julys (1998, 1999, and 2001) showing practically no sea ice of any concentration (fig. 13). The Kara Sea has a similar variability, with, for instance, July 1995 having practically no sea ice and July 1987 and 1999 having ice of at least 44-percent concentration throughout the sea (fig. 13). Similar variability can be seen in the other marginal seas and bays as well.

Areas of open water (polynyas) within the sea-ice cover appear in each of the 25 images of figure 13, and, although almost all of the polynyas are in coastal locations, their sizes and locations differ widely. All years except 2000 show a polynya just north of Canada centered in the longitude range 120–135° W. just east of Mackenzie Bay (east of the border between Alaska and Canada), but its size ranges from only a few pixels (approximately 25 km × 25 km each) in some years to a considerable area in 1998, when it covered 4° of latitude and more than 20° of longitude. Along the northern coast of Asia, 1990 stands out as having the most sizable areas of open water in July, and 1996 stands out as having the most compact ice. The most famous Arctic polynya, the North Water Polynya just west of Greenland at latitudes 75–79° N., is visible in July of several years (for example, 1979, 1980, 1998) but has broken out to become part of the open water extending to the North Atlantic Ocean in other years (1985, 2000, 2002, 2003) (fig. 13).

Antarctic Region

Images of January sea-ice concentrations in the Southern Hemisphere in each year for the period from 1979 to 2003 are presented in figure 14. As in the Arctic, all regions show significant interannual variability. In the western Weddell Sea, some Januarys show a prominent northeastward extension of the sea ice, indicative of the influence of the clockwise Weddell Gyre (1979, 1980, 1989, 1995, 1996, 2001, and 2003), but other years do not show this influence (for example, 2002). The years 1980 and 1998 are noted for the lack of January sea ice in the southernmost part of the western Weddell Sea, despite considerable sea ice further north (fig. 14).

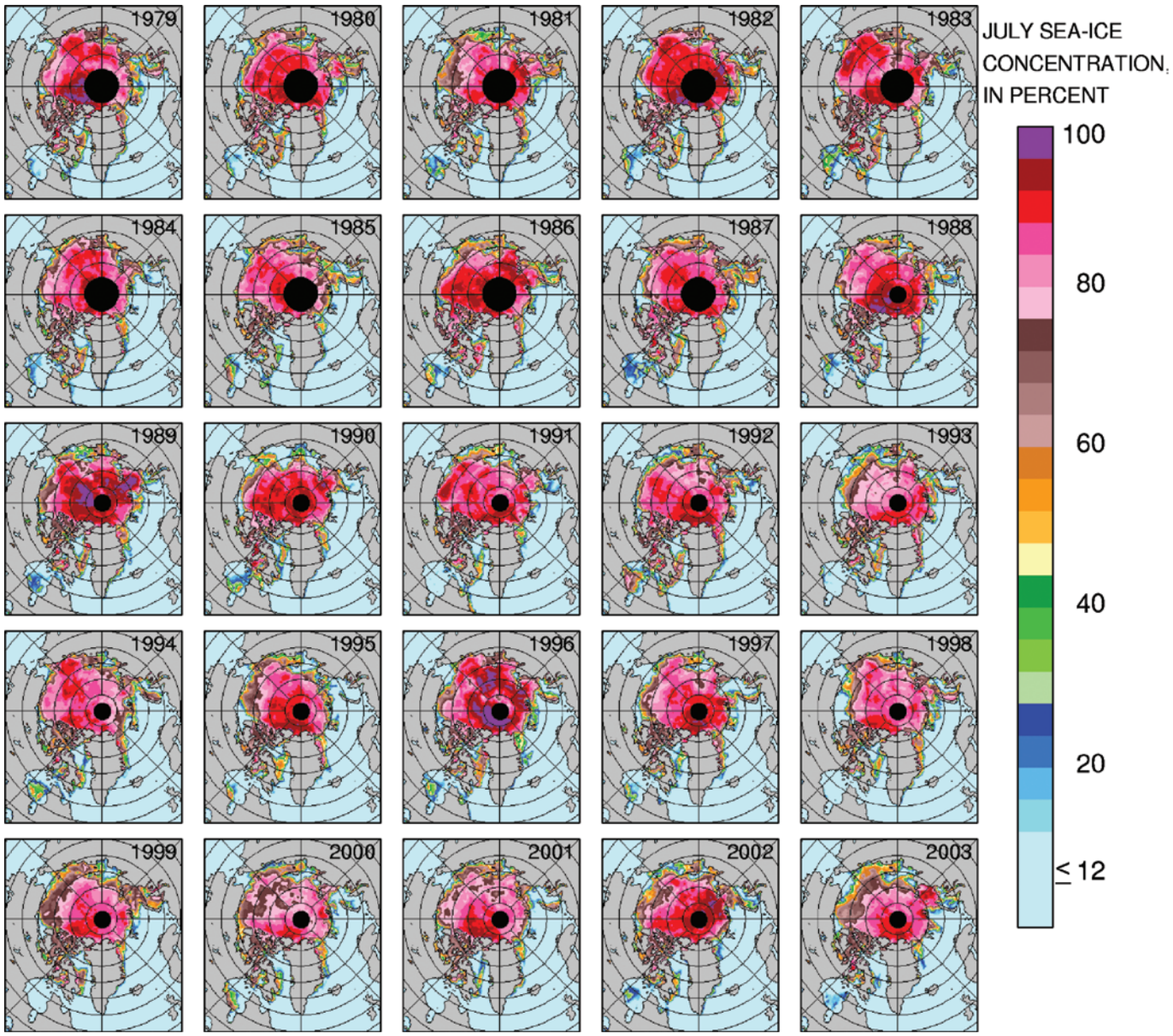

Figure 13.—*Monthly average July sea-ice concentrations in the Northern Hemisphere for each year in the period from 1979 to 2003, as derived from data from NASA's Nimbus 7 Scanning Multichannel Microwave Radiometer (SMMR) and the Defense Meteorological Satellite Program (DMSP) Special Sensor Microwave Imager (SSMI).*

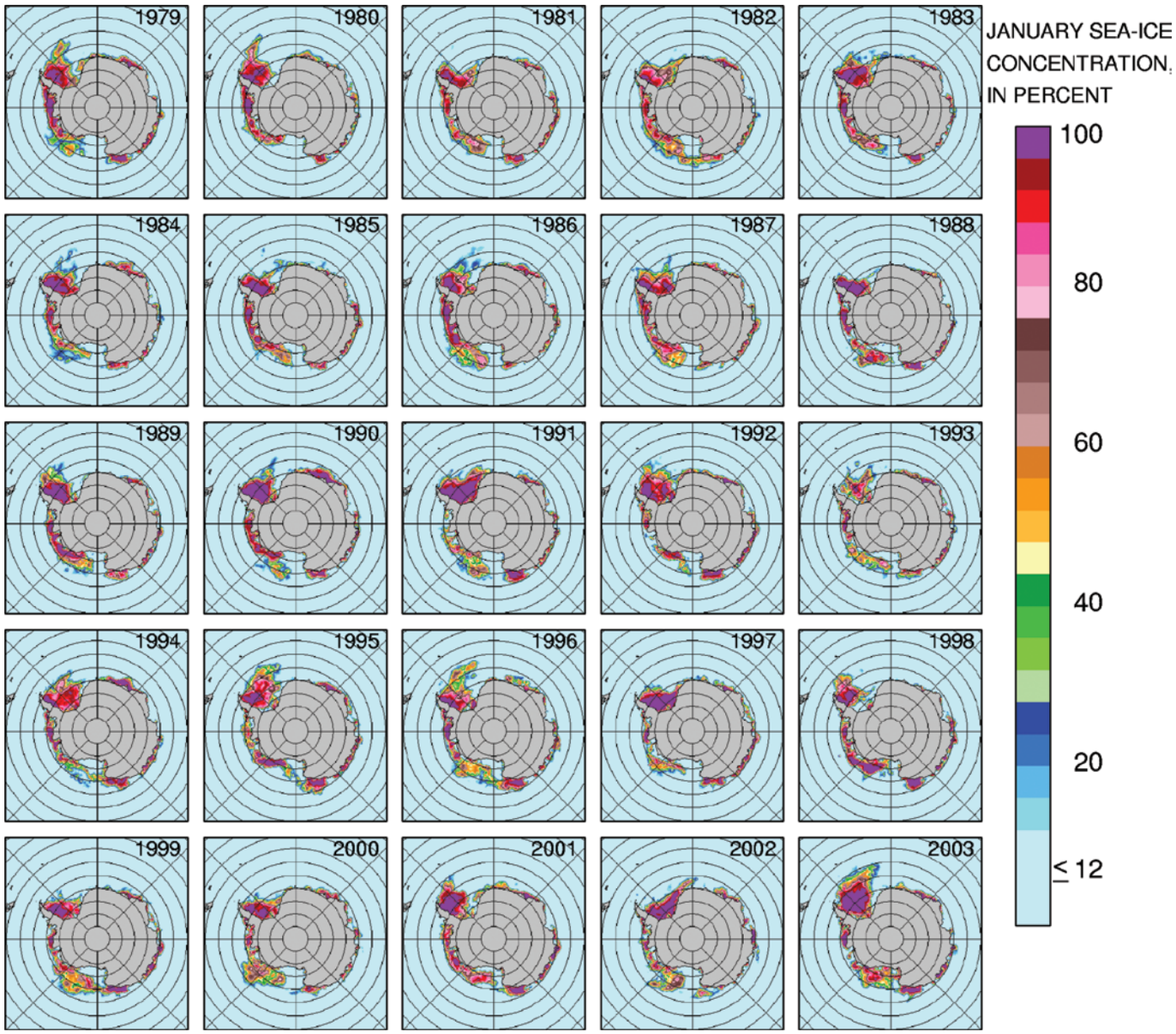

Figure 14.— *Monthly average January sea-ice concentrations in the Southern Hemisphere for each year in the period from 1979 to 2003, as derived from data from NASA's Nimbus 7 Scanning Multichannel Microwave Radiometer (SMMR) and the Defense Meteorological Satellite Program (DMSP) Special Sensor Microwave Imager (SSMI).*

In the sector encompassing the Bellingshausen and Amundsen Seas, which is noticeably "bucking the trend" toward increased Antarctic sea-ice cover (Jacobs and Comiso, 1997; Stammerjohn and Smith, 1997; Parkinson, 2002; Zwally and others, 2002), January sea ice is seen in 1979, 1980, and 1987 along almost the entire length of the western coast of the Antarctic Peninsula, whereas this coast is largely free of ice in 1989 to 1991 and 1999. The sea-ice cover in the Amundsen Sea has coastal polynyas of various sizes in most Januarys, but in January of 1992 and 2003, the sea-ice cover had retreated to the point where open water extended unhindered from the coast northward (fig. 14).

A larger polynya than the ones in the Amundsen Sea typically is present off the Ross Ice Shelf in December. This polynya typically forms in either November or December (figs. 9, 10) through the mechanism of winds or ocean currents pushing the ice northward (Bromwich and Kurtz, 1984). Often by January this polynya has broken out to join with the open water to the north. In the period from 1979 to 2003, several January averages show a continuing polynya (for example, 1982, 1996, 1999), whereas others show a small breaking out of the earlier polynya to the open ocean (for example, 1988, 1993), and many show a complete break out to the open ocean (including 1979, 1980, 1986, 1987, 1990, 1997, 2002). The final January of the record, in 2003 (fig. 14), in contrast to all others, shows a substantial sea-ice cover remaining adjacent to the ice shelf and only a relatively small polynya, perhaps due to a large tabular iceberg in the area.

These interannual variabilities in both hemispheres are connected to variabilities of the atmosphere and ocean. In the next section, we highlight a sampling of the many studies that have attempted to explain the variability of the sea-ice cover by relating it to various regional climatic oscillations and other factors in the global climate system.

Sea Ice in the Context of the Global Climate System

Satellite records provide considerable information about polar sea-ice covers, including details about the seasonal cycle, the interannual variability, which is much greater than previously recognized, and the statistically significant 25-year trends. Because sea ice is an active component of the global climate system that affects and is affected by the oceans and atmosphere, its variability and trends are almost surely closely related to variability and trends in the rest of the system. This interconnectedness is well reflected in the reports of the Intergovernmental Panel on Climate Change (IPCC), where sea ice and its changes are presented as integral elements of the global climate system and climate change (for example, Cubasch and Cess, 1990; Folland and others, 1990, 2001; Stocker and others, 2001). Quantifying the changes, however, has proven to be challenging.

Arctic Region

The decrease in Arctic sea-ice cover during the past several decades (for example, see fig. 11 for decreases during the period from 1979 to 2003) has generated particular attention because of possible connections with global climate warming (Vinnikov and others, 1999), more specifically Arctic temperature increases (Chapman and Walsh, 1993), and because of possible impacts on polar wildlife (Stirling and Derocher, 1993; Gradinger, 1995) and humans (Arctic Climate Impact Assessment, 2004). Vinnikov and others (1999) used a 5,000-year run of the NOAA Geophysical Fluid Dynamics Laboratory (GFDL) global climate model (GCM) to calculate that, based on "natural variability" as simulated by the GFDL GCM, the probability of obtaining as large a trend as the satellite-derived decrease in Arctic sea-ice extents for the period from 1978 to 1998 is less than two percent, if only natural variability is considered. Chapman and Walsh (1993) found the observed sea-ice variations and their spatial patterns to be compatible with the 1961–1990 record of temperature changes, which show warming over most of the Arctic but cooling in and near southern Greenland. Overall, average Arctic temperatures are thought to have increased during the past 100 years at a rate almost twice that for the Earth as a whole (Alley and others, 2007). The Arctic Climate Impact Assessment (2004) and other reports (Ainley and others, 2003; Derocher and others, 2004) raised concerns regarding the continued viability of the Arctic polar bear (*Ursus maritimus*) and other wildlife populations should the current warming and decreasing sea-ice coverage continue.

Despite the difficulties caused by the brevity of the satellite record and the incompleteness of the pre-satellite record, many studies have suggested possible long-term oscillatory behaviors in the Arctic sea-ice cover, related to oscillatory processes in the atmospheric and oceanic systems. In particular, connections have been made between the sea-ice cover and the North Atlantic Oscillation (NAO) (the large-scale fluctuation in atmospheric pressure between the high-pressure system near the Azores and the low-pressure system near Iceland) (Hurrell and van Loon, 1997; Johannessen and others, 1999; Kwok and Rothrock, 1999; Deser and others, 2000; Kwok, 2000; Parkinson, 2000; Vinje, 2001), the spatially broader Arctic Oscillation (Deser and others, 2000; Wang and Ikeda, 2000), the Arctic Ocean Oscillation (AOO) (Polyakov and others, 1999; Proshutinsky and others, 1999), and an interdecadal Arctic climate cycle (Mysak and others, 1990; Mysak and Power, 1992).

Of the oscillations, the NAO has received the most attention. The NAO index often is calculated as the normalized atmospheric pressure at Lisbon, Portugal, minus the normalized atmospheric pressure at Stykkishólmur, Iceland. The NAO index was positive, with strong Azores High and Icelandic Low pressure systems, during the 1980s and early 1990s (Hurrell, 1995), resulting in strong southwesterly winds across the northern North Atlantic between Iceland and Norway and strong north winds over Baffin Bay and to its south. The former winds brought warm air to the Barents and Kara Seas and the central Arctic, and the latter brought cold air to Baffin Bay and the Labrador Sea, consistent with the pattern of temperature trends found by Chapman and Walsh (1993). During the 1980s, as the NAO index increased, sea-ice extent to the east and north of Greenland tended to decrease, and sea-ice extents to the west of Greenland, in Baffin Bay, in the Labrador Sea, and in Hudson Bay, tended to increase. During the 1990s, as the NAO index decreased, sea-ice extents to the east and north of Greenland tended to increase and those to the west of Greenland tended to decrease (Parkinson, 2000). Although the overall summary is convincing of a sea ice/NAO connection, the reality of the large interannual variability in sea ice and the brevity of the record makes the results only suggestive; a longer data set and further research are needed before the connection can be fully established and understood (Parkinson, 2000).

Most of the studies described here are restricted to the past few decades. In analyzing the longer 1901 to 1997 period, through incorporating limited pre-satellite data, Walsh and Chapman (2001) conclude that the Arctic sea-ice extent has decreased substantially during the 20th century, with the summer season experiencing the largest decreases. They further find the leading mode of wintertime variability to be dominated by a pattern consistent with forcing by the NAO (Walsh and Chapman, 2001).

Antarctic Region

The modes of atmospheric variability in the Southern Hemisphere include both symmetric and asymmetric patterns, and both patterns have been examined for their effect on the sea-ice cover. A large-scale, nearly zonally symmetric mode called the Southern Annular Mode (SAM), or the Antarctic Oscillation (AO), is characterized by an alternation of atmospheric mass between middle and high southern latitudes (Rogers and van Loon, 1982). The SAM dominates atmospheric circulation (Carleton, 2003) and influences the upper Southern Ocean circulation more than it affects the Antarctic sea-ice cover (Lefebvre and others, 2004), although evidence exists suggesting that extremes in the Antarctic sea-ice cover might affect atmospheric circulation during the summer, in particular such that the SAM tends toward positive polarity under minimum sea-ice cover (Raphael, 2003). Model simulations suggest the SAM can generate sea-ice variations on interannual to centennial time scales (Hall and Visbeck, 2002), although Lefebvre and others (2004) find no connection between the long-term trends in the Antarctic sea-ice cover and the SAM index.

Asymmetric modes of atmospheric variability near Antarctica include atmospheric long waves having wave numbers 1 through 4. A typical wave 1 pattern is zonally asymmetric with areas of high and low temperature or pressure approximately 180 degrees of longitude apart. A typical wave 2 pattern has two high and two low areas alternating around the continent. A domi-

nant wave 1 pattern is observed in mean monthly surface air temperatures and results from the existence of generally colder temperatures off the coast of East Antarctica than around the rest of Antarctica. The temperature asymmetry results directly from the zonally asymmetric position of the Antarctic continent itself. In a study of one sample year, Cavalieri and Parkinson (1981) found that the first three wave numbers explained most of the variance in the 3-day averaged ice extent and atmospheric pressure fields but that the first four wave numbers were required to explain most of the variance in the sea-level pressure field.

Many of the observed connections between atmospheric modes of variability and the Antarctic sea-ice cover are regional in nature and are dominant in the Amundsen, Bellingshausen, and Weddell Seas sectors (Yuan and Martinson, 2000; Stammerjohn and others, 2003). This results, at least in part, from the effect of the tropical El Niño/Southern Oscillation (ENSO) (the combined effect of warmer than average sea-surface temperature and changes in air pressure in equatorial regions of the eastern Pacific Ocean). For example, Stammerjohn and others (2003) found possible connections between sea-ice extent in the western Antarctic Peninsula region and ENSO changes in the tropical Pacific, and Kwok and Comiso (2002) found significant retreats in the sea-ice cover in the Amundsen and Bellingshausen Seas to be associated with four ENSO events during the 17-year period from 1982 through 1998. ENSO events typically occur every 2 to 7 years. In a study of coupled oscillations in Antarctic sea ice and the atmosphere over the South Pacific, Venegas and others (2001) found interannual oscillations with 3- to 6-year periods to have dominated wintertime sea ice and atmosphere variability in the Bellingshausen, Amundsen, and Ross Seas during the period from 1979 to 1998. This result is consistent with the earlier work of Gloersen (1995), who showed statistically significant periodicities in both the Antarctic sea-ice cover and the ENSO index but considerable variability in the sea-ice response for different regions. In particular, Gloersen (1995) found a dominant quasi-quadrennial period of about 4.2 years in the Weddell Sea, a strong biennial component in the Bellingshausen and Amundsen Seas sector, and a strong quasi-triennial component in the Ross Sea sector.

In a theoretical modeling study, Rind and others (2001) found that El Niño events should lower sea-ice cover in the Pacific portion of the Southern Ocean. Using data from approximately 18 years of observations, Yuan and Martinson (2000) found that up to 34 percent of the variance observed in sea-ice extent is linearly related to ENSO but that even higher correlations exist between anomalies in sea-ice edge and tropical Pacific Ocean precipitation and sea-surface temperature in the Indian Ocean. They further found that correlations between anomalies in sea-ice edge and global surface temperature produce four significant correlation patterns, with some patterns extending into the tropics and the Northern Hemisphere.

The variations of the atmospheric long waves are an integral part of many hypothesized and observed sea-ice/atmosphere connections. Among the identified patterns are a wave 1 pattern that is represented by an oscillation in pressure between the Weddell Sea and East Antarctica sectors and a wave 2 pattern that is strongest in the Pacific Ocean and southwestern Atlantic Ocean sectors, perhaps influenced by the ENSO (Carleton, 2003). The wave 2 pattern manifests itself as the Antarctic Circumpolar Wave observed in a range of variables in the ice-ocean-atmosphere system (White and Peterson, 1996; Olbers and others, 2004). Also tied to the ENSO, a quasi-stationary wave in the southern

high latitudes, with centers in the Atlantic and Pacific Oceans, has been identified and named the Antarctic Dipole by Yuan and Martinson (2000, 2001), who found that the Antarctic Dipole exhibits high temperatures and low sea-ice amounts in the Pacific Ocean and low temperatures and larger sea-ice amounts in the Atlantic Ocean during an El Niño and the opposite conditions during a La Niña (see also Yuan, 2004, for an overview of the connections among the Antarctic Dipole, ENSO, and Antarctic sea ice). Other research suggests that a quasi-stationary atmospheric wave 3 pattern dominates the winter season and strongly affects the distribution of wintertime sea ice (Yuan and others, 1999).

The physical mechanisms explaining the interconnections between the sea-ice cover and the rest of the climate system are not fully understood for either polar region. Among the fundamental issues is whether there exists a polar amplification of global climate change (for example, see Parkinson, 2004). Many studies have quantified ice/atmosphere or ice/ocean connections for specific regions and time periods, but the picture remains far from unified and complete. Satellite monitoring of the sea-ice cover has led to a greatly improved understanding of the seasonal cycles, trends, and interannual variability of the sea ice during the period of the satellite record. Continued satellite monitoring of the sea ice and other elements of the climate system should contribute to an improved understanding of the interconnections and thereby to the possibility of improved predictions of seasonal sea-ice cover in the Arctic and Antarctic regions.

Acknowledgments

We thank Nicolo E. DiGirolamo from Science Systems and Applications, Inc. (SSAI) and Alvaro Ivanoff from ADNET Systems, Inc., both at the NASA Goddard Space Flight Center, for their skill and patience in generating the figures used in this paper through numerous iterations; Richard S. Williams, Jr., and Jane G. Ferrigno of the U.S. Geological Survey for valuable suggestions on the manuscript and for consistently editing the 11 chapters of the Satellite Image Atlas of Glaciers of the World series; the U.S. National Snow and Ice Data Center (NSIDC) for archiving and distributing the sea-ice data sets; and the Cryospheric Sciences Program at NASA Headquarters for funding this research.

State of the Earth's Cryosphere at the Beginning of the 21st Century: Glaciers, Global Snow Cover, Floating Ice, and Permafrost and Periglacial Environments—

FLOATING ICE: LAKE ICE AND RIVER ICE

By MARTIN O. JEFFRIES, KIM MORRIS, *and* CLAUDE R. DUGUAY

SATELLITE IMAGE ATLAS OF GLACIERS OF THE WORLD

Edited by RICHARD S. WILLIAMS, JR., *and* JANE G. FERRIGNO

U.S. GEOLOGICAL SURVEY PROFESSIONAL PAPER 1386–A–4–II

A broad overview is presented of seasonal and perennial lake-ice and river-ice characteristics, properties, processes, evidence for change, and the consequences of change. The long-term records of seasonal freshwater freeze-up and break-up in the Northern Hemisphere, where most of the ice occurs, show that there has been a significant reduction in ice duration due to climate warming during the 20th century, a trend which continues into the 21st century. Satellite remote sensing offers the most promising means for monitoring lake- and river-ice phenology at regional to hemispheric scales. Maintaining and even expanding the ground-based observational networks also are important to better understanding changes in this subelement of the Earth's cryosphere.

CONTENTS

STATE OF THE EARTH'S CRYOSPHERE AT THE BEGINNING OF THE 21ST CENTURY: GLACIERS, SNOW COVER, FLOATING ICE, AND PERMAFROST

FLOATING ICE: LAKE ICE AND RIVER ICE

By MARTIN O. JEFFRIES[1], KIM MORRIS[1], *and* CLAUDE R. DUGUAY[2]

Abstract

Lake ice and river ice are primarily Northern Hemisphere phenomena, where most of the ice is seasonal. That is, the ice forms in the autumn, thickens during the winter, and melts in the spring. Much more rare but no less important than seasonal ice is perennial ice that lasts for many years on a few lakes in Antarctica and at the highest latitudes in the Arctic. This part of the chapter is a broad overview of lake-ice and river-ice characteristics, properties, processes, evidence for change, and the consequences of that change. Divided into four main sections, the discussion focuses on the following: (1) freeze-up, thickening, and break-up by thermal (freezing, melting) and mechanical (deformation) processes; (2) the physical, biological, and socioeconomic consequences of seasonal- and perennial-ice covers; (3) freeze-up, break-up, and ice duration as climate indicators, evidence for climate variability and change in freshwater-ice records, and the consequences of changing ice conditions; and (4) the future of freshwater-ice research.

Introduction

Scientific and engineering studies of freshwater ice (lake and river ice) have been driven by both natural curiosity and the need to understand processes that have significant geomorphological, limnological, ecological, and socioeconomic effects. The development of the current knowledge and an understanding of freshwater-ice characteristics, properties, processes, and consequences has a long history and can be traced through comprehensive treatises, such as Barnes (1906, 1928), Michel (1971), Adams (1981), Ashton (1980, 1986), Gerard (1990), Gray and Prowse (1993), and Beltaos (1995).

Freshwater-ice events, such as floods and ice jams, can be very costly to society and the economy. For example, flooding resulting from an ice jam in 1996 on the Susquehanna River[3], Pennsylvania, caused 14 deaths and cost US $600 million (Susquehanna River Basin Commission, 2004). An ice jam on the St. Lawrence River in 1993 lasted 40 days, stopped commercial navigation, and cost the Port of Montréal an estimated CDN $200 million (Morse and

[1] Geophysical Institute, University of Alaska Fairbanks, 903 Koyukuk Drive, P.O. Box 757320, Fairbanks, AK 99775-7320

[2] Department of Geography and Environmental Management, University of Waterloo, Waterloo, ON N2L 3G1 Canada

[3] The geographic place-names given in the text conform to the usage authorized by the U.S. Board of Geographic Names for the United States and foreign countries. Unapproved place-names are shown in italics.

Hicks, 2005). Despite these events, frozen lakes and rivers are valuable recreational resources (for example, ice fishing, ice skating, and snowmobiling) and create important winter transportation and communication corridors that link remote, northern communities where hunting and trapping are an essential part of the indigenous culture. However, travel over ice can be hazardous. Each winter in rural Alaska, for example, there are numerous reports of travelers and their snowmobiles plunging through holes in the river ice.

The importance of freshwater ice extends beyond its effects on the economy and its role in society and culture. Freshwater ice also has a significant effect on the environment and is itself sensitive to environmental variability and change. Ice cover affects water properties and quality; river flow and lake circulation; heat, mass, and gas exchange between water and the atmosphere; light penetration and lake productivity; channel and shore morphology and processes; and aquatic and riparian ecosystems.

Despite its importance to society, the economy, and the environment, research support and funding for lake-ice and river-ice studies fall far behind support for the other subelements of the cryosphere as indicated by the number of scientific papers published from 1994 to 2003 (fig. 15).

Limited support for lake-ice and river-ice research means that despite a long history of scientific and engineering investigations, the knowledge and understanding of freshwater-ice characteristics, properties, processes, and consequences are incomplete. At a time when all subelements of the cryosphere, including freshwater ice, are under stress and showing significant signs of change (see Williams and Ferrigno, Hall and Robinson, Parkinson and Cavalieri, Heginbottom and others, all in this chapter), the lack of information makes it difficult to predict the consequences of climate change on freshwater ice and the natural and manmade systems that depend on and are affected by it.

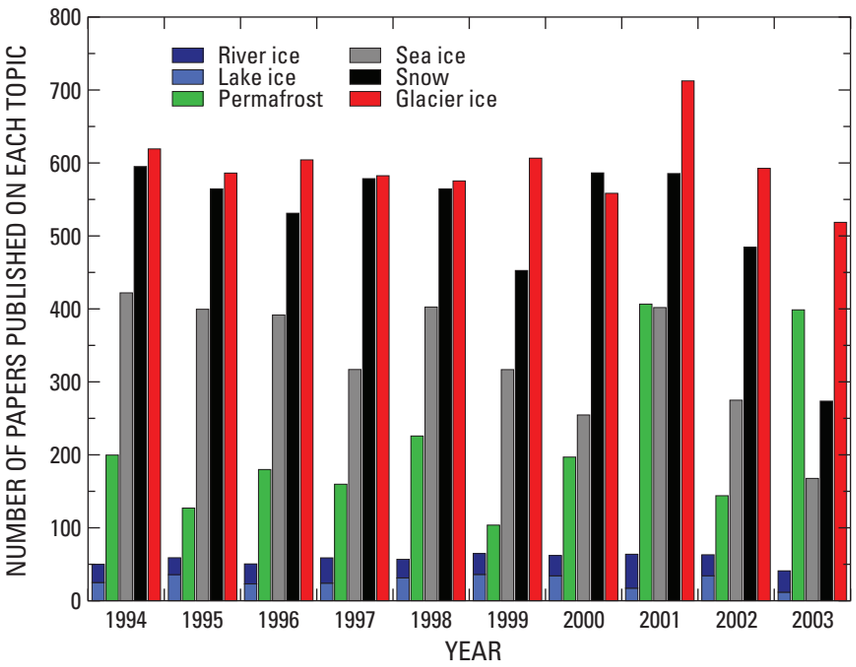

Figure 15.—*Number of papers published on topics about the Earth's cryosphere from 1994 to 2003. The data were obtained using the Biblioline online database for the Arctic and Antarctic regions (http://biblioline.nisc.com/scripts/login.dll?BiblioLine).*

Published together with companion parts on Glaciers, Global Snow Cover, Sea Ice, and Permafrost and Periglacial Environments, this part on Lake Ice and River Ice offers the opportunity to increase awareness of freshwater ice. This part begins with several definitions and descriptions of key ice events, types, and growth processes, then focuses on freeze-up, thickening, and break-up of freshwater ice. It also includes a description of the rare but important multiyear lake ice that is found in both polar regions, the physical, biological, and socio-economic importance of freshwater ice, how freshwater ice can be used as an indicator of climatic changes, and the consequences of changing ice conditions. This part of the chapter concludes with a discussion of the future of freshwater-ice research, particularly as monitoring networks of observers on the ground decrease, and whether remote sensing and numerical modeling can compensate for the decline in field-based observations and measurements.

Freeze-Up, Thickening, and Break-Up of Freshwater Ice

Background

Freeze-up often is defined as the day/date on which a lake or river reach attains a complete ice cover. Likewise, break-up often is defined as the day/date on which a lake or river reach is completely clear of ice. Freeze-up and break-up, which also are referred to as "ice on" and "ice off," respectively, are events. Freeze-up and break-up also can be considered processes or sequences of processes. Thus, freeze-up can be viewed as the period of time between initial ice formation and establishment of a complete ice cover, and break-up as the period of time between the exposure of bare ice (once all snow has melted) and complete clearance of the ice cover. Between the beginning of freeze-up and the beginning of break-up, ice thickness increases by thermal processes (freezing of water) and mechanical processes (deformation of the ice due to motion). Mechanical river-ice thickening also occurs briefly during break-up, sometimes with dramatic consequences (for example, ice jams and floods).

Most of the Earth's lake ice and river ice are in the Northern Hemisphere. The spatial and temporal variability of freeze-up, thickness, and break-up of freshwater ice in North America are documented by Bilello (1961, 1964a, 1980), Bilello and Bates (1966, 1969, 1971, 1972, 1975, 1991), Allen and Cudbird (1971), Allen (1977), Bilello and Lunardini (1996), and Assel (2003a, 2003b). Excluding alpine lakes and rivers, initial ice forms earliest (early to mid-September) in the northernmost regions and becomes progressively later at lower latitudes. Not surprisingly, the pattern of ice disappearance is the opposite of initial ice formation: the ice disappears earlier from lower latitude rivers and lakes while growth continues in the northernmost regions, where ice may persist into the summer.

Most freshwater ice is annual or first-year ice. That is, the ice grows during the autumn and winter and melts in the spring, leaving lakes and rivers open in the summer. Perennial or multiyear lake ice and river ice are rare, but there are a few high-latitude lakes in both polar regions where the ice survives year-round, often for many consecutive years (for example, Adams and others, 1989; Doran and others, 1996, 2004; Wharton and others, 1993).

Freeze-up and subsequent thickening create different ice types that reflect the complex interactions and feedbacks among the atmosphere, snow, ice, and water. Consequently, multiple terms are used to describe ice types and the processes that created them. In order to create a nomenclature for common use among investigators from different disciplines and nations, classification schemes have been proposed (Michel and Ramseier, 1971; Adams, 1976).

Two basic types of ice classification schemes are used: textural and genetic. Textural classifications describe the ice according to the size, shape, and fabric (c-axis orientation) of the ice crystals as observed in ice cores. Genetic classifications describe the ice according to its origin, as inferred from ice texture or as observed directly as ice grows on lakes and rivers. Michel and Ramseier (1971) proposed a combined textural-genetic classification scheme, and Adams (1976) proposed a genetic classification. Ultimately, any classification scheme for freshwater ice can be reduced to the three basic types of ice that predominate in lakes and rivers: frazil ice, snow ice, and congelation ice. Each of these three ice types is briefly described below. Many photographic illustrations can be found elsewhere (for example, Knight, 1962; Michel, 1971; Michel and Ramseier, 1971; Gow and Langston, 1977; Gow, 1986; Jeffries and others, 2005).

Frazil ice forms primarily in fast-flowing or turbulent reaches of rivers when the well-mixed water column has a temperature less than 0°C (supercooled). When viewed between crossed-polarizers, a thin section of consolidated frazil ice has a fine- to medium-grained polycrystalline texture of randomly oriented orbicular and tabular crystals. The somewhat small grain size of frazil ice is primarily due to the disintegration of the crystals as they collide in the flowing water prior to consolidation.

Snow ice is the product of the following sequence of events: a mass of snow that accumulates on the ice surface overcomes the buoyancy of the ice and forces its top surface below piezometric water level; water flows up to the ice surface via fractures, if they are present, and wets the base of the snow cover; the resulting slush freezes, and a layer of snow ice forms. When viewed between crossed-polarizers, a thin section of snow ice has a fine- to medium-grained polycrystalline texture of randomly oriented orbicular and polygonal crystals.

In addition to their similar textures, snow ice and frazil ice contain many air bubbles. Consequently, distinguishing between them in ice cores is primarily a matter of context. For example, frazil ice is less likely to be found in cores of lake ice than in cores of river ice. On the other hand, both frazil ice and snow ice are likely to be found in large quantities in cores of river ice. Snow ice is common in Antarctic sea-ice floes and is distinguished from the equally common frazil ice by large differences in their stable isotopic composition (Lange and others, 1989; Jeffries and others, 2001). Whether the isotopic differences are large enough to distinguish between freshwater snow ice and freshwater frazil ice has not been investigated. Snow ice often is referred to as "white ice" (fig. 16*A*), because it contains a large number of densely packed air bubbles that cause strong light scattering and a high albedo. Melting frazil ice also has a high albedo similar to that of snow ice (Prowse, 1995).

Congelation ice forms as water freezes on the bottom of the ice cover and the latent heat of crystallization is conducted upwards through the ice and snow to the atmosphere. The process of basal freezing and ice formation gives rise to two very different ice textures. The first, and perhaps most common, is the columnar texture of vertically oriented crystals with horizontal c-axes.

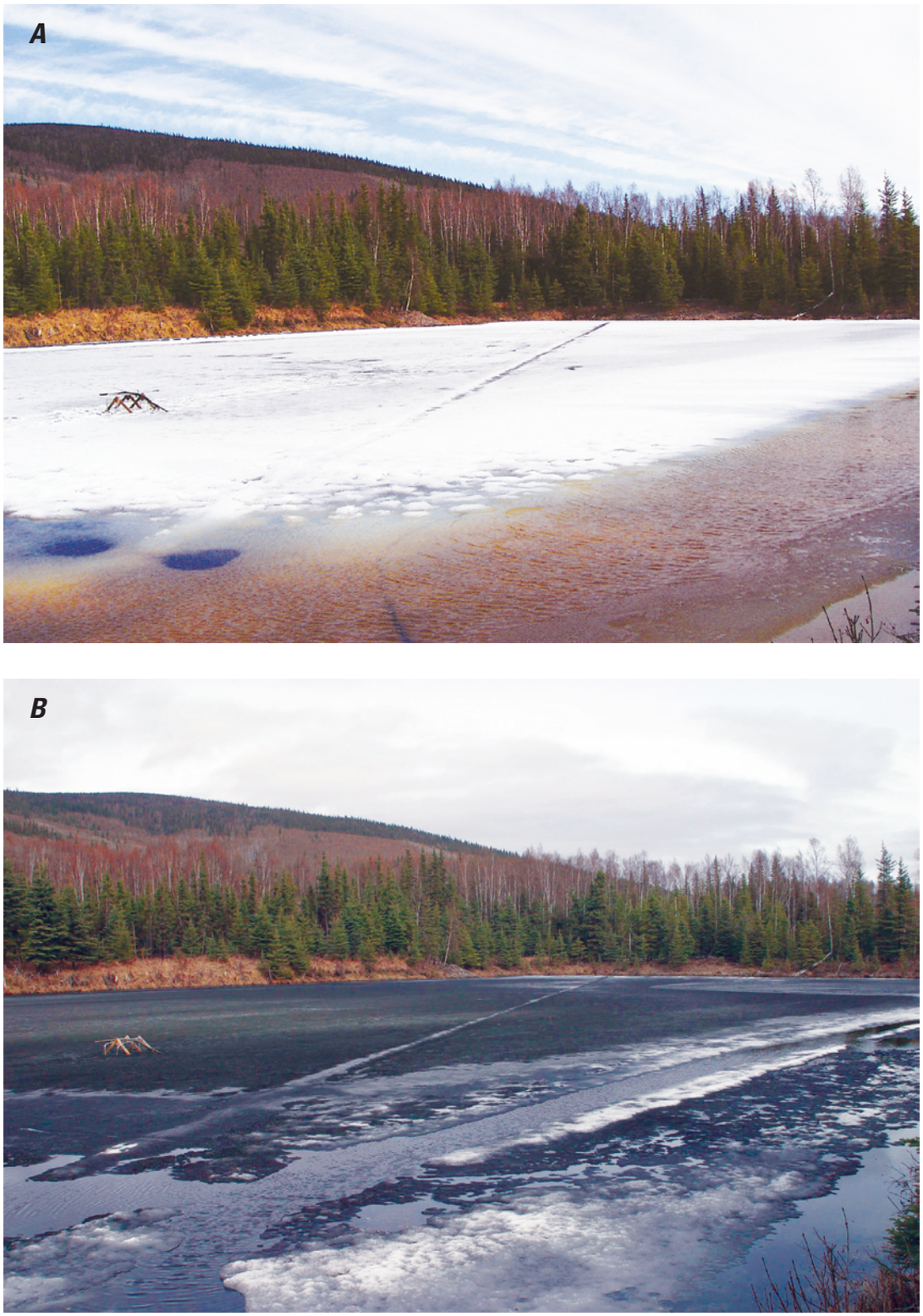

Figure 16.—*Ice break-up at 33.5 Mile Pond, Steese Highway, Alaska, showing* **A**, *the high albedo of snow ice (white ice) on 1 May 2004, and* **B**, *the low albedo of the underlying S2 congelation (black ice) on 7 May 2004, after the snow ice had melted completely. Note the low albedo of the water in the moat that accelerates ice decay around the margins. Photographs by Martin O. Jeffries, Geophysical Institute, University of Alaska Fairbanks.*

Michel and Ramseier (1971) classify this as S2 ice. The second type of congelation ice (S1; Michel and Ramseier, 1971) has macrocrystals, often many meters across, with vertical c-axes. Compared to the marked columnar texture of S2 ice, S1 ice is almost textureless, except for some vague and random stripes and striations (for example, see Gow, 1986, figs. 3, 4, and 6). Congelation ice often is referred to as "black ice" (fig. 16*B*) because it has a high optical depth that permits significant light transmission to the underlying water. During break-up, however, the textural differences between S1 and S2 ice cause significant differences in albedo (Knight, 1962), and "black ice" is no longer a recommended term for melting congelation ice.

The decay of S2 congelation ice is affected by absorption of shortwave radiation and melting along the vertically oriented, columnar crystal boundaries. This process, known as "candling," can originate simultaneously at the top and bottom of the ice (Larsen and others, 1986). Candling does not occur in S1 congelation ice; instead, tubules and air bubbles form when shortwave radiation causes melting within the macrocrystals (Knight, 1962). The different responses of S1 and S2 ice to the absorption of solar radiation are manifested as albedo differences, with S1 ice having a higher albedo than S2 ice. Melting S2 ice is shown in figure 16*B* on p. A385.

Freeze-Up Processes on Lakes and Rivers

As a lake cools to 4°C (the temperature of maximum density of freshwater), the surface waters lose heat, become more dense, and sink. This process continues until all the water in the lake is at 4°C. With further cooling (and without mechanical mixing), a stable, low-density water layer forms at the surface. As this layer cools to the freezing point, ice begins to form on the lake surface. The first ice to form is known as the initial ice skim, and it often appears first as border ice in shallow, protected areas. Sometimes, the entire lake surface can reach the freezing point simultaneously, and a continuous ice cover will appear in a matter of hours (Ragotskie, 1978).

Lake depth and volume play an important role in the autumn cooling and freeze-up of lakes (Stewart and Haugen, 1990); initial ice formation takes place later on deep, large volume lakes, because these lakes take longer to cool than shallow, low volume lakes. Lake fetch (the longest, unobstructed straight-line distance over a lake surface across which the wind has an opportunity to generate waves) also factors into this pattern, as initial ice will form earlier on small lakes with a bulk temperature (the mean temperature of the entire water column) of 2–3°C, whereas most large lakes need to cool down to a bulk temperature of less than 1°C before initial ice will form (Scott, 1964). An exception to the latter is the Laurentian Great Lakes (hereafter referred to as the Great Lakes), where, with the possible exception of Lake Erie, initial ice will form at a bulk temperature of more than 1°C (R.A. Assel, NOAA Great Lakes Environmental Research Laboratory, written commun., 2005). The effects of lake depth, volume, and fetch variability on freeze-up are clearly visible in regions with many lakes, for example, the North Slope of Alaska (Jeffries and others, 2005).

On large lakes, a considerable thickness of ice is required to resist wind forces without breaking, and initial ice-cover formation is much more dynamic than on small lakes (Michel and others, 1986). Wave action can break down the initial ice skim into small fragments, such as frazil ice, and the topmost layer of the young, consolidated ice sheet will have a polycrystalline texture.

Whether the ice thickens further by S1 or S2 congelation ice growth appears to be determined by some combination of wind speed, thermal stability of the water column, and the presence of fog particles or droplets, ice crystals or snow as the initial ice skim forms (Cherepanov, 1970; Barns and Laudise, 1985; Gow, 1986).

Border ice, which is composed of congelation ice, is usually the first ice to form in a river channel; it forms along river banks, where water flow is slower than at the center of the river (figs. 17*A*, *B*). Sheets of congelation ice also will form away from the banks in quiet reaches of a channel and then be transported downstream until the floes are arrested at a constriction (Beltaos, 1995). Away from the banks, in fast-flowing or turbulent reaches of a channel, frazil-ice crystals form and accumulate as slush, which eventually freezes completely to create the polycrystalline ice described earlier. Often, the slush will consolidate first into ice pans, which, in turn, combine and create larger ice floes (figs. 17*A*, *B*). As slush, pans, and floes are carried downstream, they can become entrained in the border ice and contribute to its expansion and further constriction of the channel.

Once a channel becomes congested and is bridged by ice, a lodgement (Gerard, 1990), also known as a surface ice jam (Beltaos, 1995), will form and affect the flow of water and movement of ice from upstream (fig. 17*C*). Lodgements form when the passage of ice along a reach is obstructed by a constriction formed by the banks and (or) border ice. Frazil ice, slush, pans, and floes can be carried under the lodgement and contribute to its thickening into a floating jam or even a grounded jam (Beltaos, 1995). Or, the frazil ice, slush, pans, and floes remain at the surface and accumulate against the jam to form a pack (Gerard, 1990). The growing pack often is rough (fig. 17*C*) due

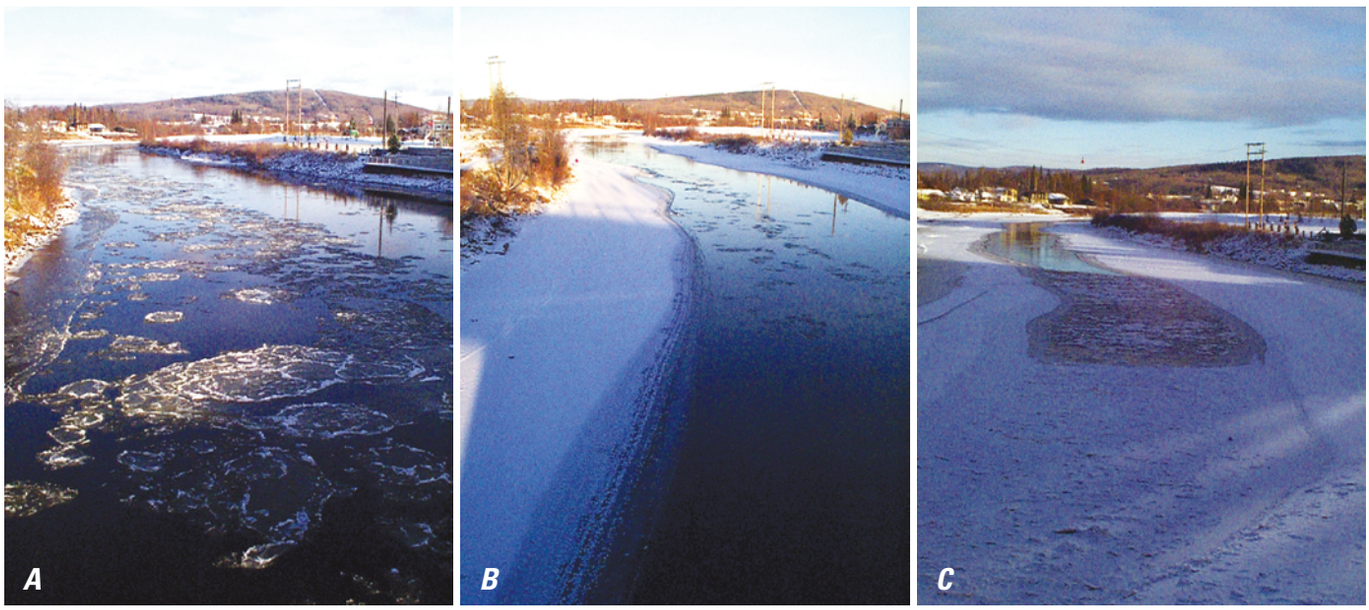

Figure 17.—*Freeze-up on the Chena River, Fairbanks, Alaska, in autumn 2001 showing,* **A**, *early, thin border ice by the left/north bank and ice pans in the channel on 21 October;* **B**, *narrowing of the open channel as the border ice expands away from the banks on 28 October; and* **C**, *closure of the channel as a lodgement forms and the pack expands upstream as ice pans are stopped at the blockage on 4 November. Photographs by Martin O. Jeffries, Geophysical Institute, University of Alaska Fairbanks.*

to rafting and ridging of the ice as it decelerates and is ultimately stopped. As more ice arrives from upstream and is blocked, the pack grows as it extends upstream. The river becomes progressively covered with ice as the pack expands at a rate that depends on the prevailing weather conditions, the discharge, and the geometry of the channel (Gerard, 1990). Where a river enters a lake, the frazil ice, slush, pans, and floes can be stopped by the lake-ice cover and accumulate in an extensive and rough mass (Leconte and Klassen, 1991).

Winter Ice Cover on Lakes and Rivers

After initial ice formation and the establishment of a consolidated ice cover on a river, open-water areas that persist all winter often remain. Sometimes known as "polynyas" (a term more commonly used in polar oceanography and sea-ice geophysics), these areas recur on fast-moving reaches and in areas of warm ground-water flow [including geothermal springs, such as at lake Mývatn, Iceland (Rist, 1970)], or lake outflow (Gerard, 1990). Like their polar-ocean counterparts, river ice polynyas are sites of significant heat and mass transfer to the atmosphere (fig. 18), but no studies about magnitude of these fluxes from rivers in winter are known.

As in polar-ocean polynyas, river polynyas are a significant source of frazil ice. Swept below the ice downstream, accumulating frazil ice can form hanging dams, which can be immense. For example, in February 1973, on La Grande Rivière, Québec, Canada, a hanging dam more than 16 km long and more than 20 m thick in places contained more than 56×10^6 m^3 of ice (Michel and others, 1986), enough frazil ice to cover an area of 7 km by 8 km to a depth of 1 m.

Frazil ice swept under an ice cover contributes to thickening as it accretes to the base and becomes an integral part of the overlying ice. When frazil ice is not present below the ice, the ice will thicken by congelation ice growth. This can be interrupted by the arrival of more frazil ice, so a river-ice sheet will develop a complex layered stratigraphy of congelation ice and frazil ice (for example, see Schwarz and others, 1986, figs. 2–7).

Figure 18.—*Heat and mass transfer from open water on the Chena River, Fairbanks, Alaska, are manifested as a fog plume on a cold (-25°C) morning, 5 March 2002. This reach of the river freezes only during the coldest weather because the water is artificially heated by a power plant located ~1 km upstream (into the page). Photograph by Martin O. Jeffries, Geophysical Institute, University of Alaska Fairbanks.*

The texture and stratigraphy of a lake-ice sheet can be complex, too. Studies on lakes in Alaska and Russia have shown that, after initial ice formation, S1 and S2 congelation ice can occur in multiple layers in the same ice sheet, and, on any given lake, S1 ice might dominate one year and S2 ice might dominate the next year (Knight, 1962; Weeks and Wettlaufer, 1996). The reasons for this variability are unclear but might include the thermal characteristics of the underlying water body (Weeks and Wettlaufer, 1996). S2 ice commonly is observed in river ice, but much less is known about the occurrence of S1 ice in frozen rivers.

Snow-ice formation adds to the complexity of the stratigraphy of lake-ice and river-ice covers. Multiple flooding events during the winter increase the thickness of the snow-ice layer. Redistribution of the snow cover by the wind will alter the distribution of mass on the ice, leading to larger quantities of snow and snow ice at the margins of the ice cover than in the center (Adams and Roulet, 1980; Adams and Prowse, 1981; Bengtsson, 1986).

In addition to snow-ice formation, ice on rivers and streams often thickens by accumulation of aufeis from water flowing across the bare ice surface (fig. 19). The water necessary for aufeis formation often is forced upward under pressure from the increasingly constricted channel below the ice, or it originates from tributaries or ground-water springs (Michel and others, 1986). Unlike snow-ice formation, which is episodic, aufeis formation is more continuous; consequently, during the course of a winter, aufeis deposits can reach thicknesses of many meters and lengths of many kilometers (Michel and others, 1986) (see Part A-5 of this chapter, figs. 32, 33, p. A466 and p. A468). Aufeis sometimes is referred to as naleds, icings, glaciation, and overflow. Aufeis, however, is the preferred term.

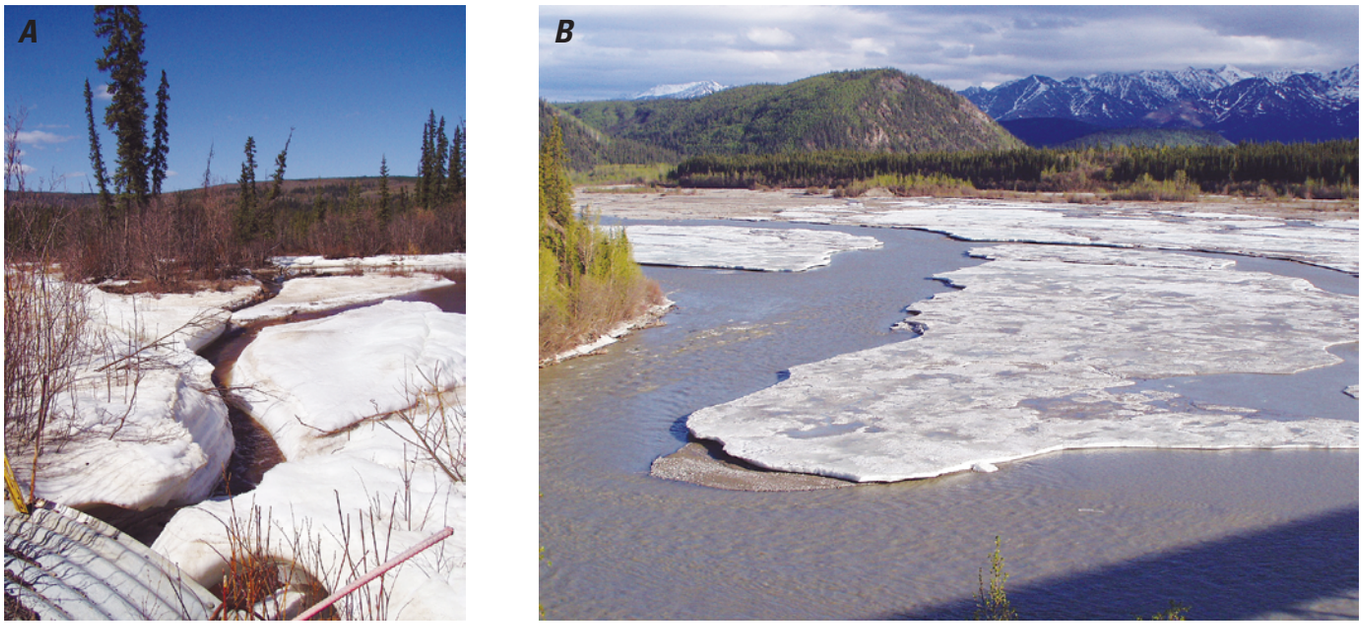

***Figure 19.*—A**, *Aufeis at Big Eldorado Creek where it enters a culvert below Goldstream Road, 6 km north of Fairbanks, Alaska, on 16 May 2006, and* **B**, *on gravel bars in the Robertson River, Alaska Highway mile 1345 (170 road miles/272 km, southeast of Fairbanks), on 27 May 2006. Photographs by Martin O. Jeffries, Geophysical Institute, University of Alaska Fairbanks.*

As freshwater ice thickens during the winter, it is subject to a number of different stresses, such as thermal pressure, wind and water drag, and water-level changes, all of which contribute to fracturing and sometimes further thickening of the ice cover (Carstens and others, 1986). Many fractures remain hidden below the snow cover, but they can be detected with passive and active microwave sensors (Melloh and others, 1991; Morris and others, 1995; Jeffries and others, 2005). Smith (2002) used an interferometric synthetic aperture radar (InSAR) technique to illustrate river-ice motion and the formation of transverse fractures in mid-winter. Transverse fractures typically precede break-up events (Beltaos, 1990, 1997). Mid-winter break-up typically is triggered by brief rain-on-snow events that occur during mid-winter thaws (S. Beltaos, National Water Research Institute, Canada, written commun., 2005). The significance of mid-winter break-up events and resultant ice jams is described in a later section.

Brief, transient events can severely disturb a lake-ice cover. For example, Jeffries and others (2005) illustrate the severe ice deformation and displacement that resulted from an M7.9-earthquake-induced seiche at Mentasta Lake, Alaska, in early November 2002. On the largest lakes, ice cover is subject to frequent disturbance, mostly by the wind, leading to the opening of fractures, the formation of new ice, and the development of pressure ridges when the fractures close and deform the thin ice (Metge, 1976). Ice fractures and ridges often are widespread (fig. 20).

The ice cover on the Great Lakes, except for shorefast ice in bays and ice grounded on shoals, rarely is static for long. Campbell and others (1987) derived mean and maximum speeds of 0.08 m s^{-1} (0.3 km h^{-1}) and 0.46 m s^{-1} (1.65 km h^{-1}), respectively, from satellite-tracked buoys deployed on Lake Erie ice. Pilant and Agarwal (1998) used sequential RADARSAT-1 synthetic aperture radar (SAR) images of Lake Superior to derive mean ice speeds of at least 0.47 m s^{-1} (1.7 km h^{-1}). At the time of annual maximum ice area, the Great Lakes rarely are totally covered with ice, and the amount of ice decreases as the depth of water increases (Assel and others, 2003). For a comprehensive description of the spatial and temporal variability of the ice cover on Great Lakes, the reader is referred to the electronic atlas created by the NOAA Great Lakes Environmental Research Laboratory (Assel, 2003a).

In shallow water, ice can become grounded on the river or lake bottom. Grounded lake ice that freezes to the bottom before the ice has attained the maximum possible thickness by freezing alone is widespread in northern tundra regions, such as Siberia and the North Slope of Alaska. Because many of the tundra lakes are so shallow (maximum depth less than or equal to 2 m), the entire area of ice freezes to the bottom; this is shown by airborne and space-borne imaging radars (Weeks and others, 1977, 1978; Mellor, 1982, 1994; Jeffries and others, 1994; Morris and others, 1995). In rivers, ice grounding is primarily associated with ice jams that form at freeze-up and during the winter, sometimes with serious consequences (for example, Beltaos, 1995).

In any given year, the maximum ice thickness of solid ice (this excludes any ice pans, ice floes, or loose accumulations of frazil ice deposited under the solid ice sheet) changes across North America. In any given location, the maximum thickness also changes from year to year, as shown by the cooperative ice-monitoring program, which was coordinated by the U.S. Army's Snow, Ice, and Permafrost Research Establishment (SIPRE) (1947–1961) and its successor organization, the U.S. Army Cold Regions Research and Engineering Laboratory (CRREL) (1961–present) from the late 1950s to the late 1970s

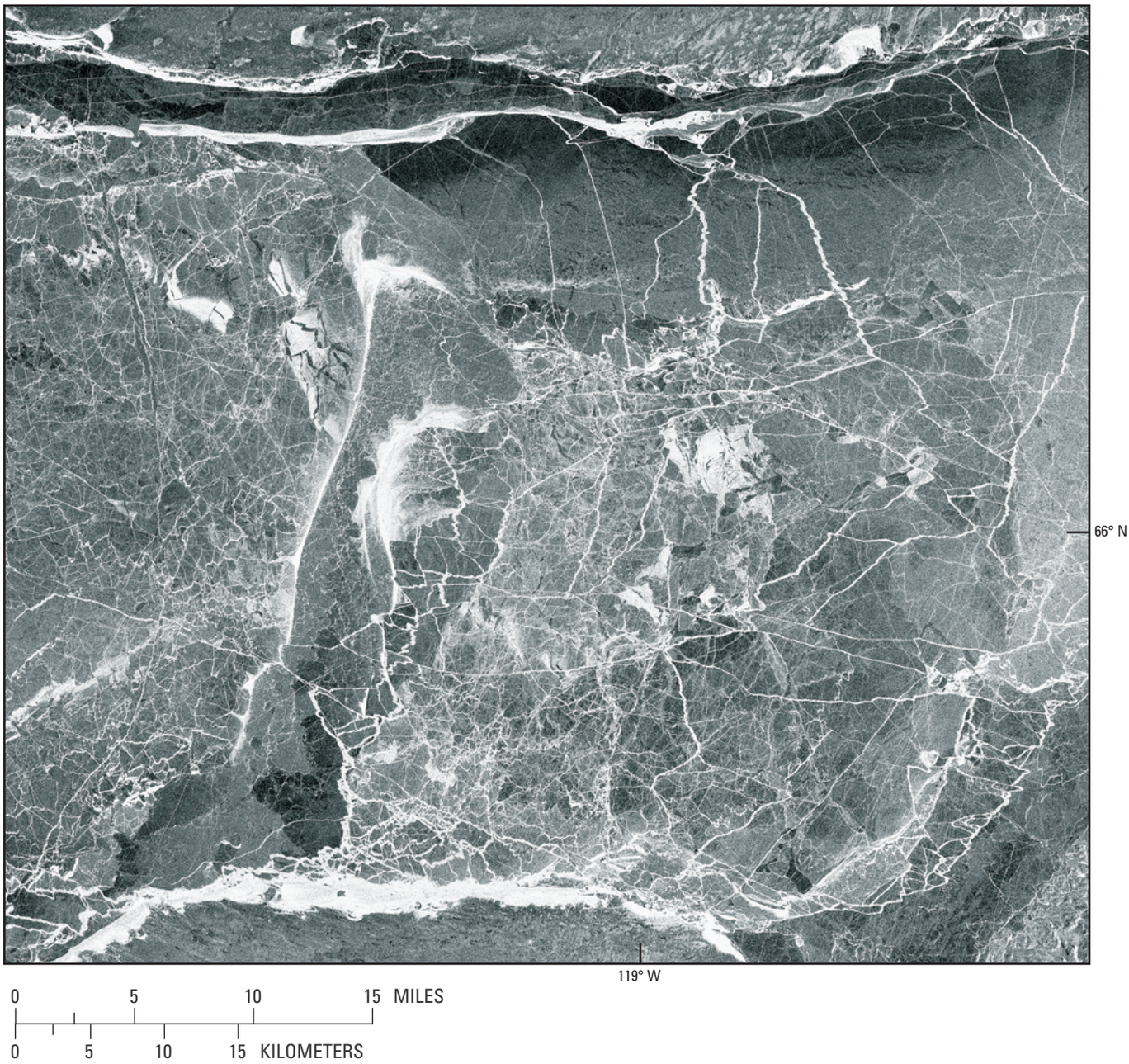

Figure 20.—*European Remote Sensing Satellite-1 (ERS-1) synthetic aperture radar (SAR) image on 1 January 1992, showing widespread ice fracturing and ridging in McTavish Arm (lat 66.1°N., long 119.00°W.), Great Bear Lake, Northwest Territories, Canada (from Morris and others, 1995). The image covers an area of 70 km by 80 km on the ground.*

(Bilello, 1961, 1964a, b, 1980; Bilello and Bates, 1966, 1969, 1971, 1972, 1975, 1991; Bilello and Lunardini, 1996). Bilello's data show that maximum ice thickness is at the end of the season (late winter/early spring) at most locations. The smallest and largest recorded maximum ice-thickness data available through 1977 can be summarized as follows: (1) the thickest ice was in the Canadian High Arctic (1.8–2.6 m); (2) the thinnest ice was in the Great Lakes/St. Lawrence River/Canadian Maritimes region (0.6–1.0 m); (3) in Alaska, the thickest ice (1.0–1.8 m) was in the northern and western regions, and the thinnest ice (1.0 m) was in the southern region (Bilello, 1980). The widespread evidence for climate change in recent decades in northern cold regions (ACIA, 2004, 2005) casts doubt on whether the above values are still a reasonable guide to the distribution of freshwater ice thickness at the end of winter in North America.

Break-Up Processes on Lakes and Rivers

Break-up involves decay (melt), fracture, transport, and removal of the ice that developed since the end of freeze-up (Prowse, 1995). Although all four processes apply to river ice, the break-up of lake ice is characterized primarily by decay and fracture; however, it is possible to envision situations where ice on large lakes might be transported and removed by outflowing rivers.

Prowse (1994, 1995) used the terms "hydrothermal" and "hydrodynamic" to describe the thermal and mechanical processes that control break-up of river ice. Beltaos (2003) preferred the terms "thermal" and "mechanical" instead of hydrothermal and hydrodynamic. Thermal break-up typically is characterized by only moderate increases in water flow and by an ice cover that has thermally deteriorated and lost much of its mechanical strength, thereby offering little resistance to water flow. In contrast, mechanical break-up usually results from the interaction of a large spring flood wave with a mechanically competent (intact and mechanically strong) ice cover.

Thermal and mechanical processes also affect the break-up of lake ice, which primarily decays thermally in place, by melting at the top and bottom and at the edges, particularly where streams and rivers flow into the lake. Lake ice also is subject to wind stress that moves and fractures the ice, particularly on large lakes (fig. 21).

Unlike initial ice formation and subsequent thermal thickening by freezing, which can be understood in terms of heat conduction driven by the surface-energy balance, thermal decay of freshwater ice is more complex because the top and bottom surfaces melt simultaneously as the ice becomes isothermal at 0°C (Larsen and others, 1986). The exception is grounded lake ice (and presumably grounded river ice), which often melts only at the top without becoming afloat (Brewer, 1958).

During river ice break-up, tributaries accelerate the decay of ice in the main channel (Pavelsky and Smith, 2004). Also, break-up does not take place simultaneously along the entire river: a river channel commonly is ice-free in some reaches and ice-covered in others. Pavelsky and Smith (2004) used Earth Observing System (EOS) Terra (EOS AM-1) and Aqua (EOS PM) satellites' Moderate Resolution Imaging Spectrometer (MODIS) and NOAA meteorological satellites' Advanced Very High Resolution Radiometer (AVHRR) imagery to show that the open and closed reaches on many rivers are in the

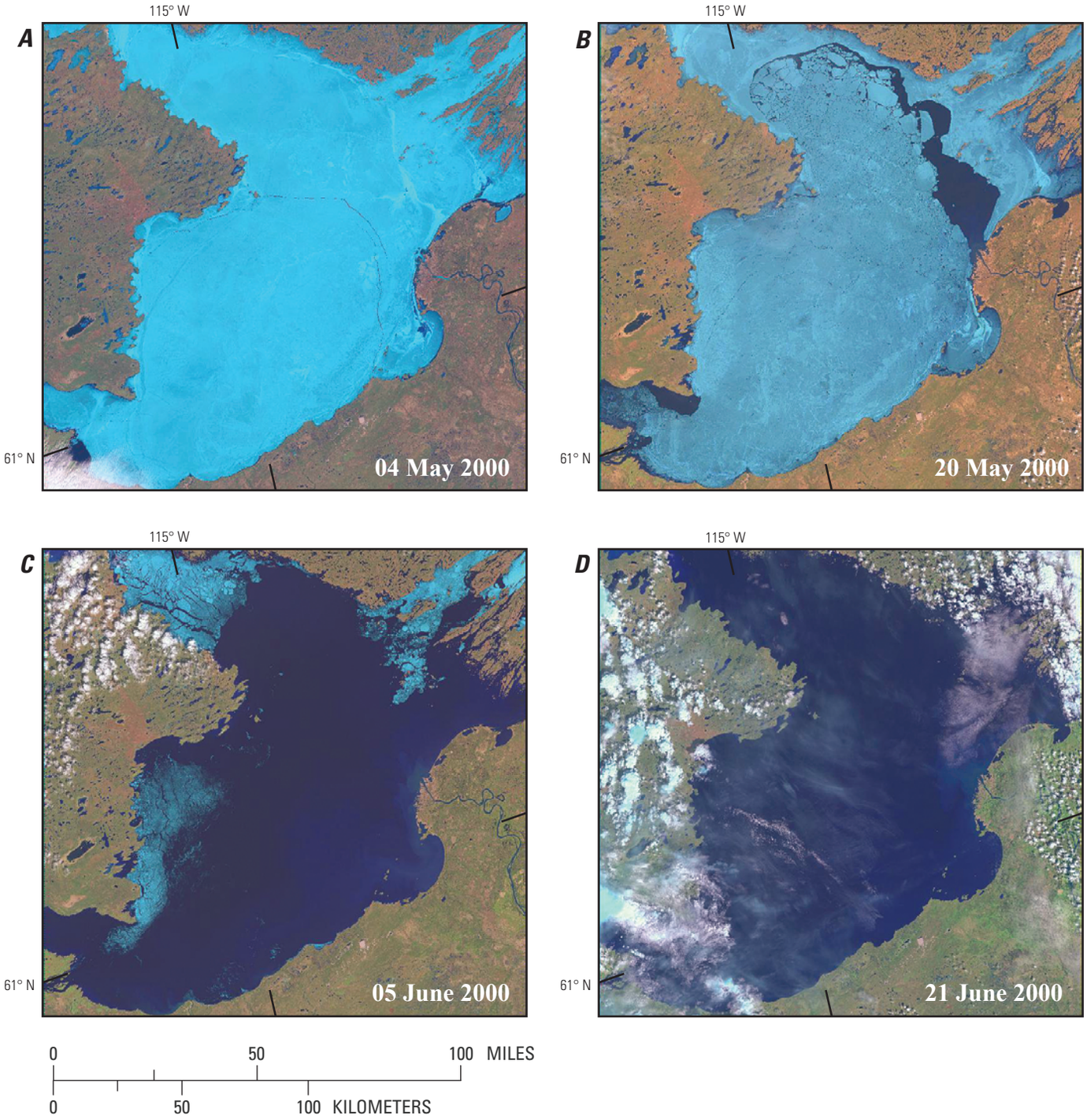

Figure 21.—*Landsat-7 ETM+ (bands 3, 4, 5) images show break-up on Great Slave Lake (lat 61.46°N., long 114.60°W.), Northwest Territories, Canada, in spring 2000:* **A**, *4 May,* **B**, *20 May,* **C**, *5 June, and* **D**, *21 June. The fracturing, weakening, and shrinkage of the ice are evident, as is the complete disappearance of ice from numerous smaller lakes long before Great Slave Lake was completely ice free. Each image covers an area of 185 km by 185 km on the ground.*

same place each year. This observation lends confidence to the use of single-point measurements from a river bank to study temporal variations in break-up and the relation between break-up and climate change.

The opening of some reaches while others remain closed can be attributed to both thermal and mechanical processes. In the case of thermal decay, the ice melts and disintegrates in place; this often occurs more rapidly in quieter reaches than in more turbulent, steeper reaches due to differences in the optical properties of ice that is exposed once the snow cover has melted (Prowse and Demuth, 1993; Prowse, 1995). The bare ice cover on quiet reaches often is predominantly congelation ice, which has a relatively low albedo (fig. 16*B*); consequently, it absorbs more shortwave radiation and decays rapidly. The bare ice cover on turbulent reaches is predominantly frazil ice, which has a relatively high albedo similar to bare snow ice (fig. 16*A*); consequently, it absorbs less shortwave radiation and decays slowly.

Sometimes, river ice may decay in a manner that is the opposite of the one described above. The ice can be thicker and thus stronger on quiet reaches, and thinner (due to high heat input and melting by fast-flowing water) and weaker in turbulent reaches; consequently, the ice on quiet reaches decays more slowly than the ice on turbulent reaches (L.C. Smith, University of California at Los Angeles, written commun., 2005). Clearly, some ambiguity remains as to the role of ice type, optical properties, and channel gradient in the decay of river ice, and further research would be needed to study this.

The role of mechanics in the opening of some reaches while others remain covered with ice relates primarily to the formation and failure of ice jams. Before an ice jam forms, the river-ice sheet must fracture so that the ice can move. Fractures form close to and parallel to the bank, down the center-line of a river (Prowse, 1995) and, most importantly, across the river-ice sheet perpendicular to the bank, for example, transverse cracks (Beltaos, 1990, 1997). Transverse cracks form when bending stresses exceed the flexural strength of the ice, sometimes in response to the passage of steep flood waves that cause vertical bending, or when flow shear and the meandering path of a channel cause horizontal bending. Once large slabs of ice that are formed between the transverse cracks are set in motion, they quickly break down into small ice blocks, and, as they move downstream, the river opens behind them. When the downstream progress of the ice blocks is stopped by an intact, mechanically competent ice cover, an ice jam forms (Beltaos, 1997).

Why and when ice jams fail are not fully known, but conditions at the toe (leading edge) of the jam, ice competence, discharge, and thermal effects probably all play a role (Beltaos, 1995). The failure of an ice jam is followed by a surge of water and ice; when the ice run or breaking front is halted by an intact ice cover further downstream, another ice jam will form. In fact, break-up over long distances in a river can be viewed as a series of surge-stall events related to the successive failure and formation of ice jams (Scrimgeour and others, 1994). It is this process that clears ice from some reaches while other reaches remain covered with ice.

Once snowmelt starts on lake ice, water collects around the margins (fig. 16*B*), where it warms as it absorbs solar radiation and accelerates melting due to positive feedback. This releases the ice cover from the shore and allows it to be moved about by the wind (Michel and others, 1986). As the ice moves and simultaneously thins and weakens, it becomes more susceptible to fracture (fig. 21), and, once fractured, it disappears quickly (Larsen and others, 1986). Michel and others (1986) suggest that the strength of lake ice (and presumably

river ice) can be maintained by the presence of snow ice, which, because of its relatively high albedo, protects the underlying congelation ice from solar radiation. However, investigations of lake ice break-up in central Alaska, as influenced by maximum ice thickness and composition (snow ice, congelation ice), indicate that the role of snow ice in break-up remains ambiguous and inconclusive (Jeffries and Morris, 2007). The size of a lake also affects break-up, with ice persisting for longer periods of time on larger lakes than on smaller lakes in the same region (fig. 21). For example, on the North Slope of Alaska, where smaller lakes also tend to be shallower and the entire ice cover freezes to the bottom, this thinner ice on smaller lakes disappears before the thicker, floating ice cover on the larger, deeper lakes (Sellmann and others, 1975).

Multiyear Ice

In some high-latitude lakes, ice survives not just one summer but many summers. The known locations of perennial lake ice in the Arctic and Antarctic are summarized by Doran and others (2004, tables 1 and 2). Although only a few perennially ice-covered lakes exist, the physical and biological consequences of multiyear ice are significant, and a brief description of the ice is warranted. A small amount of ice melts around the margins at most of these lakes each year, and a narrow moat of open water develops during the course of the summer. In the McMurdo Dry Valleys of Antarctica, for example, the moat on any lake is on the order of 1 to 3 percent of the total lake area (Spigel and Priscu, 1998).

At Colour Lake, Axel Heiberg Island, Nunavut, Canada, the ice survives for a single summer about every six years (Adams and others, 1989; Doran and others, 1996). The persistence of the ice during only occasional summers is believed to be a consequence of ice-related variations in water temperature. An end-of-summer ice cover promotes rapid freeze-up, and warm water heated during the summer is trapped in the lake. The warm water (4–5°C immediately below the ice) then persists through the winter, enhances ice melting in the spring and summer, and reduces the likelihood that the ice will survive for a second consecutive year (Doran and others, 1996).

Colour Lake is a well-mixed freshwater lake (Doran, 1993). In contrast, many of the perennially ice-covered lakes in the McMurdo Dry Valleys, Antarctica (Armitage and House, 1962; Heywood, 1972; Wharton and others, 1993; Doran and others, 2000), and northernmost Ellesmere Island, Nunavut, Canada (Hattersley-Smith and others, 1970; Jeffries and others, 2005), are meromictic lakes. These lakes rarely, if ever, experience turbulent or convective mixing and have end-of-winter water temperature maxima of more than 10°C (fig. 22) (Wilson and Wellman, 1962; Shirtcliffe and Benseman, 1964; Hattersley-Smith and others, 1970; Jeffries and Krouse, 1985; Spigel and Priscu, 1998; Belzile and others, 2001). Thus, unlike Colour Lake, the perennial lake ice in McMurdo Dry Valleys and Ellesmere Island appears to be unaffected by elevated water temperatures.

Surface ablation by melting and sublimation reduces the thickness of multiyear lake ice in the McMurdo Dry Valleys each summer, and interannual variability in the balance between summer surface ablation and winter bottom freezing leads to long-term variations in maximum ice thickness (fig. 23; McKay and others, 1985; Wharton and others, 1993). Despite interannual variations in surface ablation and bottom freezing, the increase in ice thickness

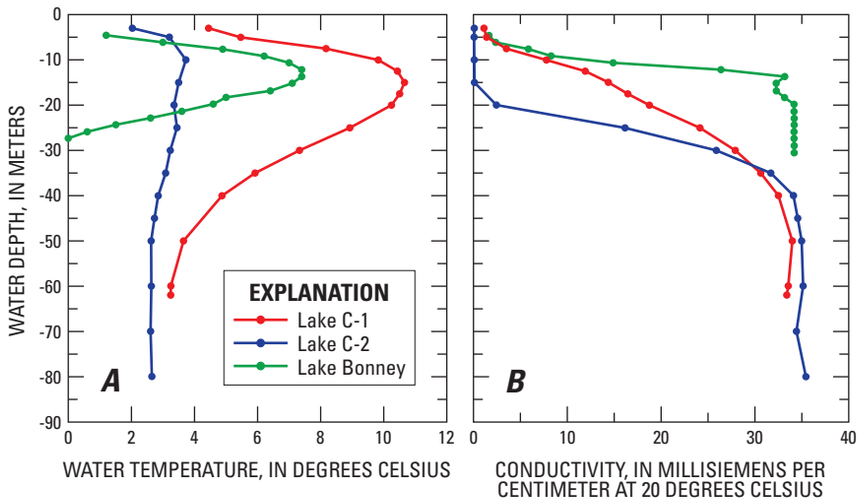

Figure 22.—**A**, *Temperature, and* **B**, *conductivity profiles in Lakes C-1 and C-2, Ellesmere Island, Nunavut, Canada, May 1985, and Lake Bonney, Taylor Valley, Antarctica, January 1963 (From Shirtcliffe and Benseman, 1964). For comparative purposes, the deepest water samples at Lakes C-1 and C-2 have salinity values of 27.4 PSU (Practical Salinity Units) and 29.3 PSU, respectively. The Lake Bonney conductivity data (Shirtcliffe and Benseman published only conductivity values) are shown as 50 percent of actual values for easier comparison with the data for Lakes C-1 and C-2.*

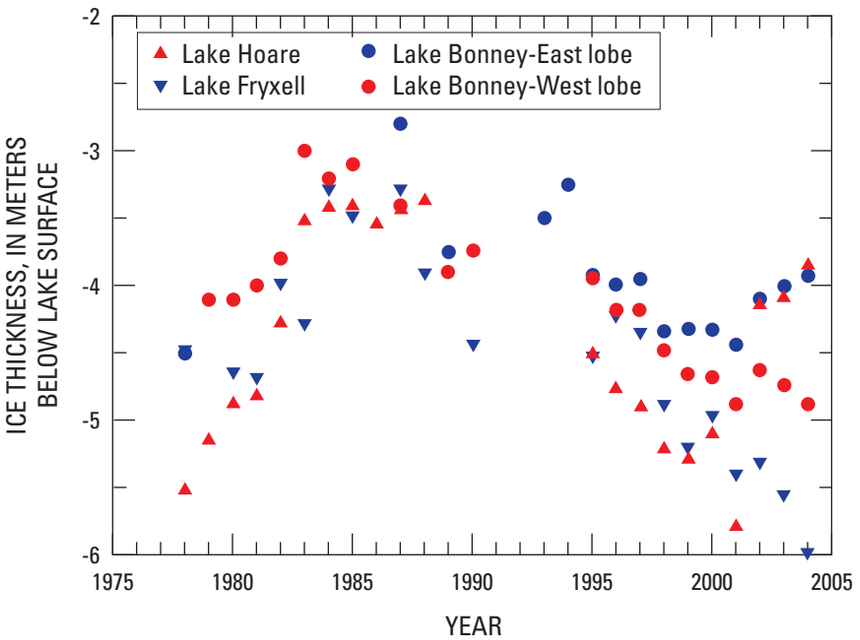

Figure 23.—*Ice-thickness variations since the late 1970s at four lakes in Taylor Valley, McMurdo Dry Valleys, Antarctica. The 1978–1988 data are from Chinn (1993). The 1989–2004 data were provided by John Priscu, Montana State University.*

from 1986 to 2000 (fig. 9) has been attributed to climate cooling (Doran and others, 2002). The McMurdo Dry Valleys lakes continue to have a perennial ice cover primarily due to the fact that the summers are too short and too cool to allow complete melting of the ice. The same explanation probably applies to the Ellesmere Island lakes; they are located only 1 to 2 km inland from the coast, where low stratus clouds affect the surface energy balance, and reduce summer air temperatures and ablation at the offshore ice shelves (Sagar, 1962; Hattersley-Smith and Serson, 1970).

The ice thickness on lakes in Taylor Valley, Antarctica, ranged from 3 m to 6 m from 1978 to 2004 (fig. 23). The ice at Lake Vida, Victoria Valley, Antarctica, about 40 km to the northwest of Taylor Valley, is much thicker than lake ice in Taylor Valley. At Lake Vida, periodic inundations of the ice surface by streams, followed by freezing, are believed to be primarily responsible for what was initially reported to be an 11.5-m ice cover (Calkin and Bull, 1967); the ice cover has since been reported to be approximately 19 m thick (Doran and others, 2003).

Only a few ice-thickness measurements have been made at the meromictic lakes on Ellesmere Island, where the ice appears to have had a fairly consistent thickness of 1 to 2 m at the end of winter from 1967 until the late 1990s (Hattersley-Smith and others, 1970; Jeffries and Krouse, 1985; Belzile and others, 2001) (see Jeffries, 2002, fig. 4, p. J152). During the summers since the late 1990s, the lake-ice covers on Ellesmere Island have experienced significant changes: at Lakes A and B, the ice has shrunk significantly and fractured, while at Lakes C-1 and C-2, the ice has melted completely (fig. 24) (Jeffries and others, 2005).

Multiyear lake ice also forms at tidewater on epishelf lakes. Epishelf lakes are bodies of freshwater that form on top of seawater that is connected to the ocean and thus subject to tidal action. Epishelf lakes form in Antarctica (for example, Doran and others, 2000) and northernmost Ellesmere Island, Nunavut, Canada (for example, Ludlam, 1996; Van Hove and others, 2001; Jeffries, 2002). At Taconite Inlet (fig. 24), the epishelf lake is 5.5 m deep (Ludlam, 1996). The overlying lake ice causes strong backscatter and a bright synthetic aperture radar (SAR) image tone, as it does on all the Ellesmere Island epishelf lakes, in contrast to the weaker backscatter and darker tone of sea ice (Jeffries, 2002). Significant melting of the epishelf lake ice on Taconite Inlet (adjacent to meromictic Lakes C-1 and C-2) after 1997 culminated in fracturing and movement of the ice in 2003 (fig. 24*G*). Extensive fracturing and movement of the perennial epishelf lake ice also took place on Disraeli Fiord, 65 km east of Taconite Inlet, in summer 2003 (Van Hove, 2005); this was only 1 year after the catastrophic drainage of the epishelf lake due to fracturing of the Ward Hunt Ice Shelf (Mueller and others, 2003; Jeffries and others, 2005).

The thickest and oldest lake ice on Earth is immediately above the subglacial lakes (145 lakes identified by early 2007) at the base of the Antarctic ice sheet (Kennicutt and Petit, 2007). At Lake Vostok, East Antarctica, for example, at a depth of 3,539 m below the ice-sheet surface, an approximately 200-m thick layer of freshwater ice many thousands of years old has accreted on the bottom of the glacier ice (Jouzel and others, 1999).

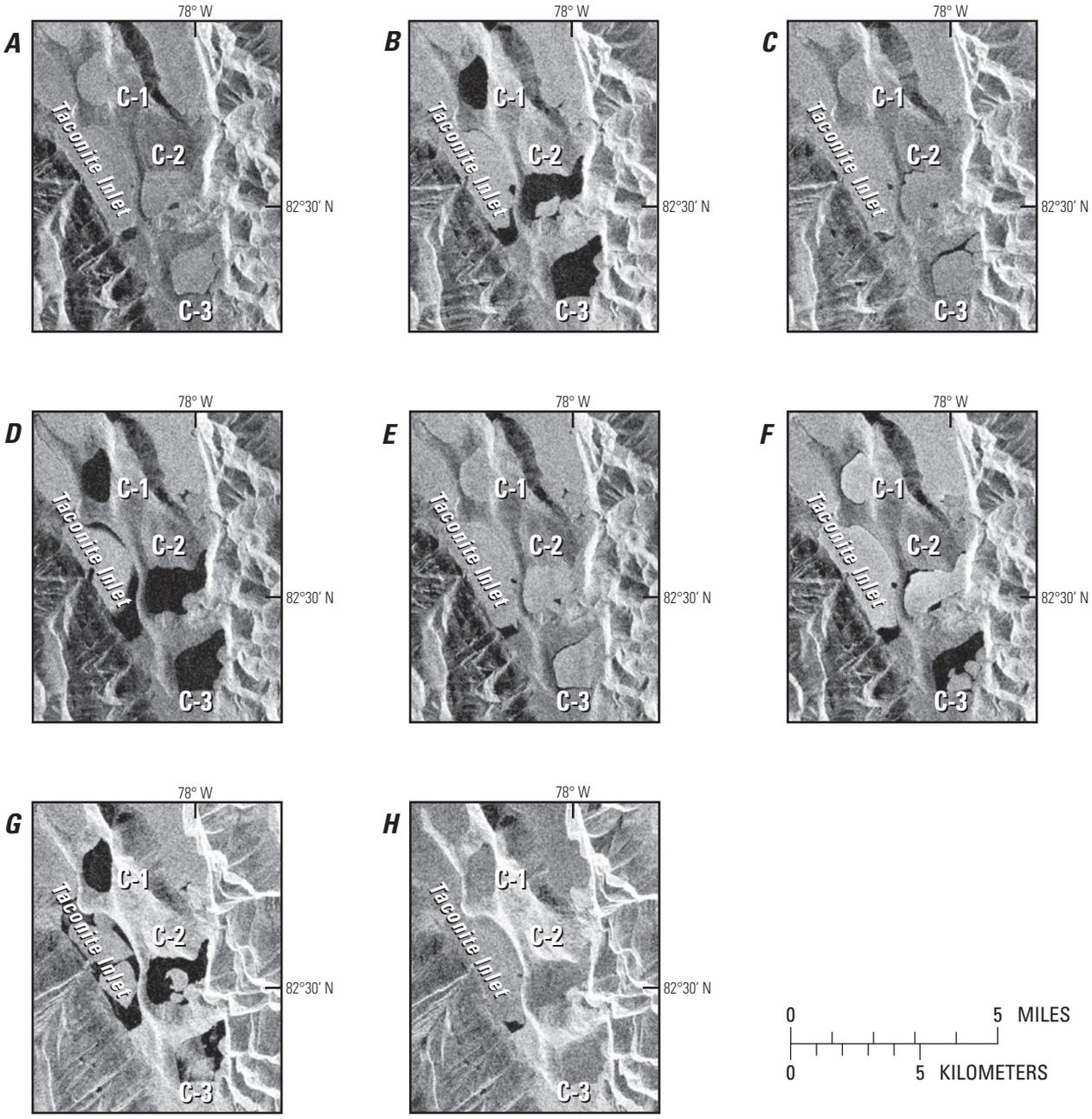

Figure 24.— *RADARSAT-1 Standard Beam synthetic aperture radar (SAR) images show fracturing, shrinkage, and complete melting of the once-perennial ice on meromictic Lakes C-1 and C-2 and the perennial epishelf lake ice in Taconite Inlet (lat 82.85°N., long 78.22° W.), Ellesmere Island, Nunavut, Canada. Lake C-3 is a well-mixed, freshwater lake.* **A***, 5 September 1997;* **B***, 26 August 1998;* **C***, 8 September 1999;* **D***, 14 August 2000;* **E***, 22 August 2001;* **F***, 21 August 2002;* **G***, 25 August 2003; and* **H***, 19 August 2004. Each image covers an area of 7 km by 8.5 km on the ground.*

Physical, Biological, and Socioeconomic Importance of Freshwater Ice

Ice on rivers and lakes affects water discharge and stage (water level) in a channel, lake water level, and seasonal storage represented by the ice itself, the snow cover it carries, and the channel and lake storage it induces (Gerard, 1990). The hydrologic significance of floating ice can be substantial; indeed, it can be argued that the hydrologic extremes of common interest, floods and low flows, are as much a function of stream processes through the action of snow and ice in the channel as they are of the catchment/landscape processes of traditional concern (Gerard, 1990). A summary of the important role of ice in river hydrology in cold and temperate regions can be found in Prowse and Beltaos (2002).

Floods and low flows in channels most often are associated with ice jams (floating or grounded), which form where the passage of ice along a reach is obstructed. An ice jam increases the hydraulic resistance and decreases the flow conveyance of the channel; consequently, water upstream from the ice jam goes into storage and the stage increases, while water downstream from the ice jam continues to flow and the stage decreases, and low flow occurs (Gerard, 1990). Upstream from freeze-up ice jams, the stage can exceed the expected summer stage maximum (Gerard and Stanley, 1988); downstream, the low flows are the annual minimum stage (Gray and Prowse, 1993). Break-up ice jams lead to flooding (fig. 25) more often than freeze-up ice jams, and riverside communities in cold regions often have more concerns about break-up floods in spring than open-water floods in summer (Gerard, 1990).

When an ice jam fails, the ensuing ice run is one of the most violent and spectacular events that can take place on a river. The stage rises very rapidly at downstream locations, and water velocities far exceed even those attained during open-water floods (Beltaos, 1995). Scouring of the riverbed and banks during major ice runs can have significant ecologic and geomorphologic effects (Prowse, 1994; Scrimgeour and others, 1994). Not all ice jams, however, fail catastrophically and cause a surge. Many simply melt in place, sometimes rapidly, and become a significant point source of additional flow that also cools the water downstream (Prowse and Marsh, 1989; Prowse, 1990). Once the ice cover has been removed from a reach, water temperatures have been known to rise from near-freezing to almost 10°C in a matter of hours (Parkinson, 1982). This warm water subsequently contributes to melting of the ice cover further downstream (Prowse, 1990).

Hydroelectric-power generation companies and their customers incur significant costs, amounting to millions of dollars, as operations are tailored to avoid high discharges that might trigger ice-jam floods downstream or low discharges that fall below the regulatory minimum (Gerard, 1990). Low discharge decreases the water supply, increases contaminant levels, and depletes oxygen, all of which have potential ecological and socioeconomic effects. High financial costs, on the order of millions of dollars, also are incurred as government agencies, businesses, and industries strive to maintain navigation and commerce on ice-covered waterways (fig. 26) and recover from periodic damage to structures and vessels caused by ice and floods (Gerard and Davar, 1995).

During break-up, aufeis can protect the river channel from what often is the major flood event of the year (Michel and others, 1986), but it also largely determines the channel routing and can act as a major flow restriction that

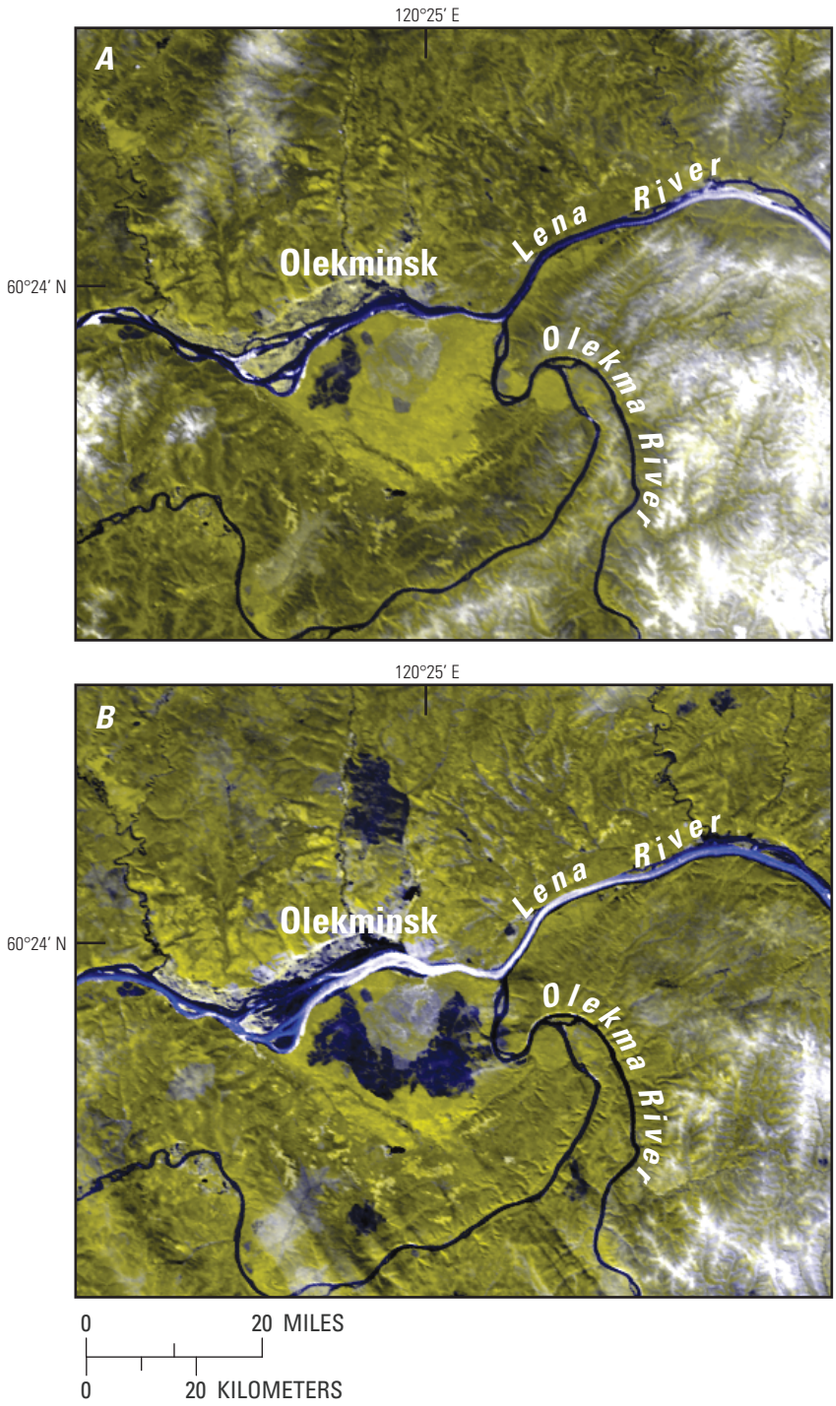

Figure 25.—*Earth Observing System (EOS) MODerate resolution Imaging Spectrometer (MODIS) (bands 1 and 2) images of the confluence of the Lena and Olekma Rivers, Russia, during break-up in spring 2000 show,* **A**, *widespread open water in both channels, except for some ice in the Lena River upstream from the confluence on 12 May, and* **B**, *an ice jam and extensive ice in the Lena River up- and downstream from the confluence causing widespread flooding on 15 May. The city of Olekminsk is located at lat 60.4°N., long 120.4°E. Each image covers an area of 105 km by 130 km on the ground.*

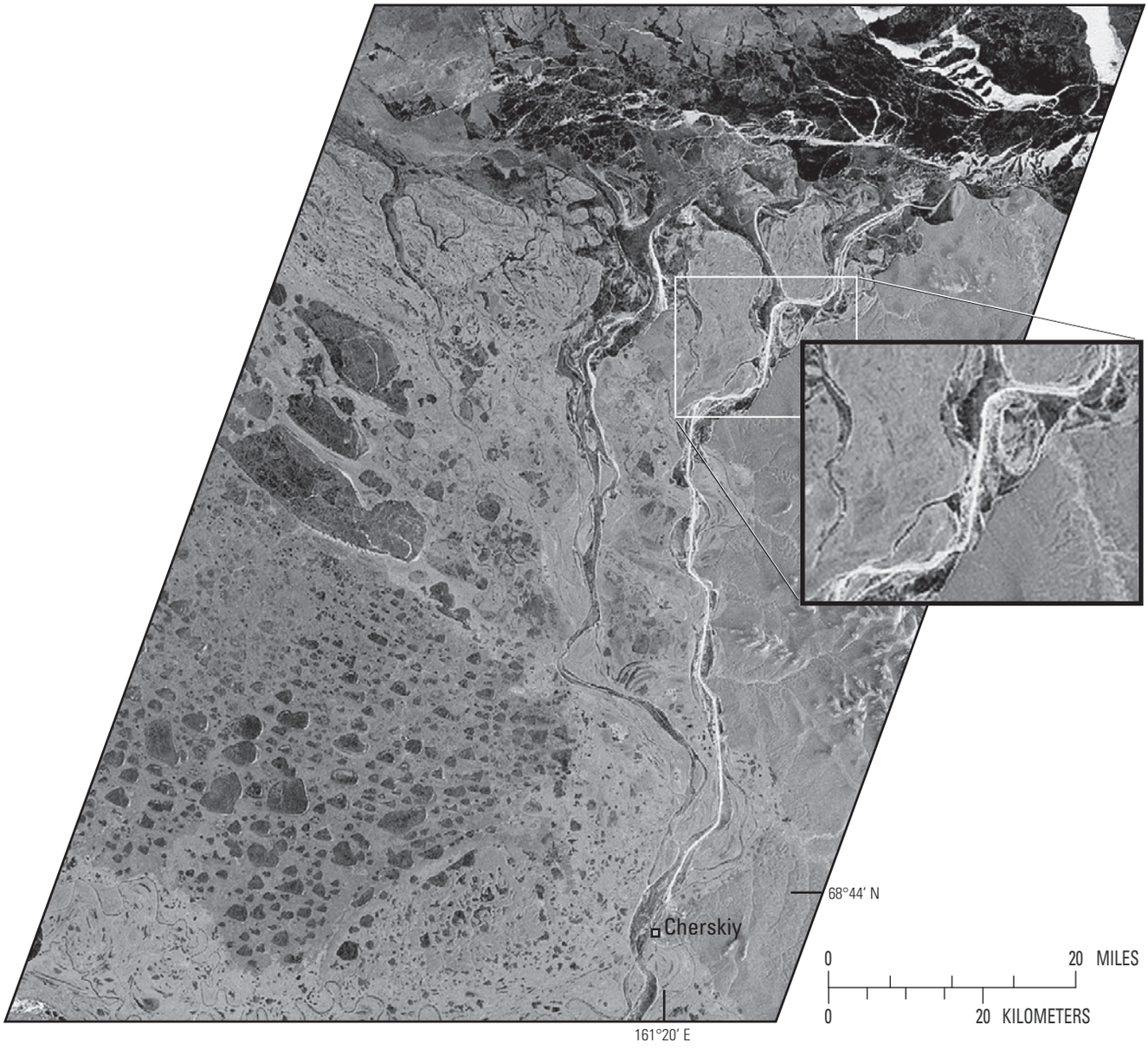

Figure 26.—*European Remote Sensing Satellite-1 (ERS-1) synthetic aperture radar (SAR) image of the Kolyma River, Russia, on 12 October 1993 showing an icebreaker track in the ice between the Arctic Ocean and the city of Cherskiy (lat 68.8°N., long 161.3°E.), a straight line distance of 100 km. The insert (center right) shows an enlarged section of the river and the icebreaker track. To the west of the river lies the Kolyma Lowland and many tundra lakes covered with new ice. The full image covers an area of 100 km by 140 km on the ground. The insert covers an area of 18 km by 24 km on the ground.*

increases flooding potential (Prowse, 1995). Aufeis can take weeks to melt after the passage of the main spring flood, and aufeis meltwater can make up a significant percentage of the summer flow in northern streams and rivers (Li and others, 1997).

Although ice-induced flooding typically has negative connotations, it also has benefits. Such floods are a major component of the water balance of lakes on the Mackenzie River delta (Marsh, 1986), where ecosystems are particularly dependent on the spring flux of sediments and nutrients that accompany the floodwater (Lesack and others, 1991). Ice-induced flooding of deltas can cause mesoscale climatic effects such as increases in air temperature that stimulate budding and early plant growth (Gill, 1974; Prowse and Reedyk, 1993). Ice-jam flooding is so integral to the function of delta ecosystems that artificial ice jams have been built on regulated rivers in an attempt to restore deltas where lakes have dried up due to the decline in natural ice-induced spring flooding (Prowse and others, 1993; Prowse, 1994).

In addition to affecting high and low discharge, ice can have a major effect on the winter hydrograph of northern streams (Gerard, 1990). The volume of water stored as ice, and as channel storage due to the increase in stage caused by the ice, can represent a significant percentage of winter flow that does not become available until spring. This is particularly important for the lake-dominated rivers of the Canadian Shield in northern Canada, where slight changes in the resistance to flow from an outlet can trigger large changes in lake storage (Gerard, 1990). On the other hand, snowfall on lake ice will increase the discharge from a lake as the snow displaces the underlying water (Jones, 1969), and in a catchment with many lakes, the effect on total river discharge can be significant (Gerard, 1990).

Through their effect on solar radiation transmission alone, an annual ice cover of long duration and the overlying blanket of snow can have a significant effect on the physics, chemistry, and biology of lakes and rivers (Adams, 1981; Scrimgeour and others, 1994). The transmission of solar radiation through the snow and ice affects the water heat budget (Likens and Ragotskie, 1965; Adams and Lasenby, 1978). Solar radiation can warm the near-surface waters to the temperature of maximum density and trigger convective mixing (Matthews and Heaney, 1987; Malm and others, 1997). This can suspend nonmotile phytoplankton in the upper water column, where light is sufficient for growth even during ice-covered periods (Matthews and Heaney, 1987; Kelley, 1997). In permafrost regions, lakes and ponds have a significant effect on the ground thermal regime (Brewer, 1958; Lachenbruch and others, 1962) and are the primary contributors to modifications of the tundra landscape (Sellmann and others, 1975). The growth and decay of ice on shallow lakes on the North Slope of Alaska play an important role in regional greenhouse gas budgets (Phelps and others, 1998) and the surface energy balance in winter (Jeffries and others, 1999).

The effects of ice on lakes are illustrated by the perennially ice-covered, meromictic lakes. The absence of mixing, or meromixis, is caused by the perennial ice that prevents turbulent mixing by the wind or convective mixing due to loss of heat from the water directly to the atmosphere (Spigel and Priscu, 1998). Consequently, the water column is very stable and often highly density-stratified, with a freshwater layer interposed between the ice and deeper saline water (fig. 22*B*). The salt gradients store solar energy leading to distinct temperature maxima and the elevated water temperatures noted earlier (fig. 22*A*). Sedimentation, biology (almost entirely microbial),

and biogeochemistry also are strongly affected by the long-term, ice-enabled water-column stability. For further information on these topics as they relate to (1) the McMurdo Dry Valleys lakes of Antarctica, see Green and Friedmann (1993) and Priscu (1998); (2) Lake A, Ellesmere Island, see Jeffries and others (1984), Belzile and others (2001), Van Hove and others (2001), and Gibson and others (2002).

Freshwater Ice and Climate

Freeze-Up, Break-Up, and Ice Duration as Climate Indicators

Meteorological factors such as air temperature, precipitation, wind speed, and radiation balance coupled with the physical characteristics of lakes and rivers (lake area, depth, volume, and fetch; river channel width, sinuosity, depth, stage, and water velocity) and of the ice itself (snow depth; ice thickness, type, and albedo) lead to complex interactions and feedbacks that affect the timing of freeze-up and break-up and thus the duration of the ice each year on lakes and rivers. Given the complexity of the system, it might seem that freeze-up, break-up, and ice duration (sometimes referred to as "phenology," a term borrowed from the biological sciences) would not be good climate indicators; however, there is ample evidence that they are primarily a function of weather and climate, particularly air temperature.

Reasons for the interest in finding relationships between ice phenology and air temperature include (1) finding a single variable that explains most of the variance in ice phenology; (2) predicting freeze-up and break-up dates for the purposes of navigation (Bilello, 1964b, 1980; Williams, 1965, 1971; Greene, 1983); (3) calibrating changes in freeze-up and break-up dates in terms of seasonal temperature anomalies and using the resultant statistical relationships to either predict the effects of climate variability and change on ice phenology or use ice phenology as a reliable indicator of future regional climate variability and change in the absence of meteorological data or other climate records (Tramoni and others, 1985; Palecki and Barry, 1986; Ginzburg and others, 1992; Robertson and others, 1992; Skinner, 1992; Soldatova, 1993; Wynne and Lillesand, 1993; Assel and Robertson, 1995; Duguay and others, 2006); and (4) using historical ice-phenology records as proxies for past climate variability and change and estimating historical changes in air temperature (Robertson and others, 1992; Assel and Robertson, 1995; Magnuson and others, 2000; Hodgkins and others, 2005).

A few examples of what has been learned about the relationship between ice phenology and air temperature at different locations and the implications for the future are provided here. In southern Finland, a 5-day change in freeze-up represents a change of 1.1°C in November mean air temperature, and a 5-day change in break-up represents a change of 1.0°C in April mean air temperature (Palecki and Barry, 1986). At Lake Mendota, Wisc., a 4.3-day change in freeze-up represents a change of 1.0°C in November–December mean air temperature, and a 3.3-day change in break-up represents a change of 1.0°C in January–March mean air temperature (Robertson and others, 1992). Should the climate continue to warm, it is predicted that the duration of the ice cover on Lake Mendota would decrease by 11 days per 1°C, and, with a warming of 4 to 5°C, there would be no ice cover every 15 to 30 years

(Robertson and others, 1992). At the current rate of decline of the ice cover at Lake Superior, it has been predicted that the lake will be ice free during typical winters from 2030 through 2040 (Austin and Colman, 2007). In the region near Great Slave Lake, Canada, a change of approximately 2.5°C in October mean air temperature would delay freeze-up by 5 to 6 days, a change of approximately 3°C in May mean air temperature would advance break-up by about 8 days, and an increase of approximately 3°C in mean air temperature between autumn and spring would reduce ice cover duration by approximately 14 days (Skinner, 1992). Relationships between ice phenology and air temperature in Russian rivers from the late 19th to the late 20th century have been used to predict freeze-up and break-up trends through 2005 (Ginzburg and others, 1992; Soldatova, 1993).

Freeze-Up, Break-Up, and Ice-Duration, Variability, and Change in the Northern Hemisphere

Long before scientists began to measure, model, and manipulate freshwater ecosystems, freshwater-ice phenology was monitored for religious and cultural reasons, for practical reasons related to transportation, and, apparently, out of simple curiosity (Magnuson and others, 2000). Today, concern about climate variability and change is another reason for continued monitoring. In addition, remote sensing can be added as a technique for observing freshwater-ice phenology over large areas, as opposed to ground-based, single-point observations that are limited by how far the human eye can see. Comparisons of satellite-derived ice phenology and ground-based, observer-derived phenology confirm the feasibility of using satellite remote sensing to contribute to future monitoring of freshwater ice (Maslanik and Barry, 1987; Wynne and Lillesand, 1993; Wynne and others, 1998), but, at the present time (2007), satellite remotely sensed records of ice phenology are few and very short compared to records of ground-based observers.

Long records of freshwater-ice phenology have been described by Magnuson and others (2000). They presented evidence for Northern Hemisphere climate change in (1) 39 records more than 100 years long of lake ice and river ice dating back as far as 1846 and (2) 3 records beginning before 1800. All these records were measured by observers on the ground. A selection of these records illustrates the key findings of Magnuson and others (2000) with regard to trends towards later freeze-up, earlier break-up, and shorter ice duration (fig. 27; table 1). On the basis of relationships between ice phenology and air temperature, such as those described in the previous section, the hemispheric changes in freeze-up and break-up correspond to an air temperature increase of 1.2°C per 100 years, consistent with greenhouse gas-forced climate warming but possibly also related to changes in solar activity (Magnuson and others, 2000).

Many long ice-phenology records are available for Russian rivers, and long-term variations and trends in freeze-up, break-up, and duration are strongly correlated with long-term air temperature variations and trends (Ginzburg and others, 1992; Soldatova, 1993; Ginzburg and Soldatova, 1996; Smith, 2000), even on regulated rivers such as the Volga (Soldatova, 1992). The Russian records also show strong regional variations in ice phenology and thus climate. For example, from the late 19th to the late 20th century, ice duration in European Russia and the Russian Far East decreased due to a combination of later freeze-up and earlier break-up, whereas in Siberia, ice duration increased

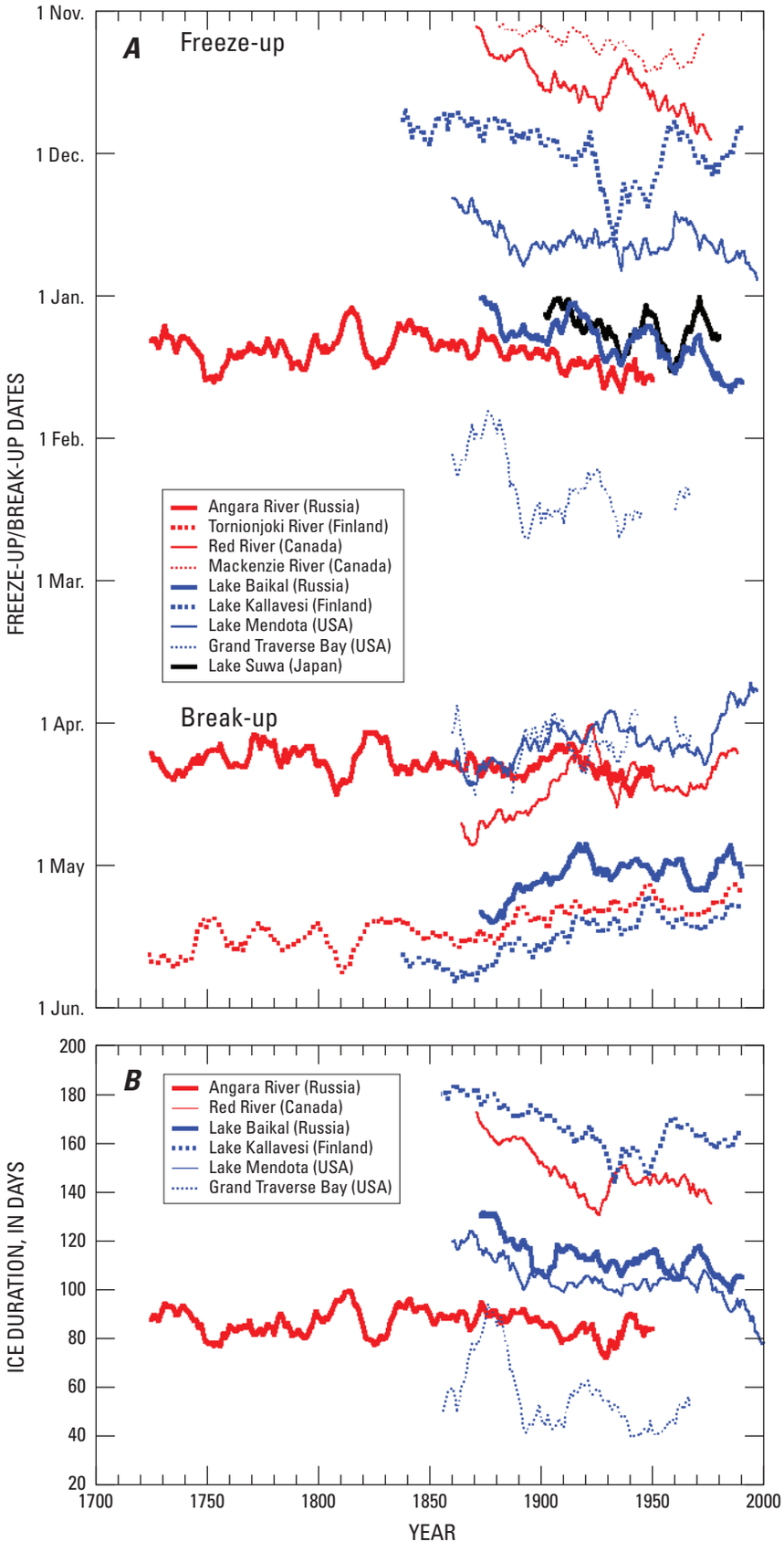

***Figure 27.—A**, Freeze-up and break-up records and **B**, ice-duration records for selected lakes and rivers in the Northern Hemisphere. The original data have been smoothed with an 11-year running average filter. Originally published by Magnuson and others (2000), the data were obtained from the National Snow and Ice Data Center, Boulder, Colo. (See also table 1.)*

Table 1.—*Trends in freeze-up, break-up, and ice duration for selected lakes and rivers*

[Locations are shown in figure 27. All values from Magnuson and others (2000); "X," no value was given by Magnuson and others (2000); —, no information available; <, less than; NA, not applicable]

Location	Freeze-up trend: days later per 100 years	*P* value	Break-up trend: days earlier per 100 years	*P* value	Ice-duration trend: days shorter per 100 years
Mackenzie River, North West Territory, Canada	6.1	0.007	X	—	—
Red River, Manitoba, Canada	13.2	<0.001	10.6	<0.001	26.1
Lake Mendota, Wisconsin, USA	6.0	0.008	7.5	0.001	13.5
Grand Traverse Bay, Michigan, USA	11.4	0.006	11.8	0.004	23.2
Tornionjoki River, Finland	X	—	6.6	<0.001	—
Lake Kallavesi, Finland	5.3	0.038	9.2	<0.001	14.5
Angara River, Eastern Russia	8.5	X	2.1	0.465	10.3
Lake Baikal, Eastern Russia	11.0	<0.001	5.1	0.004	16.1
Lake Suwa, Japan	–4.5	0.247	X	—	—
Average of above locations	[1,2]8.7	NA	[2]8.5	NA	17.2
Average of all locations	[3]5.8	NA	6.5	NA	12.3

[1]Does not include Lake Suwa because of high *P* value.

[2]Does not include Angara River because of high *P* value.

[3]Locations with records dating back as far as 1846, with the exception of Lake Suwa.

due to a combination of earlier freeze-up and later break-up (Ginzburg and others, 1992; Soldatova, 1993). Ginzburg and Soldatova (1996) predicted a further increase in duration of ice conditions in Siberia and a continued decrease in ice duration in European Russia and the Russian Far East. Regional variation in ice phenology in Russian rivers is even more evident in data from Smith (2000) than in earlier studies but this may be due primarily to methodological differences. Ginzburg and others (1992) and Soldatova (1993) analyzed regional groups of rivers, with 35 groups covering the entire continent; Smith (2000) examined the records of a single observation station on each of nine rivers flowing north to the Arctic Ocean.

Evidence for long-term changes in freshwater ice is not limited to direct measurements by observers on the ground. For example, in remote regions of the Arctic where there are no written historical records, analysis of the remains of microbiota in lake sediments has shown a climate-driven shift to shorter ice duration and a longer summer growing season since 1850 (Smol and others, 2005). This independent corroboration of the findings by Magnuson and others (2000) (later freeze-up, earlier break-up, and thus shorter ice duration since the mid-19th century) adds to the evidence for significant change in freshwater ice in the Northern Hemisphere, variability in ice phenology in Russian rivers notwithstanding.

Magnuson and others (2000) focused on the large-scale climatic implications of ice- phenology trends in a large set of records and thus reported a single, long-term temperature trend. In contrast, specific events in the ice-phenology records for Lake Mendota and Grand Traverse Bay have been examined in more detail and translated into decadal air temperature changes (Robertson and others, 1992; Assel and Robertson, 1995). At both locations,

a shift to later freeze-up and earlier break-up around 1890 indicates an early winter temperature increase of approximately 1.5°C and a late winter/early spring air temperatures increase of 1 to 1.5°C, respectively. Further transitions to earlier break-up in about 1940 and again in about 1980 correspond to an additional warming of 1.2°C in March since about 1940 and 1.1°C in January to March since about 1980, respectively.

One of the more unusual and most accurate (to the minute) records of break-up comes from the town of Nenana on the Tanana River in central Alaska. In late February or early March each year, a wooden tripod erected on the ice in the center of the river channel is connected by cable to a clock in a cabin on the south bank. The Nenana Ice Classic is then open for competition, and bets are placed on the date and time of day that the tripod will fall over, pull the cable and stop the clock, or the ice will move and carry the tripod a sufficient distance to pull the cable and stop the clock. This continuous record of the interannual variability of a specific stage of break-up dates back to 1917 (fig. 28*A*), when railroad workers first bet on when the ice would move and allow construction of a bridge across the river to begin.

A least-squares regression of the entire Nenana Ice Classic record, 1917 to 2006 (fig. 28*A*), shows that, as of spring 2004, break-up was occurring 5.4 days earlier relative to the vernal equinox than it was when the competition began (table 2). Keyser and others (2000) and Sagarin and Micheli (2001) obtained similar values for the advance of break-up through 2000. The advance of break-up is strongly related to the increase in spring mean air temperatures (Keyser and others, 2000). Sagarin and Micheli (2001) put a third-order polynomial

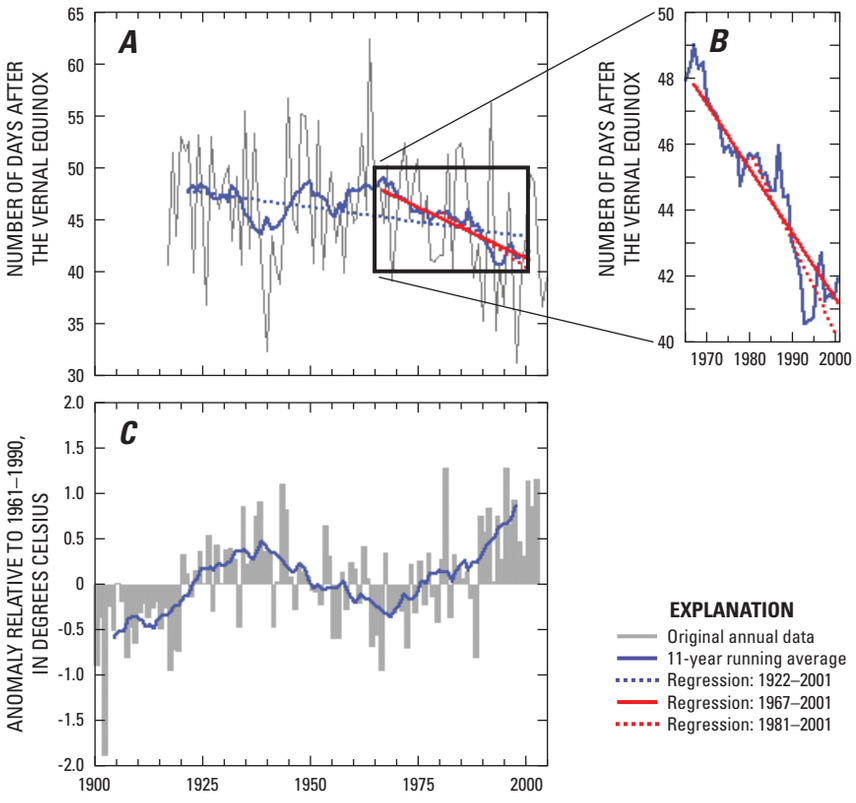

***Figure 28.**—The Nenana Ice Classic record of break-up on the Tanana River, Alaska:* **A**, *1917–2004;* **B**, *1967–2004; and* **C**, *mean annual air temperature anomalies in the Arctic, 1900–2003. Break-up is shown as number of days after the vernal equinox in order to avoid bias due to leap years (Sagarin, 2001). The area in the box in A is enlarged in B. The original break-up data were obtained from the Nenana Ice Classic Web site (http://www.nenanaakiceclassic.com/). The break-up data and the air temperature anomaly data have each been smoothed with an 11-year running average filter. (See also table 2.)*

Table 2.—*Regression analysis of filtered sections of the Nenana Ice Classic record, and change in timing of break-up relative to the vernal equinox, Tanana River, Nenana, Alaska*

[In the last column, a negative sign indicates earlier break-up and a positive sign indicates later break-up during the regression period. <, less than]

Period of filtered (and unfiltered) record	Slope	Intercept	*P* value	Coefficient of determination (r^2)	Number of days change in timing of break-up
1922–2001 (1917–2006)	–0.06	157.3	<0.0001	0.36	–5.4
1922–1969 (1917–1964)	+0.024	0.012	0.116	0.05	+1.1
1969–2001 (1964–2006)	–0.19	429.4	<0.0001	0.85	–7.8
1981–2001 (1976–2006)	–0.27	582.4	<0.0001	0.78	–8.1

regression curve through the record and related the inflections to periods of warmer (earlier break-up) and cooler (later break-up) climate during the 20th century.

Instead of a polynomial regression, the Nenana Ice Classic record has been smoothed with an 11-day moving-average filter to increase the signal-to-noise ratio (fig. 28*A*), and the results have been compared with 20th century Arctic mean annual temperature anomalies (fig. 28*C*). As reported by Sagarin and Micheli (2001), the timing of break-up on the Tanana River correlates to the major warm and cool periods of the 20th century, with relatively late break-up during the cooler 1910s–1920s and 1950s–1960s, and relatively early break-up during the warmer 1930s–1940s and since about 1970.

The smoothed record shows that break-up has been progressively earlier since the mid-1960s; since the mid-1980s, break-up has been taking place earlier than at any time since 1917. A regression analysis of the period from 1964 to 2006 (fig. 28*B*) shows that break-up was 7.8 days earlier by 2006; that is, 2.4 days longer than the change since 1917 (table 2). Prior to the mid-1960s, the timing of break-up was more variable (fig. 28*A*), and a regression analysis for 1917 to 1964 actually indicates a trend to slightly later (+1.1 days) break-up by 1964 (table 2).

At the regional level, Alaska experienced a climate change in the mid-1970s when the Pacific Decadal Oscillation (PDO) shifted from strongly negative to strongly positive; consequently, mean annual air temperature in Fairbanks, 90 km east of Nenana, increased 1.5°C (Hartmann and Wendler, 2005). The effect on break-up at Nenana has been a statistically significant post-mid-1970s shift to earlier break-up as compared to the trend from the mid-1960s to 2006 (fig. 28*C*, table 2).

Freshwater Ice and Atmospheric Teleconnections

The PDO is one of a number of indices that describe large-scale atmospheric circulation patterns, also referred to as teleconnections; a number of investigations have studied their effect on freshwater-ice phenology. El Niño, another large-scale atmospheric circulation pattern, has a greater effect

on break-up than on freeze-up throughout the Northern Hemisphere but its greatest effect is in North America (Robertson and others, 2000). El Niño causes significantly earlier break-up on lakes and rivers in Minnesota, Wisconsin, and New York, U.S.A., and Ontario, Canada (Anderson and others, 1996; Robertson and others, 2000), and also a significant reduction in the annual maximum ice area on the Great Lakes (Assel and Rodionov, 1998; Assel and others, 2003). Benson and others (2000) found 1976 North Pacific climate shift signals (PNA, Pacific/North American Pattern; WP, West Pacific Pattern) in hemispheric break-up records for lake ice, but the strongest signal was in the temperate and southern boreal regions of central and eastern North America. In Canada, Bonsal and others (2006) found the strongest responses to a variety of Pacific teleconnections (PDO, PNA, El Niño; NP, North Pacific Pattern) in the western region, with lake ice responding more strongly than river ice. Neither lake ice nor river ice respond particularly strongly to either the NAO (North Atlantic Oscillation) or AO (Arctic Oscillation) in any part of Canada, but there is a strong January–March NAO signal in the break-up record from Lake Baikal (southern Siberia, Russia) (Livingston, 1999).

Consequences of Freshwater Ice and Climate Change

The long-term records of freshwater ice freeze-up and break-up (figs. 27, 28) show a significant reduction in ice duration due to climate warming (table 1). Simulations of the effects of climate warming on lakes in cold regions predict shorter ice duration (Liston and Hall, 1995; Marsh and LeSack, 1996; Vavrus and others, 1996; Fang and Stefan, 1997a; Ménard and others, 2003) and a number of consequences, including (1) higher water temperatures and increased thermocline depth (Huttula and others, 1992; McCormick, 1990; Assel, 1991); (2) the potential elimination of anoxia and winterkill in winter but increased duration of anoxia in summer (Fang and Stefan, 1997a); and (3) decreases in fish populations and changes in species composition (Meisner and others, 1987; Hill and Magnuson, 1990). Climate warming and a reduction in ice-cover duration since 1850 on Arctic lakes and ponds also have caused significant changes in microbial ecosystems (Smol and others, 2005). In shallow lakes, ecosystems have become taxonomically more diverse and productive, with more complex community and trophic structures, while phytoplankton development has been enhanced in deeper lakes. The potential effects of climate change on the ecology of ice-covered northern rivers and lakes are discussed at length by Magnuson and others (1997).

Climate- and ice-induced changes in lake ecosystems can also take place over a very short period, as shown by observations at Experimental Lakes, Ontario, Canada (Schindler and others, 1990). From 1969 to 1987, ice duration decreased 20 days in just 18 years, as mean annual air temperature and wind speed during the open-water season increased by 2°C and 4 m s^{-1}, respectively. As the open-water season increased in length and the higher wind speeds increased mixing, the depth of the thermocline (the transition zone between warmer surface water and cooler deep water), the average lake temperature, and phytoplankton biomass and diversity increased. The microbial changes did not, however, work to the advantage of higher organisms, such as opposum shrimp and lake trout, which suffered population declines due to the warmer water. The changes observed at the Experimental Lakes are probably due to an ice-albedo positive feedback effect that has been reported at Lake Superior.

There, during the interval 1979–2006, summer water temperatures increased as the declining ice cover exposed the water to longer periods of increasing air temperatures and wind speeds (Austin and Colman, 2007).

Changes in the once-perennial ice cover on the meromictic lakes of northern Ellesmere Island (fig. 24) have produced changes in the thermal stratification of the water column. The surface mixed layer has deepened, as at the Experimental Lakes, but, unlike the Experimental Lakes, the surface waters of the Ellesmere Island lakes have cooled (D. Mueller, University of Alaska Fairbanks, written commun., 2007).

Northern lakes are sensitive to climate change because they are often covered by ice during the high solar-elevation period around the time of the summer solstice. Climate warming has the potential to greatly enhance the energy and moisture exchange over lakes by stimulating earlier thaw and increasing the absorption of solar radiation. Also, later freeze-up means more evaporative moisture can be transferred to the atmosphere (Duguay and others, 2003). At Great Slave Lake, Canada (fig. 21), for example, early break-up is in the high Sun-elevation season, which allows the low albedo (0.06) water to absorb more solar radiation. This heats the lake, promotes high evaporation in autumn and early winter prior to freeze-up, and also contributes to later freeze-up. During the 1998 El Niño, total evaporation from Great Slave Lake exceeded that of 1997 and 1999 by an average of 25 percent (Rouse and others, 2003a). Annual cumulative evaporation for 1997, 1998, and 1999 was estimated to have been 386, 505, and 420 mm, respectively (fig. 29). The difference in evaporation among the 3 years illustrates the sensitivity of the lake to both meteorological conditions and the length of the ice-free season (213 days in 1998 compared to the 1988–1999 mean of 172 days), and indicates the likely response of large northern lakes to climate warming (Rouse and others, 2003b).

The current understanding of river-ice processes is sufficient to predict that break-up will be most affected by climate change, with break-up and ice jamming becoming more or less severe, or taking place earlier, depending on local conditions (Beltaos and Burrell, 2003). The ecological consequences of

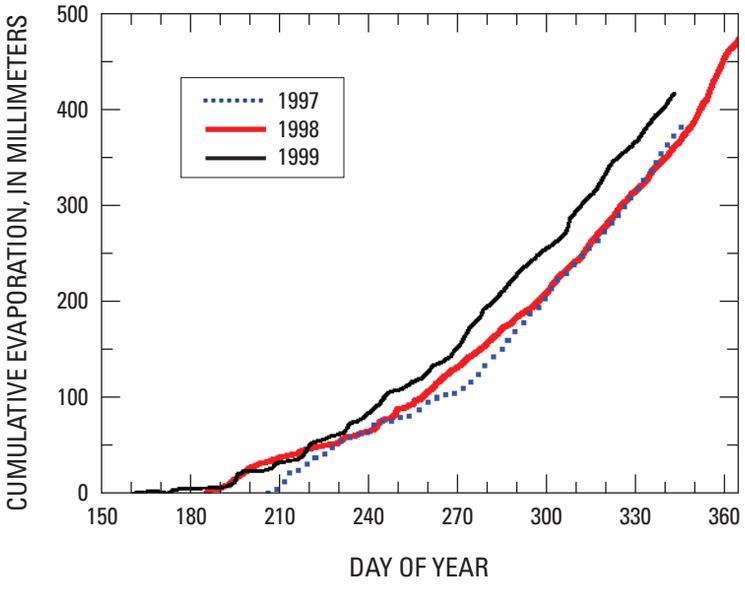

***Figure 29.**—Measured annual cumulative evaporation from Great Slave Lake for 1997, 1998, and 1999. Each curve begins at break-up and ends at freeze-up. The graph shows a longer open-water season in 1998 than in other years associated with the 1998 El Niño, which caused earlier break-up and later freeze-up.*

changes in river-ice break-up are difficult to predict because of the paucity of research on contemporary river-ice processes and their role in river ecology (Scrimgeour and others, 1994).

The trend to earlier break-up on Alaska's rivers (fig. 28) has been accompanied by a trend to more frequent thermal break-up and fewer floods (Rozell, 2005). The same phenomenon has been reported on many rivers in the Russian Arctic (Smith, 2000). A shift from intense, mechanical break-up to less severe, thermal break-up might alter aquatic and riparian community richness and structure in rivers (Scrimgeour and others, 1994; Rouse and others, 1997). A reduction in break-up flooding would benefit northern riverside communities but have adverse consequences for northern deltas, which risk desiccation and loss of habitat in the absence of spring floods (Marsh and LeSack, 1996).

Prowse and others (2002) predicted that the North American temperate zone, where mid-winter break-up events currently take place, would shift northward as winter air temperatures increased. Mid-winter break-up events are difficult to predict (Beltaos, 2002), and the associated ice jams often are more destructive than spring ice jams (S. Beltaos, National Water Research Institute, Canada, written commun., 2005). Mid-winter break-up can cause significant damage to property and infrastructure as well as serious ecological and habitat disturbance (Cunjak and others, 1998; Beltaos and others, 2003). The northward shift in the timing of mid-winter break-up is significant because of the potential for disturbance and damage in rivers that currently do not experience such events. The increased frequency of mid-winter break-up may be one of the least recognized major threats likely to result from climate change (Prowse and Bonsal, 2004).

The Future of Freshwater Ice Research

This part provides a broad overview of lake-ice and river-ice characteristics, properties, processes, evidence for change, and the consequences of change in the context of a changing climate. We have shown that, in addition to its effects on the economy and its role in society and culture, freshwater ice also has significant ecologic, hydrologic, limnologic, and geomorphologic effects. However, the smaller number of papers published on freshwater ice (fig. 15) when compared to other cryospheric subelements (for example, glaciers, snow-cover, sea ice, permafrost/periglacial phenomena) suggests that lake-ice and river-ice research has a low priority.

This conclusion is further reinforced if the historical evolution of freshwater ice observation networks across the Northern Hemisphere is examined (fig. 30). There has been a steady decrease in the number of the lake-ice and river-ice networks due to observing station closures (Shliklomanov and others, 2002), although it has been suggested that some of the decline is simply due to long delays in transferring data from the observation stations to data archives (L.C. Smith, University of California at Los Angeles, written commun., 2005). In Canada, the steep decline since the 1980s (fig. 30) can be attributed to a shift in government funding priorities that started in the 1980s and the installation of unmanned (automated) weather stations (A.E. Walker, Canadian Ice Service, Meteorological Service of Canada, written commun., 2004). Freshwater ice is a key cryospheric indicator and integrator of climate variability and change; changes can also be measured and monitored with satellite remote sensing technology.

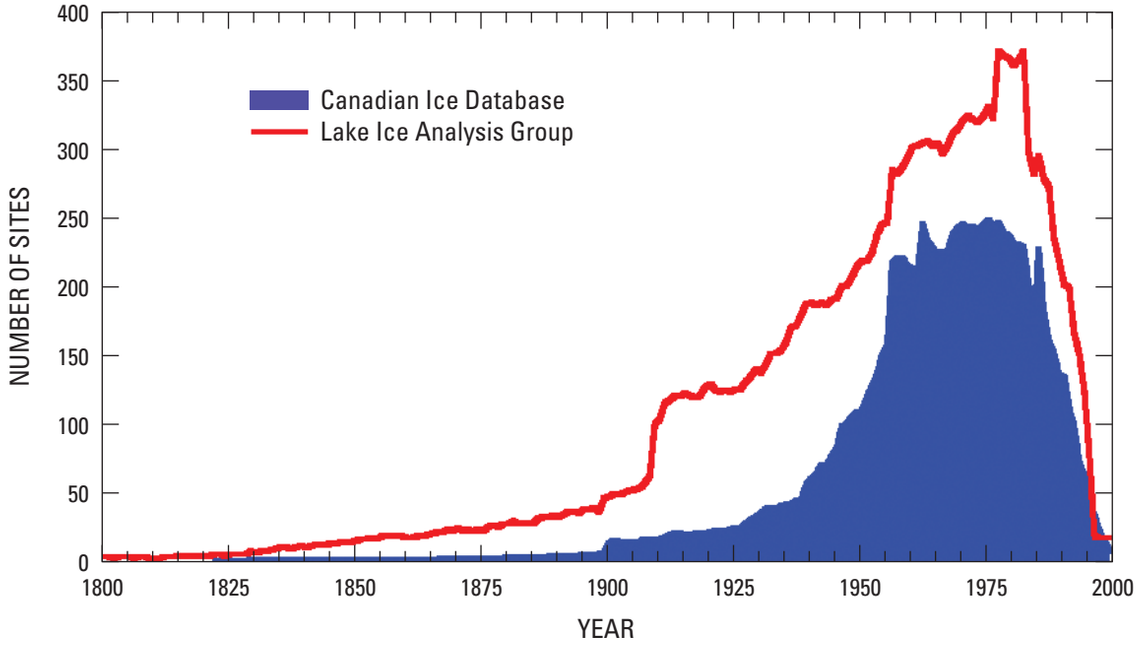

***Figure 30.**—Historical evolution of the number of lake-ice and river-ice observation sites from the Lake Ice Analysis Group (LIAG) and the Canadian Ice Database (CID) (Lenormand and others, 2002) showing a peak in the number of observation sites in the 1970s followed by a marked decline that started in the mid-1980s. The LIAG database, also known as the Global Lake and River Ice Phenology Database, is available from the National Snow and Ice Data Center (NSIDC), and the CID is available from the Canadian Cryospheric Information Network (CCIN). Some of the observations from the CID have been incorporated into the LIAG database.*

International panels of climate experts have identified and supported the need for freshwater-ice monitoring in the context of global climate-change research in reports published by the Climate and Cryosphere (CliC) Project of the World Climate Research Programme (WCRP); Global Climate Observing System (GCOS) of the World Meteorological Organization (WMO); the Integrated Global Observing Strategy (IGOS) of the United Nations Education, Scientific, and Cultural Organization (UNESCO); and the Arctic Climate Impact Assessment (ACIA) (2004, 2005).

Future progress in freshwater-ice research can be made through the support of the following activities:

- **In situ observations** can be used to improve our knowledge and understanding of freshwater-ice characteristics, properties, processes, and consequences and for the validation and improvement of remote-sensing approaches and numerical-simulation models. Existing lake-ice and river-ice sites can be reactivated and new observation sites can be added through the establishment of networks of volunteers and with schools. Such networks would have the added advantage of providing a framework for educating young students and teachers, as well as the general public, about the importance of freshwater-ice monitoring. Such observational networks have recently been established in Alaska (Alaska Lake Ice and Snow Observatory Network or ALISON: *http://www.gi.alaska.edu/alison/*) and in Canada (IceWatch: [*http://www.naturewatch.ca/english/icewatch/*].

- **Satellite remote sensing** offers the most promising means for monitoring lake-ice and river-ice phenology at regional to hemispheric scales. At present, however, few satellite remote-sensing-derived freshwater-ice products are available, and those that are available may not meet the temporal requirements set by climate programs such as GCOS (accuracy of ±1 to 2 days for freeze-up and break-up dates). In Canada, for example, the Ice Service monitors ice cover on more than 100 large lakes once every 7 days using a combination of AVHRR and RADARSAT imagery. The MODIS snow product (Hall and others, 2002) contains information on snow-covered lake-ice, but cloud cover and long periods of obscurity in winter at northern latitudes are a limiting factor, and the information has yet to be validated. MODIS also can be used for river-ice monitoring (Pavelsky and Smith, 2004) but only on large rivers due to the spatial resolution of the sensor (250 m at best). Future research should focus on (1) evaluation of the current lake-ice information provided with the MODIS snow product; (2) evaluation of the potential and limits of other sources of optical (for example, the European Space Agency Envisat [ESA] Advanced Along Track Scanning Radiometer [AATSR], and Medium Resolution Imaging Spectrometer [MERIS] instruments), and microwave (for example, NASA's EOS Aqua Advanced Microwave Scanning Radiometer [AMSR-E], ESA's Envisat Advanced Synthetic Aperture Radar [ASAR], and Canada's RADARSAT) data for ice-cover monitoring; and (3) development of approaches that make use of optical and microwave data in a synergistic manner (data fusion) to create and distribute lake- and river-ice products at a variety of spatial and temporal resolutions for operational and research needs.

- **Numerical modeling** is a useful complement to observational networks for studying the effects of climate on freshwater-ice phenology. In this context, models are useful tools for (1) determining what climatic variables are reflected in freeze-up/break-up dates and how freeze-up/break-up observations might be used as adjuncts to more conventional (for example, air temperature and precipitation) climate monitoring in data-sparse areas; (2) understanding sources of uncertainty or complications in interpreting freeze-up and break-up data (for example, confounding effects of temperature and snowfall); (3) estimating the magnitude of natural variability in freeze-up/break-up dates for use in climate-change studies; (4) estimating the potential effects of projected climate change on freeze-up and break-up dates, as well as ice thickness and ice type (congelation ice versus snow-ice); and (5) reconstructing ice phenology and filling in gaps (missing years of observations) in historical records.

- **Numerous one-dimensional thermodynamic lake-ice models** are available (for example, Liston and Hall, 1995; Vavrus and others, 1996; Fang and Stefan, 1997b; Zhang and Jeffries, 2000; Duguay and others, 2003). Each of these models has been extensively tested and shown to perform well. Jeffries and others (2005) recommended two areas for improvement: (1) ice-albedo parameterization, because current parameterizations, which are based on ice thickness rather than on albedo, do not account adequately for the large albedo difference between snow ice and congelation ice, particularly during break-up (fig. 16); and (2) the need for two- and three-dimensional lake-ice models.

- **A number of river-ice models** have been developed, mainly for engineering and process studies of a particular problem in a river reach, such as freeze-up jams, hanging dams, and break-up jams (Petryk, 1995). For an engineer or scientist, river-ice models have a number of limitations: they are often site-specific, some are proprietary, documentation may be poor, and many are simple because some processes are poorly understood (Petryk, 1995; S. Beltaos, National Water Research Institute, Canada, written commun., 2006). Simplification also can include the omission of some processes, for example mechanical break-up, which leads to poor agreement between simulated and observed ice off (for example, Greene and Outcault, 1985; Ma and Fukushima, 2002; Ma and others, 2005). Significant improvements to existing models or the development of new models will improve model-based prediction of the consequences of climate change on river ice.

Acknowledgments

This paper was written with support from National Science Foundation (NSF) grants OPP 0117645, 0326631, and 0425884 (Office of Polar Programs, Arctic Natural Sciences Program) to Martin O. Jeffries and Kim Morris, and Natural Sciences and Engineering Research Council of Canada (NSERC) and Meteorological Service of Canada (MSC) grants to Claude R. Duguay. We thank the following for their invaluable contributions: (1) the Alaska Satellite Facility and the National Aeronautics and Space Administration (NASA) for Synthetic Aperture Radar (SAR) images; (2) John C. Priscu, Montana State University, Bozeman, Montana, for the post-1988 Taylor Valley lake ice-thickness data (fig. 23); (3) Tamlin M. Pavelsky and Laurence C. Smith, University of California, Los Angeles, California, for the ice-jam flood images (fig. 25); (4) David B. Wuertz, U.S. National Climate Data Center, Asheville, North Carolina, for the Arctic temperature-anomaly data (fig. 28*C*); and (5) Wayne R. Rouse, McMaster University, Hamilton, Ontario, Canada, for the Great Slave Lake evaporation data (fig. 29). We appreciate the constructive reviews by Ray Assel, Spyros Beltaos, Peter Doran, and Larry Smith. Finally, we are very grateful to Richard S. Williams, Jr., U.S. Geological Survey, for his invitation to write this part and to be able to contribute to this introductory volume of the Satellite Image Atlas of Glaciers of the World.

References Cited

ACIA, 2004, Impacts of a warming Arctic—Arctic climate impact assessment: Cambridge, U.K., Cambridge University Press, 139 p. [*http://www.acia.uaf.edu*]

ACIA, 2005, Arctic climate impact assessment: Cambridge, U.K., Cambridge University Press, 1,042 p. [*http://www.acia.uaf.edu*]

Adams, W.P., 1976, A classification of freshwater ice: Musk-Ox, v. 18, p. 99–102.

Adams, W.P., 1981, Snow and ice on lakes, in Grey, D.M. and Male, D.H., eds., Handbook of snow and ice—Principles, processes, management and use: Toronto, Canada, Pergamon, p. 437–474.

Adams, W.P., and Lasenby, D.C., 1978, The role of ice and snow in lake heat budgets: Limnology and Oceanography, v. 23, no. 5, p. 1025–1028.

Adams, W.P., and Prowse, T.D., 1981, Evolution and magnitude of spatial patterns in the winter cover of temperate lakes: Fennia, v. 159, no. 2, p. 343–359.

Adams, W.P., and Roulet, N.T., 1980, Illustration of the roles of snow in the evolution of the winter ice cover: Arctic, v. 33, no. 1, p. 100–116.

Adams, W.P., Doran, P.T., Ecclestone, M., Kingsbury, C.M., and Allan, C.J., 1989, A rare second-year lake ice cover in the Canadian high Arctic: Arctic, v. 42, no. 4 , p. 299–306.

Ainley, D.G., Tynan, C.T., and Stirling, I., 2003, Sea ice: A critical habitat for polar marine mammals and birds, in Thomas, D.N, and Dieckmann, G.S., eds., Sea ice—An introduction to its physics, chemistry, biology and geology: Oxford, U.K., Blackwell Science, p. 240–266.

Allen, W.T.R., 1977, Freeze-up, break-up and ice thickness in Canada: Downsview, Ontario, Canada, Atmospheric Environment Service, 185 p.

Allen, W.T.R., and Cudbird, B.S.V., 1971, Freeze-up and break-up dates of water bodies in Canada: Toronto, Ontario, Canada, Meteorological Branch, Department of Transport, Report CLI-1-71, 144 p.

Alley, R., Berntsen, T., Bindoff, N.L., Chen, Z., Chidthaisong, A., and others, 2007, Climate Change 2007: The Physical Science Basis, Summary for Policymakers, Contribution of Working Group I to the Fourth Assessment Report of the Intergovernmental Panel on Climate Change, 18 p.

Anderson, W.L., Robertson, D.M., and Magnuson, J.J., 1996, Evidence of recent warming and El Niño-related variations in ice breakup of Wisconsin lakes: Limnology and Oceanography, v. 41, no. 5, p. 815–821.

Arctic Climatology Project, 2000, Environmental working group joint U.S.-Russian sea ice atlas, Tanis, F. and Smolyanitsky, V., eds: Boulder, Colorado, National Snow and Ice Data Center, CD-ROM.

Armitage, K.B., and House, H.B., 1962, A limnological reconnaissance in the area of McMurdo Sound, Antarctica: Limnology and Oceanography, v. 7, no. 1, p. 36–41.

Armstrong, T., Roberts, B., and Swithinbank, C., 1973, Illustrated glossary of snow and ice: Cambridge, U.K., Scott Polar Research Institute, Special Publication no. 4, 60 p.

Arrigo, K.R., Van Dijken, G.L., Ainley, D.G., Fahnestock, M.A., and Markus, T., 2002, Ecological impact of a large Antarctic iceberg: Geophysical Research Letters, v. 29, no. 7, doi: 10.1029/2001GL014160.

Ashton, G.D., 1980, Freshwater ice growth, motion and decay, in Colbeck, S.C., ed., Dynamics of snow and ice masses: New York, Academic Press, p. 261–304.

Ashton, G.D., ed., 1986, River and lake ice engineering: Littleton, Colorado, Water Resources Publications, 485 p.

Assel, R.A., 1991, Implications of CO_2 global warming on Great Lakes ice cover: Climatic Change, v. 18, no. 4, p. 377–395.

Assel, R.A., 2003a, An electronic atlas of Great Lakes ice cover: Ann Arbor, Michigan, NOAA Great Lakes Environmental Research Laboratory (GLERL). Available on CD-ROM and via the Internet at [*http://www.glerl.noaa.gov/data/iceatlas/*].

Assel, R.A., 2003b, Great Lakes ice cover, first ice, last ice, and ice duration: Ann Arbor, Michigan, NOAA Great Lakes Environmental Research Laboratory (GLERL), NOAA Technical Memorandum GLERL-125, 49 p.

Assel, R.A., and Robertson, D.M., 1995, Changes in winter air temperatures near Lake Michigan, 1851–1993, as determined from regional lake ice records: Limnology and Oceanography, v. 40, no. 1, p. 165–176.

Assel, R.A., and Rodionov, S., 1998, Atmospheric teleconnections for annual maximum ice cover on the Laurentian Great Lakes: International Journal of Climatology, v. 18, no. 4, p. 425–442.

Assel, R.A., Cronk, L., and Norton, D., 2003, Recent trends in Laurentian Great Lakes ice cover: Climatic Change, v. 57, nos. 1–2, p. 185–204.

Austin, J.A., and Colman, S.M., 2007, Lake Superior summer water temperatures are increasing more rapidly than regional air temperatures: A positive ice-albedo feedback: Geophysical Research Letters, v. 34, L06604, doi:10.1029/2006GL029021.

Barnes, H.T., 1906, Ice formation with special reference to anchor-ice and frazil: New York, John Wiley and Sons, 260 p.

Barnes, H.T., 1928, Ice engineering: Montréal, Québec, Renouf Publishing Company, 250 p.

Barns, R.L., and Laudise, R.A., 1985, Size and perfection of crystals in lake ice: Journal of Crystal Growth, v. 71, no. 1, p. 104–110.

Beltaos, S., 1990, Fracture and break-up of river ice cover: Canadian Journal of Civil Engineering, v. 17, no. 2, p. 173–183.

Beltaos, S., 1995, Ice jam processes, in Beltaos, S., ed., River ice jams: Highlands Ranch, Colorado, Water Resources Publications, LLC, p. 71–104.

Beltaos, S., 1997, Onset of river ice breakup: Cold Regions Science and Technology, v. 25, no. 3, p. 183–196.

Beltaos, S., 2002, Effects of climate on mid-winter ice jams: Hydrological Processes, v. 16, no. 4, p. 789–804.

Beltaos, S., 2003, Threshold between mechanical and thermal breakup of river ice cover: Cold Regions Science and Technology, v. 37, no. 1, p. 1–13.

Beltaos, S., and Burrell, B.C., 2003, Climatic change and river ice breakup: Canadian Journal of Civil Engineering, v. 30, no. 1, p. 145–155.

Beltaos, S., Ismail, S., and Burrell, B.C., 2003, Midwinter break-up and jamming on the Saint John River—A case study: Canadian Journal of Civil Engineering, v. 30, no. 1, p. 77–88.

Belzile, C., Vincent, W.F., Gibson, J.A.E., and Van Hove, P., 2001, Bio-optical characteristics of the snow, ice, and water column of a perennially ice-covered lake in the High Arctic: Canadian Journal of Fisheries and Aquatic Sciences, v. 58, no. 12, p. 2405–2414.

Bengtsson, L., 1986, Spatial variability of lake ice covers: Geografisker Annaler, v. 68A, nos. 1–2, p. 113–121.

Benson, B.J., Magnuson, J.J., Jacob, R.L., and Fuenger, S.L., 2000, Response of lake ice breakup in the Northern Hemisphere to the 1976 interdecadal shift in the North Pacific: Verhandlungen Internationale Vereingung für Limnologie, v. 27, p. 2770–2774.

Bergþórsson, P., 1969, Hafís og hitastig á liðnum öldum [Sea ice and temperature during the past centuries], in Einarsson, M.Á., ed., Hafísnn [The sea ice]: Reykjavík, Almenna Bókafélagið, p. 333–345.

Bergþórsson, P., 1970, An estimate of drift ice and temperature in Iceland in 1000 years, in Einarsson, T., ed., Symposium on drift ice and climate: Jökull, v. 19 [1969], p. 94–101.

Bilello, M.A., 1961, 1964a, Ice thickness observations—North American Arctic and Subarctic, 1958–59, 1959–60, 1960–61, 1961-62: Hanover, New Hampshire., U.S. Army Cold Regions Research and Engineering Laboratory (CRREL) CRREL Special Report 43/I, 43 p., 43/II, 87 p.

Bilello, M.A., 1964b, Method for predicting river and lake ice formation: Journal of Applied Meteorology, v. 3, no. 1, p. 38–44.

Bilello, M.A., 1980, Maximum thickness and subsequent decay of lake, river and fast sea ice in Canada and Alaska: Hanover, New Hampshire, U.S. Army Cold Regions Research and Engineering Laboratory (CRREL), CRREL Report 80–6, 160 p.

Bilello, M.A., and Bates, R.E., 1966, 1969, 1971, 1972, 1975, 1991, Ice thickness observations—North American Arctic and Subarctic, 1962–63, 1963–64, 1964–65, 1965–66, 1966–67, 1967–68, 1968–69, 1969–70, 1970–71, 1971–72, 1972–73, 1973–74: Hanover, New Hampshire, U.S. Army Cold Regions Research and Engineering Laboratory (CRREL), CRREL Special Report 43/III, 103 p., 43/IV, 127 p., 43/V, 111 p., 43/VI, 95 p., 43/VII, 103 p., 43/VIII, 127 p.

Bilello, M.A., and Lunardini, V.J., 1996, Ice thickness observations—North American Arctic and Subarctic, 1974–75, 1975–76, 1976–77: Hanover, New Hampshire, U.S. Army Cold Regions Research and Engineering Laboratory (CRREL), CRREL Special Report 43/IX, 221 p.

Bjørgo, E., Johannessen, O.M., and Miles, M.W., 1997, Analysis of merged SMMR-SSMI time series of Arctic and Antarctic sea ice parameters 1978–1995: Geophysical Research Letters, v. 24, no. 4, p. 413–416.

Bonsal, B.R., Prowse, T.D., Duguay, C.R., and Lacroix, M.P., 2006, Impacts of large-scale teleconnections on freshwater-ice duration over Canada: Journal of Hydrology v. 330, p. 340–353).

Brewer, M.C., 1958, The thermal regime of an Arctic lake: Transactions of the American Geophysical Union, v. 39, no. 2, p. 278–284.

Bromwich, D.H., and Kurtz, D.D., 1984, Katabatic wind forcing of the Terra Nova Bay polynya: Journal of Geophysical Research, v. 89, no. C3, p. 3561–3572.

Calkin, P.E., and Bull, C., 1967, Lake Vida, Victoria Valley, Antarctica: Journal of Glaciology, v. 6, no. 48, p. 833–836.

Campbell, J.E., Clites, A.H., and Greene, G.M., 1987, Measurements of ice motion in Lake Erie using satellite-tracked drifter buoys: Ann Arbor, Michigan, NOAA Great Lakes Environmental Research Laboratory (GLERL), NOAA Data Report ERL GLERL-30, 22 p.

Carleton, A.M., 2003, Atmospheric teleconnections involving the Southern Ocean: Journal of Geophysical Research, v. 108, no. C4, 8080, doi:10.1029/2000JC000379.

Carstens, T., and six others, 1986, Ice mechanics, in Ashton, G.D., ed., River and lake ice engineering: Littleton, Colorado, Water Resources Publications, p. 87–201.

Cavalieri, D.J., and Parkinson, C.L., 1981, Large-scale variations in observed Antarctic sea ice extent and associated atmospheric circulation: Monthly Weather Review, v. 109, no. 11, p. 2323–2336.

Cavalieri, D.J., Gloersen, P., and Campbell, W.J., 1984, Determination of sea ice parameters with the Nimbus-7 SMMR: Journal of Geophysical Research, v. 89, no. D4, p. 5355–5369.

Cavalieri, D.J., Gloersen, P., Parkinson, C.L., Comiso, J.C., and Zwally, H.J., 1997, Observed hemispheric asymmetry in global sea ice changes: Science, v. 278, no. 5340, p. 1104–1106.

Cavalieri, D.J., Parkinson, C.L., Gloersen, P., Comiso, J.C., and Zwally, H.J., 1999, Deriving long-term time series of sea ice cover from satellite passive-microwave multisensor data sets: Journal of Geophysical Research, v. 104, no. C7, p. 15803–15814.

Cavalieri, D.J., Parkinson, C.L., and Vinnikov, K.Y., 2003, 30-year satellite record reveals contrasting Arctic and Antarctic decadal sea ice variability: Geophysical Research Letters, v. 30, no. 18, 1970, doi:10.1029/2003GL018031.

Chapman, W.L., and Walsh, J.E., 1993, Recent variations of sea ice and air temperature in high latitudes: Bulletin of the American Meteorological Society, v. 74, no. 1, p. 33–47.

Cherepanov, N.V., 1970, Role of thermal regime of the water body in formation of the crystal structure of ice: Problems of the Arctic and the Antarctic, v. 29–32, p. 56–64.

Chinn, T., 1993, Physical hydrology of the Dry Valley lakes, in Green, W.J., and Friedmann, E.I., eds., Physical and biogeochemical processes in Antarctic lakes: Washington, D.C., American Geophysical Union, Antarctic Research Series, v. 59, p. 1–51.

Colony, R., and Thorndike, A.S., 1984, Arctic Ocean drift tracks from ships, buoys and manned research stations, 1872–1973: Boulder, Colorado, National Snow and Ice Data Center, digital media.

Comiso, J.C., Cavalieri, D.J., and Markus, T., 2003, Sea ice concentration, ice temperature, and snow depth using AMSR-E data: Institute of Electrical and Electronic Engineers (IEEE) Transactions on Geoscience and Remote Sensing, v. 41, no. 2, p. 243–252.

Croxall, J.P., Trathan, P.N., and Murphy, E.J., 2002, Environmental change and Arctic seabird populations: Science, v. 297, no. 5586, p. 1510–1514.

Cubasch, U., and Cess, R.D., 1990, Processes and modelling, in Houghton, J.T., Jenkins, G.J., and Ephraums, J.J., eds., Climate change—The IPCC scientific assessment: Published for the Intergovernmental Panel on Climate Change, Cambridge, U.K., Cambridge University Press, p. 69–71.

Cunjak, R.A., Prowse, T.D., and Parrish, D.L., 1998, Atlantic salmon (*Salmo salar*) in winter: "the season of parr discontent"?: Canadian Journal of Fisheries and Aquatic Sciences, v. 55, supplement no. 1, p. 161–180.

Dehn, W., 2002, Arctic sea ice charts, 1953–1986: W. Dehn collection: Boulder, Colorado, National Snow and Ice Data Center, digital media.

Derocher, A.N., Lunn, N.J., and Stirling, I., 2004, Polar bears in a warming climate: Integrative and Comparative Biology, v. 44, no. 2, p. 163–176.

Deser, C., Walsh, J.E., and Timlin, M.S., 2000, Arctic sea ice variability in the context of recent atmospheric circulation trends: Journal of Climate, v. 13, no. 3, p. 617–633.

Doran, P.T., 1993, Sedimentology of Colour Lake, a non-glacial High Arctic lake, Axel Heiberg Island, N.W.T., Canada: Arctic and Alpine Research, v. 25, no. 4, p. 353–367.

Doran, P.T., McKay, C.P., Adams, W.P., English, M.C., Wharton, R.A., Jr., and Meyer, M.A., 1996, Climate forcing and thermal feedback of residual ice covers in the high Arctic: Limnology and Oceanography, v. 41, no. 5, p. 839–848.

Doran, P.T., Wharton, R.A., Jr., Lyons, W.B., Des Marais, D.J., and Andersen, D.T., 2000, Sedimentology and geochemistry of a perennially ice-covered epishelf lake in the Bunger Hills Oasis, East Antarctica: Antarctic Science, v. 12, no. 2, p. 131–140.

Doran, P.T., and twelve others, 2002, Antarctic climate cooling and terrestrial ecosystem response: Nature, v. 415, no. 6871, p. 517–520.

Doran, P.T., Fritsen, C.H., McKay, C.P., Priscu, J.C., and Adams, E.E., 2003, Formation and character of an ancient 19-m ice cover and underlying trapped brine in an "ice-sealed" east Antarctic lake: Proceedings, National Academy of Sciences, v. 100, no. 1, p. 26–31.

Doran, P.T., Priscu, J.C., Lyons, W.B., Powell, R.D., Andersen, D.T., and Poreda, R.J., 2004, Paleolimnology of extreme cold terrestrial and extraterrestrial environments, in Pienitz, R., Douglas, M.S.V., and Smol, J.P., eds., Long-term environmental change in Arctic and Antarctic lakes: Dordrecht, The Netherlands, Kluwer, p. 475–507.

Duguay, C.R., Flato, G.M., Jeffries, M.O., Ménard, P., Morris, K., and Rouse, W.R., 2003, Ice cover variability on shallow lakes at high latitudes—Model simulations and observations: Hydrological Processes, v. 17, no. 17, p. 3465–3483.

Duguay, C.R., Prowse, T.D., Bonsal, B.R., Brown, R.D., Lacroix, M.P., and Ménard, P., 2006, Recent trends in Canadian lake ice cover: Hydrological Processes, v. 20, no. 4, p. 781–801.

Fang, X., and Stefan, H.G., 1997a, Simulated climate change effects on dissolved oxygen characteristics in ice-covered lakes: Ecological Modeling., v. 103, nos. 2–3, p. 209–229.

Fang, X., and Stefan, H.G., 1997b, Simulated climate change effects on ice and snow cover on lakes in a temperate region: Cold Regions Science and Technology, v. 25, no. 2, p. 137–152.

Fetterer, F., and Troisi, V., 1997, AARI 10-day Arctic Ocean EASE-grid sea ice observations: Boulder, Colorado, National Snow and Ice Data Center, digital media.

Folland, C.K., Karl, T.R., and Vinnikov, K.Y., 1990, Observed climate variations and change, in Houghton, J.T., Jenkins, G.J., and Ephraums, J.J., eds., Climate change—The IPCC scientific assessment: Published for the Intergovernmental Panel on Climate Change, Cambridge, U.K., Cambridge University Press, p. 195–238.

Folland, C.K., Karl, T.R., Christy, J.R., Clarke, R.A., Gruza, G.V., Jouzel, J., Mann, M.E., Oerlemans, J., Salinger, M.J., and Wang, S.-W., 2001, Observed climate variability and change, in Houghton, J.T., Ding, Y., Griggs, D.J., Noguer, M., van der Linden, P.J., Dai, X., Maskell, K., and Johnson, C.A., eds., Climate change 2001—The scientific basis: Contribution of Working Group I to the Third Assessment Report of the Intergovernmental Panel on Climate Change, Cambridge, U.K., Cambridge University Press, p. 99–181.

Fowler, C., 2003, Polar Pathfinder daily 25 km EASE-Grid sea ice motion vectors: Boulder, Colorado, National Snow and Ice Data Center, digital media.

Fowler, C., Maslanik, J., Haran, T., Scambos, T., Key, J., and Emery, W., 2000, Updated 2002, AVHRR Polar Pathfinder twice-daily 5 km EASE-grid composites: Boulder, Colorado, National Snow and Ice Data Center, digital media.

Gerard, R., 1990, Hydrology of floating ice, in Prowse, T.D., and Ommanney, C.S.L., eds., Northern hydrology—Canadian perspectives: Saskatoon, Saskatchewan, Canada, National Hydrology Research Institute, NHRI Science Report no. 1. p. 103–134.

Gerard, R.L., and Davar, K.S., 1995, Introduction, in Beltaos, S., ed., River ice jams: Highlands Ranch, Colorado, Water Resources Publications, LLC, p. 1–28.

Gerard, R.L., and Stanley, S., 1988, Ice jams and flood forecasting, Hay River, N.W.T.: Edmonton, Alberta, University of Alberta, Department of Civil Engineering, Water Resources Engineering Report no. 88–6, 199 p.

Gibson, J.A.E., Vincent, W.F., Van Hove, P., Belzile, C., Wang, X., and Muir, D., 2002, Geochemistry of ice-covered, meromictic Lake A in the Canadian High Arctic: Aquatic Geochemistry, v. 8, no. 2, p. 97–119.

Gill, D., 1974, Significance of spring breakup to the bioclimate of the Mackenzie Delta, in Reed, J.C., and Sater, J.E., eds., The coast and shelf of the Beaufort Sea: Arlington, Virginia, The Arctic Institute of North America, p. 543–544.

Ginzburg, B.M., and Soldatova, I.I., 1996, Long-term oscillations of river freezing and break-up dates in different geographic zones: Russian Meteorology and Hydrology, v. 6, p. 80–85.

Ginzburg, B.M., Polakova, K.N., and Soldatova, I.I., 1992, Secular changes in dates of ice formation on rivers and their relationship with climate: Soviet Meteorology and Hydrology, v. 12, p. 57–64.

Gloersen, P., 1995, Modulations of hemispheric sea-ice cover by ENSO events: Nature, v. 373, no. 6514, p. 503–506.

Gloersen, P., and Barath, F.T., 1977, A scanning multichannel microwave radiometer for Nimbus-G and SeaSat-A: Institute of Electrical and Electronics Engineers (IEEE) Journal of Oceanic Engineering, v. OE-2, no. 2, p. 172–178.

Gloersen, P., Campbell, W.J., Cavalieri, D.J., Comiso, J.C., Parkinson, C.L., and Zwally, H.J., 1992, Arctic and Antarctic sea ice, 1978–1987: Satellite passive-microwave observations and analysis: Washington, D.C., National Aeronautics and Space Administration (NASA) Special Publication, SP-511, 290 p.

Gloersen, P., Parkinson, C.L., Cavalieri, D.J., Comiso, J.C., and Zwally, H.J., 1999, Spatial distribution of trends and seasonality in the hemispheric sea ice covers: 1978–1996: Journal of Geophysical Research, v. 104, no. C9, p. 20827–20836.

Gow, A.J., 1986, Orientation textures in ice sheets of quietly frozen lakes: Journal of Crystal Growth, v. 74, no. 2, p. 247–258.

Gow, A.J., and Langston, D., 1977, Growth history of lake ice in relation to its stratigraphic, crystalline and mechanical structure: Hanover, New Hampshire, U.S. Army Cold Regions Research and Engineering Laboratory (CRREL), CRREL Report 77-1, 24 p.

Gradinger, R., 1995, Climate change and biological oceanography of the Arctic Ocean: Philosophical Transactions of the Royal Society of London, Series A, v. 352, no. 1699, p. 277–286.

Gray, D.M., and Prowse, T.D., 1993, Snow and floating ice, in Maidment, D., ed., Handbook of hydrology: New York, McGraw Hill, p. 7.1–7.58.

Green, W.J., and Friedmann, E.I., eds., 1993, Physical and biogeochemical processes in Antarctic lakes: Washington, D.C., American Geophysical Union, Antarctic Research Series, v. 59, 216 p.

Greene, G.M., 1983, Forecasting ice-cover freeze-up, growth and breakup on the St. Marys River: Ann Arbor, Michigan, NOAA Great Lakes Environmental Research Laboratory (GLERL), NOAA Technical Memorandum ERL GLERL-47, 82 p.

Greene, G.M., and Outcault, S.I., 1985, A simulation model of river ice thermodynamics: Cold Regions Science and Technology, v. 10, no. 3, p. 251–262.

Grumet, N.S., Wake, C.P., Mayewski, P.A., Zielinski, G.A., Whitlow, S.I., Koerner, R.M., Fisher, D.A., and Woollett, J.M., 2001, Variability of sea-ice extent in Baffin Bay over the last millennium: Climate Change, v. 49, nos. 1–2, p. 129–145.

Hall, A., and Visbeck, M., 2002, Synchronous variability in the Southern Hemisphere atmosphere, sea ice, and ocean resulting from the annular mode: Journal of Climate, v. 15, no. 21, p. 3043–3057.

Hall, D.K., Riggs, G.A., Salomonson, V.V., DiGirolamo, N.E., and Bayr, K.J., 2002, MODIS snow-cover products: Remote Sensing of Environment, v. 83, no. 1–2, p. 181–194.

Hall, D.K., Key, J.R., Casey, K.A., Riggs, G.A., and Cavalieri, D.J., 2004, Sea ice surface temperature product from MODIS: Institute of Electrical and Electronic Engineers (IEEE) Transactions on Geoscience and Remote Sensing, v. 42, no. 5, p. 1076–1087.

Hartmann, B., and Wendler, G., 2005, The significance of the 1976 Pacific climate shift in the climatology of Alaska: Journal of Climate, v. 18, no. 22, p. 4824–4839.

Hattersley–Smith, G., and Serson, H., 1970, Mass balance of the Ward Hunt Ice Rise and Ice Shelf—A 10 year record: Journal of Glaciology, v. 9, no. 56, p. 247–252.

Hattersley–Smith, G., Keys, J.E., Serson, H., and Mielke, J. E., 1970, Density stratified lakes in northern Ellesmere Island: Nature, v. 225, no. 5227, p. 55–56.

Heywood, R.B., 1972, Antarctic limnology—A review: British Antarctic Survey Bulletin, v. 29, p. 35–65.

Hill, B.T., Ruffman, A., and Drinkwater, K., 2002, Historical record of the incidence of sea ice on the Scotian Shelf and the Gulf of St. Lawrence, in Squire, V.A., and Langhorne, P.J., eds., Ice in the environment: International Association of Hydraulic Engineering and Research (IAHR), 16th International Symposium on Ice in the Environment (Dunedin, New Zealand, 2–6 December 2002) Proceedings: Department of Physics, University of Otago, v. 3, p. 16–24.

Hill, D.K., and Magnuson, J.J., 1990, Potential effects of global climate warming on the growth and prey consumption of Great Lakes fish: Transactions of the American Fisheries Society, v. 119, no. 2, p. 265–275.

Hodgkins, G.A., Dudley, R.W., and Huntington, T.G., 2005, Changes in the number and timing of days of ice-affected flow on northern New England rivers, 1930–2000: Climatic Change, v. 71, no. 3, p. 319–340.

Hurrell, J.W., 1995, Decadal trends in the North Atlantic Oscillation—Regional temperatures and precipitation: Science, v. 269, no. 5224, p. 676–679.

Hurrell, J.W., and van Loon, H., 1997, Decadal variations in climate associated with the North Atlantic Oscillation: Climatic Change, v. 36, nos. 3/4, p. 301–326.

Huttula, T., Peltonen, A., Bilaletdin, A., and Saura, M., 1992, The effects of climatic change on lake ice and water temperature: Aqua Fennica, v. 22, no. 2, p. 129–142.

Ito, H., 1982, Sea ice atlas of northern Baffin Bay: Zürich, Switzerland, Swiss Federal Institute of Technology, Department of Geography, 142 p.

Jacobs, S.S., and Comiso, J.C., 1997, Climate variability in the Amundsen and Bellingshausen Seas: Journal of Climate, v. 10, no. 4, p. 697–709.

Jeffries, M.O., 2002, Ellesmere Island ice shelves and ice islands, in Williams, R.S., Jr., and Ferrigno, J.G., eds. Satellite Image Atlas of Glaciers of the World: U. S. Geological Survey Professional Paper 1386-J (Glaciers of North America), p. J147–J164.

Jeffries, M.O., and Krouse, H.R., 1985, Isotopic and chemical investigations of two stratified lakes in the Canadian Arctic: Zeitschrift für Gletscherkunde und Glazialgeologie, v. 21, p. 71–78.

Jeffries, M.O., and Morris, K., 2007, Some aspects of ice phenology on ponds in central Alaska: Annals of Glaciology, v. 46, p. 397–403.

Jeffries, M.O., Krouse, H.R., Shakur, M.A., and Harris, S.A., 1984, Isotope geochemistry of stratified Lake "A", Ellesmere Island, N.W.T., Canada: Canadian Journal of Earth Sciences, v. 21, no. 9, p. 1008–1021.

Jeffries, M.O., Morris, K., Weeks, W.F., and Wakabayashi, H., 1994, Structural-stratigraphic features and ERS-1 SAR backscatter characteristics of ice growing on shallow lakes in N.W. Alaska, winter 1991–92: Journal of Geophysical Research., v. 99, no. C11, p. 22459–22471.

Jeffries, M.O., Li, S., Jaña, R.A., Krouse, H.R., and Hurst-Cushing, B., 1998, Late winter first-year ice floe thickness variability, seawater flooding and snow ice formation in the Amundsen and Ross seas, in Jeffries, M.O., ed., Antarctic sea ice—Physical processes, interactions and variability: Washington, D.C., American Geophysical Union, Antarctic Research Series, v. 74, p. 69–87.

Jeffries, M.O., Zhang, T., Frey, K., and Kozlenko, N., 1999, Estimating late winter heat flow to the atmosphere from the lake-dominated Alaskan North Slope: Journal of Glaciology, v. 45, no. 150, p. 315–324.

Jeffries, M.O., Krouse, H.R., Hurst-Cushing, B., and Maksym, T., 2001, Snow ice accretion and snow cover depletion on Antarctic first-year sea ice floes: Annals of Glaciology, v. 33, p. 51–60.

Jeffries, M.O., Morris, K., and Duguay, C.R., 2005, Lake ice growth and decay in central Alaska—Observations and computer simulations compared: Annals of Glaciology, v. 40, p. 195–199.

Jeffries, M.O., Morris, K., and Kozlenko, N., 2005, Ice characteristics & processes, and remote sensing of frozen rivers and lakes, in Duguay, C.R., and Pietroniero, A. , eds., Remote sensing in northern hydrology—Measuring environmental change: Washington, DC, American Geophysical Union, AGU Monograph 163, p. 91–118.

Jevrejeva, S., 2001, Severity of winter seasons in the northern Baltic Sea between 1529 and 1990: Reconstruction and analysis: Climate Research, v. 17, no. 1, p. 55–62.

Johannessen, O.M., Miles, M., and Bjørgo, E., 1995, The Arctic's shrinking sea ice: Nature, v. 376, no. 6536, p. 126–127.

Johannessen, O.M., Shalina, E.V., and Miles, M.W., 1999, Satellite evidence for an Arctic sea ice cover in transformation: Science, v. 286, no. 5446, p. 1937–1939.

Jones, J.A.A., 1969, The growth and significance of white ice at Knob Lake, Québec: Canadian Geographer, v. 8, no. 4, p. 354–372.

Jouzel, J., and nine others, 1999, More than 200 meters of lake ice above subglacial Lake Vostok: Science, v. 286, no. 5447, p. 2138–2141.

Kawanishi, T., Sezai, T., Ito, Y., Imaoka, K., Takeshima, T., Ishido, Y., Shibata, A., Miura, M., Inahata, H., and Spencer, R.W., 2003, The Advanced Microwave Scanning Radiometer for the Earth Observing System (AMSR-E), NASDA's contribution to the EOS for global energy and water cycle studies: Institute of Electrical and Electronics Engineers (IEEE) Transactions on Geoscience and Remote Sensing, v. 41, no. 2, p. 184–194.

Kelley, D.E., 1997, Convection in ice-covered lakes—Effects on algal suspension: Journal of Plankton Research, v. 19, no. 12, p. 1859–1880.

Kennicutt, II, M., and Petit, J.-R., 2007, Future directions in subglacial environments research: EOS (Transactions, American Geophysical Union), v. 88, no. 11, p. 129 and p. 131.

Key, J., and Haefliger, M., 1992, Arctic ice surface temperature retrieval from AVHRR thermal channels: Journal of Geophysical Research, v. 97, no. D5, p. 5885–5893.

Keyser, A.R., Kimball, J.S., Nemani, R.R., and Running, S.W., 2000, Simulating the effects of climate change on the carbon balance of North American high-latitude forests: Global Change Biology, v. 6, Supplement no. 1, p. 185–195.

Knight, C.A., 1962, Studies of Arctic lake ice: Journal of Glaciology, v. 4, no. 33, p. 319–335.

Koch, L., 1945, The East Greenland ice: Meddelelser om Grønland, v. 130, no. 3, p. 1–375.

Kukla, G., and Gavin, J., 1981, Summer ice and carbon dioxide: Science, v. 214, no. 4520, p. 497–503.

Kwok, R., 2000, Recent changes in Arctic Ocean sea ice motion associated with the North Atlantic Oscillation: Geophysical Research Letters, v. 27. no. 6, p. 775–778.

Kwok, R., and Comiso, J.C., 2002, Spatial patterns of variability in Antarctic surface temperature—Connections to the Southern Hemisphere Annular Mode and the Southern Oscillation: Geophysical Research Letters, v. 29, no. 14, doi:10.1029/2002GL015415.

Kwok, R., and Rothrock, D.A., 1999, Variability of Fram Strait ice flux and North Atlantic Oscillation: Journal of Geophysical Research, v. 104, no. C3, p. 5177–5189.

Kwok, R., Zwally, H.J., and Yi, D., 2004, ICESat observations of Arctic sea ice: A first look: Geophysical Research Letters, v. 31, L16401, doi:10.1029/2004GL020309.

Lachenbruch, A.H., Brewer, M.C., Greene, G.W., and Marshall, B.V., 1962, Temperatures in permafrost: Temperature—its measurement and control in science and industry, v. 3, no. 1, p. 791–803.

Lange, M., Schlosser, P., Ackley, S.F., Wadhams, P., and Dieckmann, G.S., 1989, ^{18}O concentrations in sea ice of the Weddell Sea: Journal of Glaciology, v. 36, no. 124, p. 315–323.

Larsen, P., and five others, 1986, Thermal regime of lakes and rivers, in Ashton, G.D., ed., River and lake ice engineering: Littleton, Colorado, Water Resources Publications, p. 203–260.

Laxon, S., Peacock, N., and Smith, D., 2003, High interannual variability of sea ice thickness in the Arctic region: Nature, v. 425, no. 6961, p. 947–950.

Leconte, R., and Klassen, P.D., 1991, Lake and river ice investigations in northern Manitoba using airborne SAR imagery: Arctic, v. 44, Supplement no. 1, p. 153–163.

LeDrew, E., Barber, D., Agnew, T., and Dunlap, D., 1992, Canadian sea ice atlas from microwave remotely sensed imagery: July 1987 to June 1990: Ottawa, Canada, Canada Communication Group-Publishing, 80 p.

Lefebvre, W., Goosse, H., Timmermann, R., and Fichefet, T., 2004, Influence of the Southern Annular Mode on the sea ice-ocean system: Journal of Geophysical Research, v. 109, no. C9, C09005, doi:10.1029/2004JC002403.

Lenormand, F., Duguay, C.R., and Gauthier, R., 2002, Development of a historical ice database for the study of climate change in Canada: Hydrological Processes, v. 16, no. 18, p. 3707–3722.

Lesack, L.W.F., Hecky, R.E., and Marsh, P., 1991, The influence of frequency and duration of flooding on the nutrient chemistry of Mackenzie Delta lakes, in Marsh, P., and Ommanney, C.S.L., eds., Mackenzie Delta, environmental interactions and implications of development: Saskatoon, Saskatchewan, National Hydrology Research Institute, NHRI Symposium no. 4, p. 19–36.

Li, S., Benson, C., Shapiro, L., and Dean, K., 1997, Aufeis in the Ivishak River, Alaska, mapped from satellite radar interferometry: Remote Sensing of Environment, v. 60, no. 2, p. 131–139.

Likens, G.E., and Ragotskie, R.A., 1965, Vertical water motion in a small, ice-covered lake: Journal of Geophysical Research, v. 70, no. 10, p. 2333–2344.

Liston, G.E., and Hall, D.K., 1995, Sensitivity of lake freeze-up and break-up to climate change—A physically based modelling study: Annals of Glaciology, v. 21, p. 387–393.

Liu, A.K., Zhao, Y., and Wu, S.Y., 1999, Arctic sea ice drift from wavelet analysis of NSCAT and special sensor microwave imager data: Journal of Geophysical Research, v. 104, no. C5, p. 11529–11538.

Livingston, D.M., 1999, Ice break-up on southern Lake Baikal and its relationship to local and regional air temperatures in Siberia and the North Atlantic Oscillation: Limnology and Oceanography, v. 44, no. 6, p. 1486–1497.

Long, D.G., Hardin, P.J., and Whiting, P.T., 1993, Resolution enhancement of spaceborne scatterometer data: Institute of Electrical and Electronics Engineers (IEEE) Transactions on Geoscience and Remote Sensing, v. 31, no. 3, p. 700–715.

Ludlam, S.D., 1996, Stratification patterns in Taconite Inlet, Ellesmere Island, N.W.T.: Journal of Paleolimnology, v. 16, no. 2, p. 205–215.

Ma, X., and Fukushima, Y., 2002, A numerical model of the river freezing process and its application to the Lena River: Hydrological Processes, v. 16, no. 11, p. 2131–2140.

Ma, X., Yasunari, T., Ohata, T., and Fukushina, Y., 2005, The influence of river ice on spring runoff in the Lena River, Siberia: Annals of Glaciology, v. 40, p. 123–127.

Magnuson, J.J., and eleven others, 1997, Potential effects of climate change on aquatic systems—Laurentian Great Lakes and Precambrian Shield Region: Hydrological Processes, v. 11, no. 8, p. 825–871.

Magnuson, J.J., and thirteen others, 2000, Historical trends in lake and river ice cover in the northern hemisphere: Science, v. 289, no. 5485, p. 1743–1746.

Malm, J., and six others, 1997, Temperature and salt content regimes in three shallow ice-covered lakes—1. Temperature, salt content and density structure: Nordic Hydrology, v. 28, no. 2, p. 99–128.

Marsh, P., 1986, Modelling water levels for a lake in the Mackenzie Delta, in Kane, D.L., ed., Cold Regions Hydrology Symposium, Proceedings: Bethesda, Maryland, American Water Resources Association, p. 23–29.

Marsh, P., and LeSack, L.F.W., 1996, Hydrologic regime of perched lakes in the Mackenzie Delta—Potential responses to climate change, in Symposium on Regional Assessment of Freshwater Ecosystems and Climate Change in North America, Leesburg, Virginia, 24–26 October 1994, Proceedings, p. 849–856.

Maslanik, J.A., and Barry, R.G., 1987, Lake ice formation and breakup as an indicator of climate change—Potential for monitoring using remote sensing techniques, in The influence of climate change and climatic variability on the hydrologic regime and water resources, Proceedings of the Vancouver Symposium, August 1987: International Association of the Hydrological Sciences IAHS Publication no. 168, p. 153–160.

Massom, R.A., 1991, Satellite remote sensing of polar regions: London, Belhaven Press, 307 p.

Matthews, P.C., and Heaney, S.I., 1987, Solar heating and its influence on mixing in ice-covered lakes: Freshwater Biology, v. 18, no. 1, p. 135–149.

Maykut, G.A., 1978, Energy exchange over young sea ice in the central Arctic: Journal of Geophysical Research, v. 83, no. C7, p. 3646–3658.

McCormick, M.J., 1990, Potential changes in thermal structure and cycle of Lake Michigan due to global warming: Transactions, American Fisheries Society, v. 119, no. 2, p. 183–194.

McKay, C.P., Clow, G.D., Wharton, R.A., Jr., and Squyres, S.W., 1985, Thickness of ice on perennially frozen lakes: Nature, v. 313, no. 6003, p. 561–562.

McLaren, A.S., Walsh, J.E., Bourke, R.H., Weaver, R.L., and Wittmann, W., 1992, Variability in sea-ice thickness over the North Pole from 1977 to 1990: Nature, v. 358, no. 6383, p. 224–226.

Meisner, J.D., Goodier, J.L., Regier, H.A., Shuter, B.J., and Christie, W.J., 1987, An assessment of the effects of climate warming on Great Lakes basin fishes: Journal of Great Lakes Research, v. 13, no. 3, p. 340–352.

Melloh, R.A., Eppler, D.T., Farmer, L.D., Gatto, L.W., and Chacho, E.F., 1991, Interpretation of passive microwave imagery of surface snow and ice, Harding Lake, Alaska: Hanover, New Hampshire, U.S. Army Cold Regions Research and Engineering Laboratory, (CRREL), CRREL Report 91–11, 30 p.

Mellor, J.C., 1982, Bathymetry of Alaskan Arctic lakes—a key to resource inventory with remote sensing methods: Ph.D. dissertation, University of Alaska, Fairbanks, Alaska, 342 p.

Mellor, J.C., 1994, ERS-1 SAR use to determine lake depths in arctic and subarctic regions, in Second ERS–1 Symposium—Space at the Service of our Environment, Hamburg, Germany, 11–14 October 1993, Proceedings: Paris, European Space Agency, Special Publication SP–361, p. 1141–1146.

Melnikov, I.A., 1997, The Arctic sea ice ecosystem: Amsterdam, Gordon and Breach Science Publishers, 204 p.

Ménard, P., Duguay, C.R., Pivot, F.C., Flato, G.M., and Rouse, W.R., 2003, Sensitivity of Great Slave Lake ice cover to climate variability and climatic change, in Squire, V.A., and Langhorne, P.J., eds., Ice in the environment: International Association of Hydraulic Engineering and Research (IAHR), 16th International Symposium on Ice in the Environment, (Dunedin, New Zealand, 2–6 December 2002), Proceedings: Department of Physics, University of Otago, v. 3, p. 57–63.

Metge, M., 1976, Thermal cracks in lake ice: Ph.D. dissertation, Queen's University, Kingston, Ontario, Canada, 204 p.

Michel, B., 1971, Winter regimes of lakes and rivers: Hanover, New Hampshire, U.S. Army Cold Regions Research and Engineering Laboratory (CRREL), CRREL Monograph 111-B1a, 130 p.

Michel, B., and Ramseier, R., 1971, Classification of river and lake ice: Canadian Geotechnical Journal, v. 8, no. 1, p. 36–45.

Michel, B., and eight others, 1986, Hydraulics, in Ashton, G.D., ed., River and lake ice engineering: Littleton, Colorado, Water Resources Publications, p. 261–371.

Morris, K., Jeffries, M.O., and Weeks, W.F., 1995, Ice processes and growth history on arctic and sub-arctic lakes using ERS-1 SAR data: Polar Record, v. 31, no. 177, p. 115–128.

Morse, B., and Hicks, F., 2005, Advances in river ice hydrology, 1999–2003: Hydrological Processes, v. 19, no. 1, p. 247–263.

Mueller, D.R., Vincent, W.F., and Jeffries, M.O., 2003, Break-up of the largest Arctic ice shelf and associated loss of an epishelf lake: Geophysical Research Letters, v. 30, no. 20, 2031, doi:10.1029/2003GL01793.

Mysak, L.A., and Power, S.B., 1992, Sea-ice anomalies in the western Arctic and Greenland-Iceland Sea and their relation to an interdecadal climate cycle: Climatological Bulletin/Bulletin Climatologique, v. 26, no. 3, p. 147–176.

Mysak, L.A., Manak, D.K., and Marsden, R.F., 1990, Sea-ice anomalies observed in the Greenland and Labrador Seas during 1901–1984 and their relation to an interdecadal Arctic climate cycle: Climate Dynamics, v. 5, no. 2, p. 111–133.

NSIDC, 2004, Morphometric characteristics of ice and snow in the Arctic basin: Aircraft landing observations from the Former Soviet Union, 1928–1989, Romanov, I.P., compiler: Boulder, Colorado, National Snow and Ice Data Center, digital media.

Olbers, D., Borowski, D., Volker, C., and Wolff, J.-O., 2004, The dynamical balance, transport and circulation of the Antarctic Circumpolar Current: Antarctic Science, v. 16, no. 4, p. 439–470.

Palecki, M.A., and Barry, R.G., 1986, Freeze-up and break-up of lakes as an index of temperature changes during the transition seasons—A case study for Finland: Journal of Climate and Applied Meteorology, v. 25, no. 7, p. 893–902.

Parkinson, C.L., 2000, Recent trend reversals in Arctic sea ice extents: Possible connections to the North Atlantic Oscillation: Polar Geography, v. 24, no. 1, p. 1–12.

Parkinson, C.L., 2002, Trends in the length of the Southern Ocean sea-ice season, 1979–99: Annals of Glaciology, v. 34, p. 435–440.

Parkinson, C.L., 2004, Southern Ocean sea ice and its wider linkages: Insights revealed from models and observations: Antarctic Science, v. 16, no. 4, p. 387–400, doi:10.1017/S0954102004002214.

Parkinson, C.L., Comiso, J.C., Zwally, H.J., Cavalieri, D.J., Gloersen, P., and Campbell, W.J., 1987, Arctic sea ice, 1973-1976: Satellite passive-microwave observations: Washington, D.C., National Aeronautics and Space Administration (NASA) Special Publication, SP-489, 296 p.

Parkinson, C.L., Cavalieri, D.J., Gloersen, P., Zwally, H.J., and Comiso, J.C., 1999, Arctic sea ice extents, areas, and trends, 1978–1996: Journal of Geophysical Research, v. 104, no. C9, p. 20837–20856.

Parkinson, F.E., 1982, Water temperature observations during break-up on the Liard-Mackenzie river system, in Andres. D.D., and Gerard, R., eds., Workshop on Hydraulics of Ice-Covered Rivers (Edmonton, Alberta, 1–2 June 1982), Proceedings: National Research Council of Canada, p. 261–295.

Pavelsky, T.M., and Smith, L.C., 2004, Spatial and temporal patterns in Arctic river ice breakup observed with MODIS and AVHRR time series: Remote Sensing of Environment, v. 93, no. 3, p. 328–338.

Petryk, S., 1995, Numerical modelling, in Beltaos, S., ed., River ice jams: Highlands Ranch, Colorado, Water Resources Publications, LLC, p. 147–172.

Phelps, A.R., Peterson, K., and Jeffries, M.O., 1998, Methane efflux from high latitude lakes during spring ice-melt: Journal of Geophysical Research, v. 103, no. D2, p. 29029–29036.

Pilant, A.N., and Agarwal, A., 1998, A study of Lake Superior ice features and dynamics using RADARSAT-1 ScanSAR imagery, in RADARSAT ADRO Final Symposium, Montréal, Québec, Canada, 13–15 October 1998, Proceedings (on CD-ROM).

Poe, G., St. Germain, K., Bobak, J., Swadley, S., Wessel, J., Thomas, B., Wang, J., and Burns, B., 2001, DMSP calibration/validation plan for the Special Sensor Microwave Imager Sounder (SSMIS): Washington, D.C., Naval Research Laboratory (28 November 2001), 190 p. (unpub. report).

Polyakov, I.V., Alekseev, G.V., Bekryaev, R.V., Bhatt, U.S., Colony, R., Johnson, M.A., Karklin, V.P., Walsh, D., and Yulin, A.V., 2003, Long-term ice variability in Arctic marginal seas: Journal of Climate, v. 16, no. 12, p. 2078–2085.

Polyakov, I.V., Proshutinsky, A.Y., and Johnson, M.A., 1999, Seasonal cycles in two regimes of Arctic climate: Journal of Geophysical Research, v. 104, no. C11, p. 25761–25788.

Priscu, J., ed., 1998, Ecosystem dynamics in a polar desert—The McMurdo Dry Valleys, Antarctica: Washington, D.C., American Geophysical Union, Antarctic Research Series, v. 72, 369 p.

Proshutinsky, A.Y., Polyakov, I.V., and Johnson, M.A., 1999, Climate states and variability of Arctic ice and water dynamics during 1946–1997: Polar Research, v. 18, no. 2, p. 135–142.

Prowse, T.D., 1990, Heat and mass balance of an ablating ice jam: Canadian Journal of Civil Engineering, v. 17, no. 4, p. 629–635.

Prowse, T.D., 1994, Environmental significance of ice to streamflow in cold regions: Freshwater Biology, v. 32, no. 2, p. 241–259.

Prowse, T.D., 1995, River ice processes, in Beltaos, S., ed., River ice jams: Highlands Ranch, Colorado, Water Resources Publications, LLC, p. 29–70.

Prowse, T.D., and Beltaos, S., 2002, Climatic control of river-ice hydrology—A review: Hydrological Processes, v. 16, no. 4, p. 805–822.

Prowse, T.D., and Bonsal, B.R., 2004, Historical trends in river-ice break-up—A review: Nordic Hydrology, v. 35, no. 4, p. 281–293.

Prowse, T.D., and Demuth, M.N., 1993, Strength variability of major river-ice types: Nordic Hydrology, v. 24, nos. 2–3, p. 169–182.

Prowse, T.D., and Marsh, P., 1989, Thermal budget of river ice covers during break-up: Canadian Journal of Civil Engineering, v. 16, no. 1, p. 62–71.

Prowse, T.D., and Reedyk, S., 1993, Thermal and climatologic effects, in Prowse, T.D., and Gridley, N.C., eds., Environmental aspects of river ice: Saskatoon, Saskatchewan, National Hydrology Research Institute, NHRI Science Report no. 5, p. 60–75.

Prowse, T.D., Demuth, M.N., and Peterson, M., 1993, Proposed artificial river ice damming to induce flooding of a delta ecosystem, in 50th Eastern Snow Conference (Québec City, Québec, 8–10 June 1993), Proceedings:, p. 331–338.

Prowse, T.D., Bonsal, B.R., and Lacroix, M.P., 2002, Trends in river-ice break-up and related temperature controls, in Squire V.A., and Langhorne, P.J., eds., Ice in the environment: International Association of Hydraulic Engineering and Research (IAHR), 16th International Symposium on Ice in the Environment (Dunedin, New Zealand, 2–6 December 2002), Proceedings: Department of Physics, University of Otago, v. 3, p. 64–71.

Ragotskie, R.A., 1978, Heat budgets of lakes, in Lerman, A., ed., Lakes—Chemistry, geology, physics: New York, Springer-Verlag Inc., p. 1–19.

Raphael, M.N., 2003, Impact of observed sea-ice concentration on the Southern Hemisphere extratropical atmospheric circulation in summer: Journal of Geophysical Research, v. 108, no. D22, 4687, doi:10.1029/2002JD003308.

Rayner, N.A., Parker, D.E., Horton, E.B., Folland, C.K., Alexander, L.V., Rowell, D.P., Kent, E.C., and Kaplan, A., 2003, Global analyses of sea surface temperature, sea ice, and night marine air temperature since the late nineteenth century: Journal of Geophysical Research, v. 108, no. D14, 4407, doi:10.1029/2002JD002670.

Riggs, G.A., Hall, D.K., and Salomonson, V.V., 2003, MODIS sea ice user's guide: *http://modis-snow-ice.gsfc.nasa.gov/siugkc.html*.

Rind, D., Chandler, M., Lerner, J., Martinson, D.G., and Yuan, X., 2001, Climate response to basin-specific changes in latitudinal temperature gradients and implications for sea ice variability: Journal of Geophysical Research, v. 106, no. D17, p. 20161–20173.

Rist, S., 1970, Lake-ice of Mývatn: Jökull, v. 19 [1969], p. 121–127.

Robertson, D.M., Ragotskie, R.A., and Magnuson, J.J., 1992, Lake ice records used to detect historical and future climatic changes: Climatic Change, v. 21, no. 4, p. 407–427.

Robertson, D.M., Wynne, R.H., and Chang, W.Y.B., 2000, Influence of El Niño on lake ice and river ice cover in the Northern Hemisphere from 1900 to 1995: Verhandlungen Internationale Vereingung für Limnologie, v. 27, p. 2784–2788.

Rogers, J.C., and van Loon, H., 1982, Spatial variability of sea level pressure and 500 mb height anomalies over the Southern Hemisphere: Monthly Weather Review, v. 110, no. 10, p. 1375–1392.

Rothrock, D.A., Yu, Y., and Maykut, G.A., 1999, Thinning of the Arctic sea-ice cover: Geophysical Research Letters, v. 26, no. 23, p. 3469–3472.

Rouse, W.R., and ten others, 1997, Effects of climate change on the freshwaters of Arctic and Subarctic North America: Hydrological Processes, v. 11, no. 8, p. 873–902.

Rouse, W.R., Oswald, C.M., Binyamin, J., Blanken, P.D., Schertzer, W.M., and Spence, C., 2003a, Interannual and seasonal variability of the surface energy balance and temperature of central Great Slave Lake: Journal of Hydrometeorology, v. 4, no. 4, p. 720–730.

Rouse, W.R., and fifteen others, 2003b, Energy and water cycles in a high-latitude, north-flowing river system: Bulletin of the American Meteorological Society, v. 84, no. 1, p. 73–87.

Rozell, N., 2005, Breakup has been milder in recent years: Heartland Magazine (Fairbanks Daily News Miner), 10 April 2005, p. H–7.

Sagar, R.B., 1962, Meteorological and glaciological studies—Ice rise station, Ward Hunt Island, May to September 1960: Hanscom Field, Bedford, Massachusetts, Air Force Cambridge Research Laboratories, Report no. AFCRL-62-848; Arctic Institute of North America, Research Report no. 24, 87 p.

Sagarin, R., 2001, False estimates of the advance of spring: Nature, v. 414, no. 6864, p. 600.

Sagarin, R., and Micheli, F., 2001, Climate change in nontraditional data sets: Science, v. 294, no. 5543, p. 811.

Schindler, D.W., and nine others, 1990, Effects of climatic warming on the lakes of the central boreal forest: Science, v. 250, no. 4983, p. 967–970.

Schnack-Schiel, S.B., 2003, The macrobiology of sea ice, in Thomas, D.N. and Dieckmann, G.S., eds., Sea ice—An introduction to its physics, chemistry, biology and geology: Oxford, U.K., Blackwell Science, p. 211–239.

Schwarz, J., and seven others, 1986, Ice physics, in Ashton, G.D., ed., River and lake ice engineering: Littleton, Colorado, Water Resources Publications, p. 19–85.

Scott, J. T., 1964, A comparison of the heat balance of lakes in winter: Ph.D. dissertation, University of Wisconsin, Madison, 152 p.

Scrimgeour, G.J., Prowse, T.D., Culp, J.M., and Chambers, P.A., 1994, Ecological effects of river ice break-up—A review and perspective: Freshwater Biology, v. 32, no. 2, p. 261–275.

Sellmann, P.V., Brown, J., Lewellen, R.I., McKim, H., and Merry, C., 1975, The classification and geomorphic implications of thaw lakes on the Arctic Coastal Plain, Alaska: Hanover, New Hampshire, U.S. Army Cold Regions Research and Engineering Laboratory (CRREL), CRREL Research Report 344, 21 p.

Shiklomanov, A.I., Lammers, R.B., and Vorosmarty, C.Y., 2002, Widespread decline in hydrological monitoring threatens pan-Arctic research: EOS (Transactions of the American Geophysical Union), v. 83, no. 2, p. 13, 16–17.

Shirtcliffe, T.G.L., and Benseman, R.F., 1964, A sun-heated Antarctic lake: Journal of Geophysical Research, v. 69, no. 16, p. 3355–3359.

Skinner, W.R., 1992, Lake ice conditions as a cryospheric indicator for detecting climate variability in Canada: Downsview, Ontario, Canadian Climate Centre, Atmospheric Environment Service, Report no. 92-4, 46 p. (unpublished manuscript).

Smith, L.C., 2000, Trends in Russian Arctic river-ice formation and breakup. 1917–1994: Physical Geography, v. 21, no. 1, p. 46–56.

Smith, L.C., 2002, Emerging applications of interferometric synthetic aperture radar in geomorphology and hydrology: Annals of the Association of American Geographers, v. 92, no. 3, p. 385–398.

Smol, J.P. and twenty five others, 2005, Climate-driven regime shifts in the biological communities of arctic lakes: National Academy of Sciences, Proceedings, v. 102, no. 12, p. 4397–4402.

Soldatova, I.I., 1992, Causes of variability of ice appearance dates in the lower reaches of the Volga: Soviet Meteorology and Hydrology, v. 2, p. 62–66.

Soldatova, I.I., 1993, Secular variations in river breakup dates and their relation to climate changes: Russian Meteorology and Hydrology, v. 9, p. 70–76.

Spigel,, R.H., and Priscu, J.C., 1998, Physical limnology of the McMurdo Dry Valleys lakes, in Priscu, J.C., ed., Ecosystem dynamics in a polar desert—The McMurdo Dry Valleys, Antarctica: Washington, D.C., American Geophysical Union, Antarctic Research Series, v. 72, p. 153–187.

Stammerjohn, S.E., and Smith, R.C., 1997, Opposing Southern Ocean climate patterns as revealed by trends in regional sea ice coverage: Climatic Change, v. 37, no. 4, p. 617–639.

Stammerjohn, S.E., Drinkwater, M.R., Smith, R.C., and Liu, X., 2003, Ice-atmosphere interactions during sea-ice advance and retreat in the western Antarctic Peninsula region: Journal of Geophysical Research, v. 108, no. C10, 3329, doi:10.1029/2002JC001543.

Stewart, K.M., and Haugen, R.K., 1990, Influence of lake morphometry on ice dates: Verhandlungen Internationale Vereingung für Limnologie, v. 24, p. 122–127.

Stirling, I., and Derocher, A.E., 1993, Possible impacts of climate warming on polar bears: Arctic, v. 46, no. 3, p. 240–245.

Stocker, T.F., Clarke, G.K.C., Le Treut, H., Lindzen, R.S., Meleshko, V.P., Mugara, R.K., Palmer, T.N., Pierrehumbert, R.T., Sellers, P.J., Trenberth, K.E., and Willebrand, J., 2001, Physical climate processes and feedbacks, in Houghton, J.T., Ding, Y., Griggs, D.J., Noguer, M., van der Linden, P.J., Dai, X., Maskell, K., and Johnson, C.A., eds., Climate change 2001—The scientific basis: Contribution of Working Group I to the Third Assessment Report of the Intergovernmental Panel on Climate Change, Cambridge, U.K., Cambridge University Press, p. 417–470.

Susquehanna River Basin Commission, 2004, Congressman Platts praises river ice observer program and its volunteers—Susquehanna River flood forecasting and warning system highlighted: Harrisburg, Pennsylvania, Susquehanna River Basin Commission (Press release, 19 February 2004), (*http://www.srbc.net/Press%20Releases/FF&WS%20press%20conf.pdf*).

Swithinbank, C., 1972, Arctic pack ice from below, in Karlsson, Th., ed., Sea ice, Proceedings of an International Conference: Reykjavík, National Research Council, p. 246–254.

Thoroddsen, Þ., 1916–17, Hafís við strendur Íslands [Sea ice near the coast of Iceland], in Thoroddsen Þ., Árferði á Íslandi í þúsand ár [Climate in Iceland during a thousand years]: Kaupmannahöfn, S.L. Møller, Hinu íslenska fræðafjelagi, p. 355–432.

Tramoni, F.R., Barry, R.G., and Key, J., 1985, Lake ice cover as a temperature index for monitoring climate perturbations: Zeitschrift für Gletscherkunde und Glazialgeologie, v. 21, p. 43–49.

Van Hove, P., 2005, Limnologie du Nord del' Île d'Ellesmere—Réponse et sensibilité aux changements de climat dans les environnements extrêmes [Limnology of northern Ellesmere Island—Response and sensitivity to climate change in extreme environments]: Ph.D. dissertation, Department of Biology, Université Laval, Montréal, Québec, Canada, 119 p.

Van Hove, P., Swadling, K.M., Gibson, J.A.E., Belzile, C., and Vincent, W.F., 2001, Farthest north lake and fjord populations of calanoid copepods *Limnocalanus macrurus* and *Drepanopus bungei* in the Canadian High Arctic: Polar Biology, v. 24, no. 4, p. 303–307.

Vavrus, S.J., Wynne, R.H., and Foley, J.A., 1996, Measuring the sensitivity of southern Wisconsin lake ice to climate variations and lake depth using a numerical model: Limnology and Oceanography, v. 41, no. 5, p. 822–831.

Venegas, S.A., Drinkwater, M.R., and Shaffer, G., 2001, Coupled oscillations in Antarctic sea ice and atmosphere in the South Pacific sector: Geophysical Research Letters, v. 28, no. 17, p. 3301–3304.

Vilmundarson, Þ., 1969, Heimildir um hafís á síðari öldum [Record of sea ice during the last centuries], in Einarsson, M.Á., ed., Hafísinn [The sea ice]: Reykjavík, Almenna Bókafélagið, p. 313–332.

Vinje, T., 2001, Anomalies and trends of sea-ice extent and atmospheric circulation in the Nordic Seas during the period 1864–1998: Journal of Climate, v. 14, no. 3, p. 255–267.

Vinnikov, K.Y., Robock, A., Stouffer, R.J., Walsh, J.E., Parkinson, C.L., Cavalieri, D.J., Mitchell, J.F.B., Garrett, D., and Zakharov, V.F., 1999, Global warming and Northern Hemisphere sea ice extent: Science, v. 286, no. 5446, p. 1934–1937.

Vyas, N.K., Bhandari, S.M., Dash, M.K., Pandey, P.C., Khare, N., Khanolkar, A., and Sharma, N., 2004, An atlas of Antarctic sea ice from Oceansat-1 MSMR (June 1999–September 2001): Goa, India, National Centre for Antarctic and Ocean Research, 64 p.

Wadhams, P., and Davis, N.R., 2000, Further evidence of ice thinning in the Arctic Ocean: Geophysical Research Letters, v. 27, no. 24, p. 3973–3975.

Walsh, J.E., and Chapman, W.L., 2001, 20th-century sea-ice variations from observational data: Annals of Glaciology, v. 33, p. 444–448.

Walsh, J.E., and Johnson, C.M.,1979, An analysis of Arctic sea ice fluctuations, 1953–77: Journal of Physical Oceanography, v. 9, no. 3, p. 580–591.

Wang, J., and Ikeda, M., 2000, Arctic Oscillation and Arctic sea-ice oscillation: Geophysical Research Letters, v. 27, no. 9, p. 1287–1290.

Watkins, A.B., and Simmonds, I., 2000, Current trends in Antarctic sea ice: The 1990s impact on a short climatology: Journal of Climate, v. 13, no. 24, p. 4441–4451.

Weeks, W.F., and Wettlaufer, J.S., 1996, Crystal orientations in floating ice sheets, in Arsenault, R.J., and six others, eds., The Johannes Weertman Symposium, Anaheim, California, 4–8 February 1996, Proceedings: Warrendale, Pennsylvania, Minerals, Metals & Materials Society, p. 337–350.

Weeks, W.F., Sellmann, P.V., and Campbell, W.J., 1977, Interesting features of radar imagery of ice-covered North Slope lakes: Journal of Glaciology, v. 18, no. 78, p. 129–136.

Weeks, W.F., Fountain, A.J., Bryan, M.L., and Elachi, C., 1978, Differences in radar returns from ice-covered North Slope lakes: Journal of Geophysical Research, v. 8, no. C8, p. 4069–4073.

Wharton, R.A., Jr., McKay, C.P., Clow, G.D., and Andersen, D.T., 1993, Perennial ice covers and their influence on Antarctic lake ecosystems, in Green W.J., and Friedmann, E.I., eds., Physical and biogeochemical processes in Antarctic lakes: Washington, D.C., American Geophysical Union, Antarctic Research Series, v. 59, p. 53–70.

White, W.B., and Peterson, R.G., 1996, An Antarctic circumpolar wave in surface pressure, wind, temperature and sea ice extent: Nature, v. 380, no. 6576, p. 699–702.

Williams, G.P., 1965, Correlating freeze-up and break-up with weather conditions: Canadian Geotechnical Journal, v. 11, no. 4, p. 313–326.

Williams, G.P., 1971, Predicting the date of lake ice break-up: Water Resources Research, v. 7, no. 2, p. 323–333.

Wilson, A.T., and Wellman, H.W., 1962, Lake Vanda—An Antarctic lake: Nature, v. 196, no. 4860, p. 1171–1173.

Wingham, D.J., Francis, C.R., Baker, S., Bouzinac, C., Brockley, D., Cullen, R., de Chateau-Thierry, P., Laxon, S.W., Mallow, U., Mavrocordatos, C., Phalippou, L., Ratier, G., Rey, L., Rostan, F., Viau, P., and Wallis, D.W., 2006, CryoSat: A mission to determine the fluctuations in Earth's land and marine ice fields: Advances in Space Research, v. 37, no. 4, p. 841–871.

Winsor, P., 2001, Arctic sea ice thickness remained constant during the 1990s: Geophysical Research Letters, v. 28, no. 6, p. 1039–1041.

Worby, A.P., Jeffries, M.O., Weeks, W.F., Morris, K., and Jaña, R., 1996, The thickness distribution of sea ice and snow cover during late winter in the Bellingshausen and Amundsen Seas, Antarctica: Journal of Geophysical Research, v. 101, no. C12, p. 28441–28455.

Worby, A.P., Massom, R.A., Allison, I., Lytle, V.I., and Heil, P., 1998, East Antarctic sea ice: A review of its structure, properties and drift, in Jeffries, M.O., ed., Antarctic sea ice: Physical processes, interactions and variability: Washington, D.C., American Geophysical Union, Antarctic Research Series, v. 74, p. 41–67.

Wynne, R.H., and Lillesand, T.M., 1993, Satellite observation of lake ice as a climate indicator—Initial results from statewide monitoring in Wisconsin: Photogrammetric Engineering and Remote Sensing, v. 59, no. 6, p. 1023–1031.

Wynne, R.H., Lillesand, T.M., Clayton, M.K., and Magnuson, J.J., 1998, Satellite monitoring of lake ice breakup on the Laurentian Shield (1980–1994): Photogrammetric Engineering and Remote Sensing, v. 64, no. 6, p. 607–617.

Yuan, X., 2004, ENSO-related impacts on Antarctic sea ice: A synthesis of phenomenon and mechanisms: Antarctic Science, v. 16, no. 4, p. 415–425.

Yuan, X., and Martinson, D.G., 2000, Antarctic sea ice extent variability and its global connectivity: Journal of Climate, v. 13, no. 10, p. 1697–1717.

Yuan, X., and Martinson, D.G., 2001, The Antarctic Dipole and its predictability: Geophysical Research Letters, v. 28, no. 18, p. 3609–3612.

Yuan, X., Martinson, D.G., and Liu, W.T., 1999, Effect of air-sea-ice interaction on winter 1996 Southern Ocean subpolar storm distribution: Journal of Geophysical Research, v. 104, no. D2, p. 1991–2007.

Zhang, T., and Jeffries, M.O., 2000,. Modelling inter-decadal variations of lake ice thickness and sensitivity to climatic change in northernmost Alaska: Annals of Glaciology, v. 31, p. 339–347.

Zwally, H.J., Comiso, J.C., Parkinson, C.L., Campbell, W.J., Carsey, F.D., and Gloersen, P., 1983, Antarctic sea ice, 1973–1976: Satellite passive-microwave observations: Washington, D.C., National Aeronautics and Space Administration (NASA) Special Publication, SP-459, 206 p.

Zwally, H.J., Comiso, J.C., Parkinson, C.L., Cavalieri, D.J., and Gloersen, P., 2002, Variability of Antarctic sea ice 1979–1998: Journal of Geophysical Research, v. 107, no. C5, doi: 10.1029/2000JC000733.

Zwally, H.J., Schutz, R., Bentley, C., Bufton, J., Herring, T., Minster, J., Spinhirne, J., and Thomas, R., 2003 (updated to current year), GLAS/ICESat L2 sea ice altimetry data V018, 15 October to 18 November 2003: Boulder, Colorado, National Snow and Ice Data Center, digital media.